A Novel Strategy to Restore Meaningful Function to Permanently Denervated Skeletal Muscles

by

Asal Yans

Submitted in partial fulfilment of the requirements
for the degree of Doctor of Philosophy

at

Dalhousie University
Halifax, Nova Scotia
December 2024

Dalhousie University is located in Mi'kma'ki, the
ancestral and unceded territory of the Mi'kmaq.
We are all Treaty people.

DEDICATION

To Mehdi

My beloved husband, my best friend and steadfast partner, who has stood by me through every challenge, frustration, and triumph along this journey. Your patience, encouragement, and unwavering belief in me have been my strength and solace. Thank you for always having my back, for being my anchor, and for loving me unconditionally. This accomplishment is as much yours as it is mine.

Table of Contents

LIST OF FIGURES

ABSTRACT

Skeletal muscles rely on neuromuscular junctions (NMJs) and motoneuron control for function. Permanent denervation, caused by spinal cord injuries (SCIs), peripheral nerve injuries (PNIs), or motoneuron diseases like Amyotrophic Lateral Sclerosis (ALS), leads to muscle paralysis and atrophy, with the inability to regenerate or reinnervate. Despite advances in neuroprosthetics, restoring movement in fully denervated muscles remains a challenge due to the lack of neural connections. This thesis explores new techniques to regenerate and restore function in permanently denervated skeletal muscles. First, a protocol was developed to differentiate mouse embryonic stem (ES) cells into functional skeletal muscle cells *in vitro*. These myofibres expressed muscle markers, and developmental analysis revealed the progression of cells from a quiescent to a differentiated state. The cells were engineered to express external genes, including tdTomato or channelrhodopsin-2 (ChR2), facilitating their identification or optical control post-transplantation *in vivo*. Additionally, ChR2 gene expression also was achieved using adeno-associated virus (AAV) vectors, allowing ChR2-expressing myofibres to be used for optical control of muscles. In the second study, irradiated soleus muscles followed by muscle fibres degradation using notexin, a myotoxic agent, were transplanted with ES cell-derived myoblasts expressing ChR2 or tdTomato. The transplanted myoblasts successfully engrafted and regenerated the muscles. tdTomato-expressing muscles showed increased mass but smaller fibres, and ChR2-expressing muscles responded to light stimulation, producing contractile forces comparable to neural stimulation, demonstrating the effectiveness of optogenetics in restoring function in denervated muscles. The next study focused on *ex vivo* anatomical and physiological analysis of transplanted muscles. Regenerated tdTomato-expressing muscles were innervated by endogenous motor axons, and showed normal responses to nerve stimulation, with largely normal synaptic transmission. The innervation rate between endogenous motor axons and exogenous muscle fibres was more 80% with newly formed NMJs at their original sites. Interestingly, the regenerated muscles contained only fast-twitch fibres, unlike the typical slow-twitch composition of the soleus muscle. Lastly, in search of alternative methods to introduce external genes into muscle cells, I explored lipid nanoparticles (LNPs) as non-viral vectors for gene delivery into ES cell-derived muscle cells. LNPs efficiently transfected muscle cells with minimal cytotoxicity and high specificity for muscle cells, with apolipoprotein E (ApoE) enhancing transfection efficiency. This work underscores the potential of LNPs in muscle transfection and paves the way for future *in vivo* experiments.

LIST OF ABBREVIATIONS AND SYMBOLS USED

ACh	Acetylcholine
AChR	Acetylcholine receptor
AAV	Adeno-associated virus
cAMP	Adenylyl cyclase
ALS	Amyotrophic Lateral Sclerosis
ApoE	Apolipoprotein E
α-BTX	α-Bungarotoxin
bFGF	Basic fibroblast growth factor
BMD	Becker Muscular Dystrophy
$BaCl_2$	Barium chloride
ChR	Channelrhodopsin
ChR1	Channelrhodopsin-1
ChR2	Channelrhodopsin-2
CNS	Central Nervous system
BPI	Brachial Plexus Injuries
CSA	Cross-sectional area
CREB	cAMP response element binding protein
μCTX	μ-conotoxin
DMD	Duchenne muscular dystrophy
ES	Embryonic stem
EPP	End-plate potential
EYFP	Enhanced yellow fluorescent protein
ECM	Extracellular Matrix
EDL	Extensor digitorum longus

GAPDH	Glyceraldehyde 3-phosphate dehydrogenase
GC	Genome copies
HBSS	Hanks' Balanced Salt Solution
H & E	Hematoxylin and Eosin
HLV	Hydrodynamic limb vein
hiPSC	Human Induced pluripotent stem cell line
LNP	Lipid nanoparticles
LDLR	Low-density lipoprotein receptors
MTOC	Mitomycin C
mEPP	Miniature end-plate potential
mN	Millinewton
ms	Millisecond
MU	Motor unit
MRF	Myogenic regulatory factor
MHC	Myosin heavy chain
MOI	Multiplicity of Infection
mRNA	Messenger RNA
NMJ	Neuromuscular junction
PAX7	Paired Box Transcription Factor 7
PFA	Paraformaldehyde
PBS	Phosphate-buffered saline
PNI	Peripheral nerve injury
PNS	Peripheral nervous system
pDNA	Plasmid DNA
PSCs	Presynaptic Schwann cells

PMEF	Primary mouse embryonic fibroblasts
rAAVs	Recombinant adeno-associated viruses
Rh	Rhodopsin
SCI	Spinal cord injury
siRNA	Small interfering RNA
SV2	Synaptic vesicle protein 2
TA	Tibialis anterior
T-tubules	Transverse-tubules
VLDLR	Very low-density lipoprotein receptors
VML	Volumetric muscle loss
HSA	α-skeletal actin

ACKNOWLEDGMENTS

I would like to express my sincere gratitude to my supervisor, Dr. Victor Rafuse, for his guidance and intellectual support throughout this research journey. Navigating the complexities of scientific research has been challenging, yet his encouragement and insights helped me persevere through each step. His direction contributed significantly to my growth, enabling me to expand my skills, broadened my vision and provided numerous innovative ideas to explore, for which I am truly appreciative.

I extend my heartfelt appreciation to my committee members, Dr. Ying Zhang and Dr. Sean Christie, for their invaluable feedback and support over the years. I am also grateful to Dr. Adam Johnston, who joined the committee for my defense in Dr. Zhang's absence and provided thorough feedback on my PhD thesis. Additionally, I would like to thank my external examiner, Dr. David Bennett, for his insightful comments and critical review, which helped strengthen my work.

To the members of the Rafuse Lab, both past and present, I owe a deep appreciation for their companionship and support. A special thank you to our incredible lab manager, Cindee Leopold, for her unwavering assistance, kindness, and invaluable mentorship. Cindee’s dedication and expertise, particularly with cell culture, were instrumental in advancing my research. My heartfelt gratitude goes to Dr. Borbala Podor for her true friendship, her genuine efforts to help me, and her thoughtful feedback on this thesis, as well as for performing all the intracellular recordings. I am also deeply thankful to Dr. Laura Dumas—who carried out the AAV cell transfection— Dr. Julia Harrison, Jack Guthrie, and Arul Jude Cline Asainayagam for their kind friendship and generous support throughout this project. Finally, my thanks go to Simone Laforest, who was always there to assist with animal care.

I wish to extend my appreciation to Dr. William Baldridge, current Graduate Coordinator and previous Head of Department, and to Pauline Fraser, Assistant to the Department Head & Graduate Programs, for their generous support and for always being there whenever I needed assistance.

Additionally, I am deeply grateful to the funding sources that made my PhD work possible. My sincere thanks go to the Natural Sciences and Engineering Research Council of Canada (NSERC) and the Canadian Institutes of Health Research (CIHR), as well as to the Abdul Majid Bader Graduate Scholarship, the Nova Scotia Health Research Foundation (NSHRF), and the Dalhousie Medical Research Foundation (DMRF) for their generous support.

To my parents, Farah and Karim, who have always dreamed of seeing me reach the highest levels of academic achievement—thank you for your unconditional love and belief in me.

Although my dear father passed away before witnessing this accomplishment, his inspiration and guidance have been a constant presence in my life.

I am also grateful to my family: my brother Arash, my brother-in-law Alireza, and my in-laws Mansooreh and Ali, for their unwavering moral support, love, and encouragement.

And finally, to my best friend and life partner, my husband Mehdi. Thank you for standing by my side through all the highs and lows of this journey. This achievement would not have been possible without your love, support, and companionship.

Chapter 1: Introduction

1.1 Skeletal Muscle

Skeletal muscles are highly plastic and dynamic tissues (Frontera & Ochala, 2015) that make up approximately 40% to 45% of the human body's mass (J. Liu et al., 2018). These muscles play a crucial role in numerous bodily processes. Mechanically, their primary function is to convert chemical energy into mechanical force, enabling movement, power generation, posture maintenance, and activity. This allows individuals to participate in social and work-related activities, supports overall health, and fosters independence in daily life. Metabolically, skeletal muscles are involved in basal energy metabolism, serve as storage for essential nutrients like amino acids and carbohydrates, produce heat to regulate core body temperature, and consume the majority of oxygen and energy substrates during exercise. Notably, skeletal muscle also acts as a reservoir of amino acids, which are needed by organs such as the skin, brain, and heart for synthesizing specific proteins (Frontera & Ochala, 2015; Wolfe, 2006).

Unlike smooth and cardiac muscle, skeletal muscle contraction is controlled by the somatic nervous system, which allows for voluntary contractions. The human body contains more than 600 skeletal muscles, varying in size and contractile abilities, enabling body movements that range from powerful to delicate, maintaining posture, and supporting breathing (Dumont et al., 2015). Skeletal muscles possess a high capacity to regenerate after damage, largely due to satellite cells—a type of dormant stem cell that becomes activated to repair or regenerate muscle fibres (Dumont et al., 2015; Laumonier & Menetrey, 2016; Morgan & Partridge, 2003).

However, certain conditions, including volumetric muscle loss (VML) and diseases such as muscular dystrophy, surpass the muscle's ability to self-repair (Aguilar et al., 2018; Guiraud & Davies, 2019; Ribeiro et al., 2019). Moreover, severe injuries such as spinal cord injuries (SCIs) or peripheral nerve injuries (PNIs), like brachial plexus injuries (BPI), can lead to muscle denervation, permanent muscle paralysis, loss of motor function, and total muscle atrophy, which impairs muscle regeneration. Depending on the injury's severity and location, critical movements such as hand grasping may become severely compromised (Carpaneto & Micera, 2015; Fu & Gordon, 1995; T. Gordon, 2020). In SCI cases, motoneuron apoptosis leads to muscle denervation, atrophy, and the formation of fibrous tissue, further hindering recovery (X. Xu et al., 2023). In PNIs, while motor axons can regenerate (Fu & Gordon, 1997; Gaudet et al., 2011; T. Gordon, 2020; T. Gordon & Borschel, 2017; Lieberman, 1971), the slow pace of axon regrowth—about 1 mm per day in humans—means that by the time these nerves reconnect with muscles, typically a year or more has passed. Significant muscle atrophy and fat replacement occur in that time. Prolonged denervation causes severe, irreversible damage to muscle tissue, reducing functional recovery to just 10% (Fu & Gordon, 1995).

Paralysis resulting from SCIs and PNIs severely impacts a patient's mobility and ability to perform essential movements. While full recovery from paralysis is the ultimate goal, even partial improvements can greatly enhance quality of life (Anderson, 2004; Collinger et al., 2013). Surveys of quadriplegic patients have identified regaining hand function as a top priority, as restoring hand movements significantly improves independence and daily living (Anderson, 2004). Various strategies have been explored to restore hand function, such as neuroprosthetics that combine wearable orthoses with electrical stimulation of

peripheral nerves to control paralyzed muscles. However, these devices often fail when there is permanent muscle denervation, as no nerves remain for stimulation (Prochazka et al., 2001; C. K. Thomas et al., 1997). At present, there are no medical treatments capable of fully restoring function to permanently denervated muscles.

A novel approach to restoring some function in permanently denervated skeletal muscles involves replacing damaged muscle fibres with engineered fibres that can be activated using optogenetics and ChR2 expression. Previous work in our lab has shown that transgenic expression of ChR2 in skeletal muscle fibres enables controlled muscle contraction through blue light stimulation. This method helped prevent atrophy in denervated muscles by maintaining muscle activity (Magown et al., 2015). In this research, we accomplished cell replacement therapy by transplanting embryonic stem (ES) cell-derived muscle cells carrying ChR2 gene into completely degraded mouse soleus muscles that were prevented from regenerating. We successfully induced muscle contractions in response to blue light, generating optical force comparable to neural force.

In this chapter, we reviewed in detail how skeletal muscles function and produce force, how muscles regenerate after injury, the impact of SCIs and PNIs on muscle function, and the principles of optogenetics and its application to muscle tissue.

1.2 Motor Unit

Muscle function is achieved by interaction of muscle and nervous system. A motor unit (MU) is fundamentally described as a single motor neuron and the collection of skeletal muscle fibres it innervates and activates, representing the key operational unit in neuromuscular activities. This concept underscores the synergy between the structural and

functional aspects of the neuromuscular system, emphasizing the crucial route through which the central nervous system (CNS) governs skeletal muscle fibres. The diversity in MU size, the type of motor neuron, and the specific muscle fibres it targets enables precise control over muscle contractions, ranging from fine, subtle movements to robust, forceful contractions (R. E. Burke, 1981; Henneman & Mendell, 1981; Purves D, Augustine GJ, Fitzpatrick D, et al., 2001) Based on their contractile capabilities and resistance to fatigue, MUs are classified into three primary types: slow (type I), fast fatigue-resistant (type IIA), and fast fatigable (type IIX). Slow MUs excel in maintaining contractions over long durations without succumbing to fatigue, crucial for maintaining posture and performing endurance tasks. On the other hand, fast fatigable MUs, while capable of generating potent contractions, fire rapidly and are best suited for short, intense exertions. Fast fatigue-resistant MUs offer a compromise, providing both strength and endurance (Enoka & Duchateau, 2008; Henneman et al., 1965a). The CNS selectively recruits the MU types in a process governed by the size principle, orchestrating muscle force and action type with remarkable precision. This orderly activation pattern, from the least to the most potent units, facilitates nuanced muscle force production and optimizes energy use (Bawa et al., 2014; Cope & Sokoloff, 1999; Henneman et al., 1965a).

Furthermore, the innervation ratio—the number of muscle fibres per motor neuron—differs across muscles to match their specific functional roles. Muscles involved in delicate, precise tasks, like ones controlling the fingers and eyes, exhibit low innervation ratios for better control. In contrast, muscles tasked with generating large, forceful movements, such as in the legs and arms, display higher innervation ratios (Duchateau & Enoka, 2011; Fuglevand et al., 1993). The innervation ratio is closely linked to

motoneuron size, and this relationship explains the observed connection between MU force and the size of the motoneuron (Henneman & Mendell, 1981; Rafuse et al., 1997).

1.3 Muscle Neuromuscular Junction

The dynamic between motoneurons and muscle fibres, modulated by neurotransmitters at the neuromuscular junction (NMJ), translates electrical impulses from the CNS into mechanical muscle actions. The NMJ serves as a critical chemical synapse connecting motoneurons with skeletal muscle cells, enveloped by Schwann cells (Hong & Etherington, 2011; Hui et al., 2021; L. Li et al., 2018; Rodríguez Cruz et al., 2020), which plays a crucial role in enabling physical movement and everyday activities. Impairments in its development and upkeep can lead to neurological conditions such as congenital myasthenic syndrome and myasthenia gravis (L. Li et al., 2018). This synapse forms at a distinct region of the sarcolemma known as the endplate. This area is characterized by a unique "pretzel-like" shape in healthy mammalian muscles, a form attributed to the branching pattern of the motor neuron's ending. At the tip of each neuron arborization, there are enlargements called presynaptic boutons or motor-nerve terminals, filled with vesicles containing the neurotransmitter acetylcholine (ACh). These boutons are precisely aligned with the sarcolemma's post-synaptic indentations, known as junctional folds, where there are densely packed groupings of acetylcholine receptors (AChRs) (S. R. Iyer et al., 2021; Lovering et al., 2020). Non-myelinating Terminal Schwann cells or presynaptic Schwann cells (PSCs) are interlocked between post-junctional folds and serve as glial cells essential for the NMJ's structural integrity and functional regulation (Feng & Ko, 2007; S. R. Iyer et al., 2021; Ko & Robitaille, 2015). NMJ functions by transmitting action potentials from the motor neurons, which then prompt the release of the ACh to the

synaptic cleft to bind to receptors on the muscle fibres, causing them to depolarize. As a result of depolarization, calcium from the sarcoplasmic reticulum is released, and causes muscle contraction. As such, the NMJ plays a vital role in enabling physical movement and facilitating our everyday activities (S. R. Iyer et al., 2021; Kuo & Ehrlich, 2015; L. Li et al., 2018).

The NMJ has a dynamic nature, with both structural and functional plasticity that undergoes physiological and morphological changes, highlighting its ability to remodel and repair. This plasticity is essential for muscle recovery after injury, in response to exercise (Deschenes, 2019; Fambrough, 1979; L. Li et al., 2018; M. H. Wilson & Deschenes, 2005) and for compensating for motor neuron loss up to a certain point in various diseases (Y. Wang et al., 2021). However, aging can compromise this adaptability, leading to a decline in NMJ function that contributes to muscle weakness and atrophy (L. Li et al., 2018). Interestingly, NMJ compensatory sprouting mainly occurs in slow MUs, while fast fatigable MUs are more prone to neurodegeneration and easily lose the NMJ (Gulino, 2023).

Denervation, resulting from various pathologies like injuries, aging, or cancer cachexia, often leads to muscle dysfunction and atrophy as its most pronounced and detrimental effects. Within these processes, the degeneration of the NMJ is identified as a critical event (Huang et al., 2022). Based on Criss Hartzell & Fambrough (1972) and Fambrough, (1974) studies, changes in the density and sensitivity of the AChRs after denervation in rat models were reported. Also, they noticed a decrease in intrajunctional AChRs and an increase in extrajunctional AChRs within 14 days post-denervation. Similar findings were reported by Steinbach (1981) in the cat model. Increase in the number of extrajunctional AChRs

that are distributed along the muscle fibre membrane, beyond the confines of the NMJ, in contrast to the densely packed intrajunctional AChRs found within the synaptic area, represents a natural compensatory response, designed to boost the muscle fibre's sensitivity to ACh when direct nerve connections are lost and plays a crucial role in preserving some level of muscle functionality and preparing the muscle for potential reconnection with nerves (Fambrough, 1979). Also, Motor endplates (MEPs) became fragmented and broke apart along the lamella clusters following denervation until they ultimately vanished completely both in mice (X. Yin et al., 2019) and human (Gupta et al., 2021). In addition to the internal alterations at the NMJ, presynaptic cells like PSCs that play a role in the maintenance of the NMJ also undergo alterations and cannot support axon and NMJ regeneration after denervation (Huang et al., 2022).

Functional recovery of NMJ is essential for determining the success of treatments aimed at addressing denervation, such as surgeries involving nerve grafting or transplants (Huang et al., 2022). Interestingly, studies investigating AChRs and NMJs locations on the regenerated skeletal muscles after injury and denervation found that new synapses form at their original sites (Burden et al., 1979; Harris, 2003; Marshall et al., 1977). The distribution of AChR on regenerating skeletal muscle fibres was examined in the absence of nerve terminals by Burden et al. (1979) They found that the new synapses, formed by regenerating axons, were precisely located at the sites of the muscle's original synapses, despite the original muscle fibres degenerating and being removed. The basal lamina sheaths of muscle fibres remained intact, serving as guides for the regenerating muscle cells and marking the original synaptic sites. This finding demonstrated that the precise reconnection of nerve and muscle does not require the original muscle cells but instead

relies on cues external to the muscle cell, such as the basement membrane or possibly PSCs, to reestablish synaptic connections accurately.

1.4 Muscle Contraction

In the NMJ, the motoneuron action potential causes depolarization, leading to the opening of voltage-gated calcium (Ca^{2+}) channels on the presynaptic membrane. As calcium enters the nerve terminal, ACh vesicles are released into the NMJ, where ACh travels across the synaptic gap and binds to AChRs on the motor endplates. This binding triggers the depolarization of the muscle fiber, generating action potentials within the muscle (Pham & Puckett, 2023). The nicotinic AChRs at the motor endplate respond by opening channels that allow sodium ions to flow in, resulting in endplate depolarization and action potential formation in the plasma membrane of muscle cells, known as the sarcolemma (Karlin, 2002; Martyn et al., 2009; Rudolf & Straka, 2019). The action potential travels along the membrane surrounding the myofibrils and enters specific structures called transverse-tubules (T-tubules), which transmit the electrical signal from the surface to the deeper regions of the muscle fiber. These T-tubules contain dihydropyridine receptors, situated next to the terminal cisternae of the sarcoplasmic reticulum, the muscle's calcium store. When the T-tubules depolarize, the dihydropyridine receptors undergo a conformational change, interacting with ryanodine receptors on the sarcoplasmic reticulum. This interaction prompts the ryanodine receptors to open, releasing Ca^{2+} from the sarcoplasmic reticulum into the muscle cell cytosol (Kawaguchi & Fujita, 2024). The influx of Ca^{2+} binds to troponin C, a part of the regulatory complex on the thin filaments. This binding process is cooperative, meaning that each Ca^{2+} ion that attaches to troponin C increases its affinity for additional Ca^{2+}, allowing up to four Ca^{2+} ions to bind per troponin C molecule.

As Ca^{2+} binds, it triggers a structural shift in the troponin complex, which moves tropomyosin away from the myosin-binding sites on actin. This exposes the sites, enabling myosin on the thick filaments to bind to actin and initiate muscle contraction (Ohtsuki & Morimoto, 2008).

The cross-bridge cycle is a process during excitation-contraction coupling in which thick and thin filaments slide past each other to produce muscle contraction. The cycle begins when myosin is tightly bound to actin, with no ATP attached to myosin, a state known as rigor. In contracting muscles, this is a temporary state, but in the absence of ATP, such as after death, it becomes permanent, leading to rigor mortis. When ATP binds to the myosin head, it induces a conformational change that reduces myosin's affinity for actin, allowing myosin to detach. The myosin head then moves into a cocked position, directed toward the sarcomere. ATP is hydrolyzed into ADP and inorganic phosphate, which remain attached to myosin. Myosin then binds to a new site on actin and generates a power stroke that pulls the actin filament. This process repeats as long as Ca^{2+} remains bound to troponin C. Finally, ADP is released, returning myosin to the rigor state, where it again binds tightly to actin in the absence of ATP (Fitts, 2008; Pham & Puckett, 2023).

Muscle relaxation occurs after contraction when Ca^{2+} is actively transported back into the sarcoplasmic reticulum by the Ca^{2+}/ATPase pump (SERCA) on the sarcoplasmic reticulum membrane. This process lowers intracellular Ca^{2+} levels, maintaining them at low concentrations when the muscle is at rest. Within the sarcoplasmic reticulum, a protein called calsequestrin binds to Ca^{2+}, reducing free Ca^{2+} concentration and easing the workload of the SERCA pump. As intracellular Ca^{2+} levels fall, Ca^{2+} detaches from

troponin C, allowing tropomyosin to once again block the myosin-binding sites on actin, leading to muscle relaxation (Paolini et al., 2007).

1.5 Muscle Force

The generation of force within skeletal muscles is a complex interplay of various intrinsic (A. Gordon et al., 1966), and extrinsic factors, coupled with the types of muscle contractions—namely isometric and isotonic. At the heart of muscle force generation are intrinsic properties such as the cross-sectional area (CSA) of the muscle, which is directly proportional to its force capacity. Larger muscles with greater CSA can generate more force due to the increased number of actin and myosin filaments available for cross-bridge cycling during contractions (Maughan et al., 1983). Muscle fibre composition also significantly impacts force production; type II fibres produce greater force at a faster rate than type I fibres, which are more fatigue-resistant and suited for endurance activities (Bottinelli & Reggiani, 2000). Additionally, the length-tension relationship describes how muscle length at the initiation of contraction influences force output, with optimal force generated when there is maximal overlap between actin and myosin filaments (A. Gordon et al., 1966).

External conditions affecting muscle force generation include neural activation and the pattern of MU recruitment. Increased neural drive enhances MU recruitment and firing rates, thereby elevating muscle force (Enoka & Duchateau, 2008). The force-velocity relationship also plays a crucial role, indicating that muscles produce less force at higher contraction velocities due to a decrease in the time available for cross-bridge formation (Hill, 1938). Moreover, external loading and mechanical constraints during various exercises influence the engagement of muscles and the force they generate.

Isometric contractions occur when muscles generate force without changing length, essential for joint stabilization and posture maintenance. Muscle force in isometric contractions adheres to the length-tension relationship, with maximal force production achieved at optimal sarcomere overlap (A. Gordon et al., 1966). Isotonic contractions, characterized by muscle length change under constant force, are divided into concentric (muscle shortens) and eccentric (muscle lengthens under tension) types. The force-velocity relationship dictates that concentric contractions see diminished force with increased velocity, while eccentric contractions can generate higher forces, underscoring the versatility of muscle adaptations to varying demands (Hill, 1938).

1.6 Muscle Regeneration

In normal conditions, mammalian adult skeletal muscle is a stable tissue, but it also possesses an amazing capacity for self-healing following damages (Juhas & Bursac, 2013; Khodabukus et al., 2018; Relaix et al., 2021; H. Yin et al., 2013) Regeneration of muscle after damage or trauma involves a complex and critical process essential for the restoration of muscle functionality and structure. Satellite cells, key myogenic stem cells nestled between the basal lamina and the plasma membrane of muscle fibres, play a pivotal role in this regenerative ability. Normally inactive under standard physiological conditions, these cells are activated by muscle injury and trauma, triggering a series of repair and regeneration actions (Bischoff, 1990; Day et al., 2009; Le Grand & Rudnicki, 2007; Morgan & Partridge, 2003; Relaix & Zammit, 2012). Once activated, satellite cells commence the cell cycle, undergoing proliferation and differentiation into myoblasts, which then merge to either form new muscle fibres or mend the existing ones. The process of activation involves a sophisticated mix of signals from the injured muscle, such as

mechanical stress and inflammatory cytokines, rousing the satellite cells from their dormant state (H. Yin et al., 2013). Besides generating progeny that differentiate, satellite cells also preserve their population through self-renewal, thereby meeting the essential characteristics of a stem cell (Collins et al., 2005; Singh & Dilworth, 2013).

The process through which satellite cells are activated and differentiated is directed by a series of transcriptional activities and signaling pathways. Notably, the Notch, Wnt, and TGF-β pathways play significant roles in managing cell growth and differentiation, ensuring effective muscle tissue regeneration (Bentzinger et al., 2012; Gerrard et al., 2021; Girardi & Le Grand, 2018). The role of myogenic regulatory factors (MRFs) like MyoD, Myf5, myogenin, and MRF4 is crucial in the transition of satellite cells to myoblasts. The transcription factor Pax7 is vital for satellite cell maintenance and self-renewal, acting as a dominant regulator in preserving the satellite cell reservoir throughout the regeneration phase (Olguín & Pisconti, 2012; Seale et al., 2000; Von Maltzahn et al., 2013). Moreover, the secretion of growth factors such as FGF, HGF, and IGF-1 by muscle or pro-inflammatory macrophages plays a significant role in satellite cell proliferation and myogenic differentiation, emphasizing the critical role of the surrounding microenvironment in muscle regeneration (R. E. Allen et al., 1995; Boonen & Post, 2008; Johnson et al., 2023; Srikuea et al., 2010).

Furthermore, the success of muscle regeneration is significantly affected by the satellite cells' niche, comprising the extracellular matrix (ECM) and diverse cell types present within the muscle tissue. Even minor changes to the niche ECM can significantly impact stem cells localization, activation, self-renewal, proliferation, and differentiation. The ECM not only offers structural support but also preserves the satellite cells' identity and

influences its functions by binding to growth factors and altering their availability (Cosgrove et al., 2009; Gattazzo et al., 2014; K. Thomas et al., 2015). Additionally, interactions between satellite cells and other cells like fibroblasts and endothelial cells are key in modulating satellite cell functions and facilitating the reconstruction of muscle tissue post-injury (Gillies & Lieber, 2011; Johnson et al., 2023). The removal of fibroblasts disrupts satellite cell dynamics, causing early differentiation, a reduction in the initial satellite cell population, and the formation of smaller regenerated myofibres (Murphy et al., 2011), and endothelial cells play a role in promoting satellite cells' activation (Johnson et al., 2023; Mierzejewski et al., 2023).

Progress in understanding the detailed molecular and cellular mechanisms of satellite cell activation, growth, and differentiation, alongside their interactions within their niche, is essential for the development of specific treatments for muscle conditions and for improving outcomes of muscle repair after injuries. This growing knowledge base holds significant promise for addressing muscular dystrophies, combating age-associated muscle loss, and aiding recovery from sports injuries.

To understand muscle denervation injuries, we need to review SCIs and PNIs, which lead to muscle denervation and paralysis.

1.7 Spinal Cord Injury

A SCI refers to any damage to the spinal cord that leads to temporary or permanent disruptions in its function. These injuries are classified into two categories based on their origin: traumatic and non-traumatic (Ahuja et al., 2017; Ge et al., 2018; Mcdonald & Sadowsky, 2002). Traumatic SCI is caused by external forces, such as vehicular collisions,

falls, sports accidents, or violent acts, that directly injure the spinal cord. In contrast, non-traumatic SCI arises from conditions like tumours, infections, or degenerative disc diseases, which result in spinal cord damage (Ahuja et al., 2017; Ge et al., 2018; Jain et al., 2015).

SCIs cause severe physical, social, and vocational impacts on affected individuals and their families, significantly reducing their independence and increasing the risk of mortality over their lifetime. The research conducted by Thorogood et al. (2023) presents a comprehensive analysis of the trends in SCIs in Canada, documenting a noticeable increase in the annual incidence of such injuries over a 14-year period, from 2005 to 2019. Their findings indicate that the number of new SCI cases annually escalated from 874 to 1,199 incident cases, highlighting a significant rise in the prevalence of SCIs within the Canadian population. Economically, SCI imposes significant burdens, with an estimated lifetime cost of $336,000 per person in Ontario, Canada. This cost is even higher for patients with high-level SCIs. The financial implications of SCI underscore the need for comprehensive healthcare strategies and support systems to alleviate the economic impact on individuals and healthcare systems (Y. Liu et al., 2023).

The spinal cord acts as the main conduit between the brain and the rest of the body by relaying motor and sensory signals. It is composed of vertically aligned spinal tracts, known as white matter, that encase the central regions, referred to as gray matter. This gray matter is where the majority of the spinal cord's neuronal cell bodies are found, organized into distinct segments that contain both sensory and motor neurons. Sensory neuron axons enter the spinal cord, while motor neuron axons exit it through segmental nerves or roots, facilitating the flow of sensory inputs to the brain and motor commands

to the body (Maynard et al., 1997). There is a huge damage of gray and white matter at the lesion centre in SCI which affects motor, sensory, and autonomic functions at and below the site of the injury (Grumbles & Thomas, 2017; Rupp, 2020).

Paralysis and profound weakness and atrophy of muscles observed following a SCI can be attributed to the chronic muscle denervation as a result of motor neuron loss and/or changes in muscle use. Muscle paralysis occurs due to motoneuron death, severance of CNS axons, or demyelination of central or peripheral axons (Grumbles & Thomas, 2017; C. K. Thomas & Noga, 2003; C. K. Thomas & Zijdewind, 2006; X. Xu et al., 2023). In the CNS, neurons have a notably limited capacity for regeneration (Harvey et al., 2005). In cases of demyelination, CNS axon innervation may remain intact, allowing patterned electrical stimulation to restore some function or facilitate activity-based rehabilitation (Grumbles & Thomas, 2017). Some researches suggest that introducing a supportive environment, such as a peripheral nerve graft, at the injury site may enable certain central neurons to extend their severed axons over considerable distances (David & Aguayo, 1981; Richardson et al., 1980). However, the study by Harvey et al. (2005) demonstrated that there is no significant efficacy in regenerating cervical-level spinal cord axons, even after peripheral nerve grafting and daily electrical stimulation in rats.

If motoneurons die, complete denervation occurs, eliminating voluntary control over the affected muscle fibres (Grumbles & Thomas, 2017). In this case, patterned electrical stimulation can no longer be used to restore function due to the high current required to excite fully denervated muscle, which can cause significant damage to the muscle (Gilman & Arbor, 1983; Grumbles & Thomas, 2017). In such difficult cases, it is crucial to replace motoneurons and re-establish muscle innervation. This process restores muscle

excitability and fibre size, supports muscle conditioning, promotes the advantages of physical activity, and enables electrical stimulation of muscles to perform various functions, such as walking, grasping, breathing, and controlling the bladder or bowel (Grumbles & Thomas, 2017). However, denervated muscles undergo atrophy over time and become resistant to reinnervation. Therefore, even successful engraftment of motoneurons may not be effective in the case of severely wasted muscles. To overcome this challenge, directly activating denervated muscles by introducing opsins such as ChR2 into the muscle fibres and using optical stimulation might restore some level of muscle function (Magown et al., 2015).

1.8 Peripheral Nerve Injury

PNI are a significant clinical problem due to their impact on sensory and motor function. Peripheral nerves, due to their location in the body, and their delicate structure are more exposed to damage from injury or illness compared to the CNS structures. The CNS is well-protected by the skull, spine, meninges, and the chemical defence of the blood-brain barrier, while peripheral nerves lack these layers of physical and chemical protection. Consequently, damage to peripheral nerves can result from numerous incidents, ranging from mechanical injuries such as compression, stretching, or cutting, to non-mechanical factors including diseases, genetic conditions, or the effects of medications (Caillaud et al., 2019).

Despite the fact that axons in the PNS are capable of regrowth after the injury, to reinnervate their target muscles or sense organs (Fu & Gordon, 1997; Gaudet et al., 2011; T. Gordon, 2020; T. Gordon & Borschel, 2017; Lieberman, 1971), a significant proportion of PNIs lead to poor functional outcomes, inadequate nerve regeneration, and the loss of

sensory and motor functions which are often accompanied by incomplete recovery, muscle atrophy, chronic pain, and severe weakness (Lopes et al., 2022; M. L. Wang et al., 2019). The time between the initial nerve injury, and muscle or organ reinnervation by regrowing motor axons is the most important detector of the functional recovery anticipation (Scheib & Höke, 2013). The main challenge for proper healing in PNI is the speed of axonal growth, which is very slow at 1-3 mm daily until reaching to distal motor endplates (Lopes et al., 2022; Slavin et al., 2021). In most cases of PNIs, the damage site is located at a long distance from the target motor endplates, and in cases like brachial plexus it takes more than a year that axons could reach to distal muscle to reinnervate them (T. Gordon, 2020). Prolonged denervation causes muscle atrophy and fibrosis (T. Gordon, 2020), and muscles not able to fully recover from atrophy because of satellite cells exhaustion. Also, intramuscular neural sheets become destroyed in the long-term denervation. Thus, very low number of motor axons could innervate these muscles, and functional recovery reduces by up to 90% (Fu & Gordon, 1995).

Based on the nerve gap and other factors in PNI surgical or non-surgical treatments might be performed. Deciding to undertake surgical intervention is complex; performing surgery too early can hinder the potential for spontaneous recovery. Conversely, relying on the lesion's ability to recover spontaneously carries risks, as there is a critical period during which surgery can significantly enhance the recovery potential (Lopes et al., 2022).

However, surgical treatments are essential for addressing PNI, though effective solutions remain difficult. For small gaps under 1 cm, neurorrhaphy (suturing nerve ends) is commonly used, but it is limited to short gaps to avoid excessive tension that could hinder regeneration. Fibrin glue offers an alternative by reducing inflammation and providing

quicker results (Lopes et al., 2022; Vijayavenkataraman, 2020). For larger gaps, nerve grafting is common, with nerve autografts being the most effective for gaps over 3 cm (Grinsell & Keating, 2014). However, autografts come with drawbacks such as the need for a second surgery, donor site morbidity, limited donor nerves, and long recovery times (Kehoe et al., 2012). Nerve allografts may be used for gaps too large for autografts (more than 3 cm in humans), but they require long-term (18- 24 months) immunosuppressive therapy, and high risk of opportunistic infections and other systemic issues. Therefore, this method is only used in severe cases that cannot be treated otherwise. Recently, advances in artificial nerve guide conduits aim to reduce reliance on allografts (Lopes et al., 2022).

Non-surgical treatments, such as exercise and electrical stimulation, are often combined with surgery to promote nerve regeneration, but the outcomes, especially in PNIs with a nerve gap longer than 3 cm, are unknown. While exercise can aid axonal growth and pain relief (Maugeri et al., 2021), low-frequency electrical stimulation has shown promise in improving nerve healing (Alvites et al., 2018), though high-frequency stimulation can worsen and intensify muscle atrophy. It is crucial to standardize factors such as the duration of electrical stimulation, consider potential side effects on healthy surrounding tissues, and account for variations caused by the type and extent of injury. As mentioned earlier, although these efforts to find PNI treatments are promising, it remains challenging to develop a perfect method that effectively reduces neuropathic pain and fully could restore nerve function (Lopes et al., 2022; Vijayavenkataraman, 2020).

1.8.1 Brachial Plexus Injuries

The brachial plexus is a complex network of nerves emerging from the spinal cord segment located in the neck, which controls the muscles and sensations in the shoulder, arm, and

hand (Bayot et al., 2023; Smania et al., 2012). Adult traumatic BPIs, a type of PNI, are severe and debilitating, significantly affecting functional abilities and daily activities. These injuries cause major physical impairments and create substantial social, economic, and psychological challenges, frequently leading to lifelong disabilities as patients often lose their arm and hand functions (Breyer et al., 2021; Thatte et al., 2013). Patients undergoing BPI surgery experience a high prevalence of mental health issues, with 38% having coded depression, 42% coded anxiety, and 25% having both coded depression and anxiety in the year preceding the operation (Yannascoli et al., 2018).

The primary consequences of BPI include muscle atrophy, sensory deficits, pain, and psychological distress. Muscle atrophy, a key result of denervation, begins as early as 2 to 3 months post-injury, with a 50% reduction in fibre diameter. By 2 to 4 months, there is activation of satellite cells, a decrease in fibrils, and death of myofibres and capillaries, accompanied by significant interstitial collagen deposition. Over time, nuclear chromatin condenses and fragments and mitochondrial matrix staining density decreases. As denervation progresses, mitochondria shrink, become more globular, and have fewer cristae, reducing the muscle's repair ability. From 2 to 7 months, muscle and fibre atrophy continue, with dense collagen fibres forming around remaining muscle fibres. By a year, initial streak rarefaction occurs, and by 18 months, there is a significant reduction in CSA and changes in the sarcoplasmic reticulum. After two years, muscle fibres fragment and disintegrate, with adipose and fibrous connective tissue replacing the lost muscle fibres within 1 to 3 years (Smania et al., 2012).

Neuropathic pain, often associated with nerve damage and paralysis, is a significant issue, especially for individuals with complete palsy, affecting nearly 80% of cases. This pain

typically begins either immediately or within a few days following the injury and may last for months or even years (Bertelli & Ghizoni, 2010).

Somatosensory deficits following BPI significantly impact functional recovery, particularly of the upper limb and hand (Oud et al., 2007). The extent of sensory impairment generally depends on the specific nerve roots involved, and the affected area usually follows a dermatomeric distribution (Russell, 2015). Sensory impairments can include loss of touch, proprioception, and pain sensation, which can severely disrupt limb use. The recovery process for sensory functions after BPI is often slow and incomplete and full restoration of sensory function is rare (Smania et al., 2012).

1.9 Muscle Optogenetics

Optogenetics is a technique that introduces a foreign gene into a cell to make it light-sensitive. This method is mainly used on electrically excitable cells, allowing for the regulation of cellular activity using light, which can either excite or inhibit the cells based on the context. Initially developed to control neuronal activity, it employs light-sensitive proteins like channelrhodopsins (ChRs) to regulate ion flow across cell membranes in response to specific light wavelengths (Boyden et al., 2005; Ferenczi et al., 2019; Yizhar et al., 2011).

Bacteriorhodopsin was identified as an ion pump in 1971 that can be swiftly triggered by visible light photons (Oesterhelt & Stoeckenius, 1971). This concept of controlling cellular functions with a single gene and component persisted, leading to the later discovery of other family members: halorhodopsin (Matsuno-Yagi & Mukohata, 1977), channelrhodopsin 1 (ChR1) (Nagel et al., 2002), and channelrhodopsin 2 (ChR2) (Nagel

et al., 2003). Boyden et al. (2005), introduced ChR2 into mammalian neurons for the first time using lentiviral gene delivery, making neurons responsive to light. This groundbreaking study, lead to a spike in optogenetic research in neurons. By 2010, it was demonstrated that ChR, bacteriorhodopsin, and halorhodopsin could all effectively, safely and rapidly activate or deactivate neurons in response to different light colours (Deisseroth, 2011).

ChR2, one of the most common proteins used in optogenetics, is a seven transmembrane helix protein from the rhodopsin (Rh) family with 737 amino acids (Abilez et al., 2011; Müller et al., 2011; Natasha et al., 2013) which acts as a nonselective ion channel, permitting the flow of sodium, potassium, proton, and calcium ions across the cell membrane. It is optimally activated by light at a wavelength of 470 nm, featuring a rapid activation time of less than 1.5 millisecond (ms) and a closure rate between 10 and 13 ms. However, ChR2 can exhibit high levels of desensitization, which may result in inconsistent responses during repetitive or continuous light stimulation (Ishizuka et al., 2006; J. Y. Lin et al., 2009). To address these limitations, the ChR2-H134R variant was developed, offering reduced desensitization and enhanced expression in mammalian tissues (Nagel et al., 2005). This variant of ChR2 has been extensively studied, demonstrating its efficient expression and kinetic properties that align well with the requirements for inducing muscle excitation-contraction coupling, making it a pivotal tool in optogenetic applications within muscle research.

1.9.1 Indirect Muscle Optical Stimulation

The earliest demonstration of light-induced muscle contraction involved the optogenetic stimulation of ChR2-expressing excitatory motoneurons in the layer 5 vibrissal motor

cortex, which triggered whisker movement in freely moving mice and rats (Aravanis et al., 2007). This technique was later expanded to stimulate the phrenic nucleus and spinal respiratory interneurons, restoring diaphragm movement and breathing in rats with SCI (Alilain et al., 2008).

Currently, indirect optical muscle stimulation refers to introducing an optogenetic opsin into peripheral motoneurons controlling muscle functions, which has been developed as an alternative to electrical stimulation (Cohen et al., 2023; Gundelach et al., 2020). The first optical stimulation of peripheral motoneurons to activate skeletal muscles was conducted in transgenic mice expressing ChR2-YFP in both CNS and peripheral nervous system (PNS) neurons, to recruit MUs in an orderly fashion based on size. This approach overcame a key limitation of electrical stimulation, which activates larger MUs before smaller ones, causing fatigue even at low intensities (Llewellyn et al., 2010). Another key study utilized an adeno-associated virus (AAV) 6 vector to introduce the ChR2 gene into the sciatic nerve of rats, indirectly activating the tibialis anterior (TA) and gastrocnemius muscles through light stimulation of the sciatic nerve (Towne et al., 2013). Additionally, Bryson et al. (2014) conducted another study of indirect optical muscle activation by transplanting ChR2-expressing motoneurons into the tibial nerve of mice. Upon illumination with blue light, these transplanted neurons were activated, inducing downstream skeletal muscle contraction. Further examples of indirect optical muscle activation include regulating ankle joint positioning by optically stimulating peripheral nerves in the lower limb (Srinivasan et al., 2018). However, this method presents challenges. First, it may lack precision. It is difficult to ensure that only the target motor neuron is affected, which can lead to unintended activation of other nerves, such as afferent

(sensory) nerves. This can result in off-target effects (Cohen et al., 2023). Additionally, stimulating an entire motor neuron, which controls a whole muscle or part of a muscle, complicates precise localized control of muscle contraction. This lack of precision in controlling individual muscle fibres limits the usefulness of indirect stimulation for fine-tuned muscle movement. Moreover, the effectiveness of this method is largely restricted to scenarios where the neuromuscular system retains some degree of functionality. When target motoneurons are damaged, as in neuromuscular diseases like motor neuron disease, nerve avulsion, and SCI, indirect stimulation may not be effective. Direct optogenetic stimulation of muscles may offer a safer and less harmful alternative to electrical methods, potentially improving muscle function without the associated risks of nerve-based stimulation (Cohen et al., 2023).

1.9.2 Direct Muscle Optical Stimulation

Skeletal muscles, being electrically excitable tissues, present an ideal platform for direct optogenetic applications. By expressing ChR2 in these cells, it is possible to control muscle activation directly with light, bypassing the traditional neuromuscular pathway. The direct expression of opsins in muscles marks a new era of research, though relatively few studies have been conducted so far. Some have explored direct optical stimulation of cardiac muscles to treat cardiac arrhythmias (Bruegmann et al., 2010; Crocini et al., 2016; Nyns, Poelma, Volkers, Plomp, et al., 2019; Scardigli et al., 2018; Zaglia et al., 2015).

The first expression of ChR2 in skeletal muscle was achieved in the body wall and egg-laying muscles of Caenorhabditis elegans nematodes (Nagel et al., 2005). *In vivo* direct optical stimulation of skeletal muscles was elegantly demonstrated by Magown et al. (2015), who showed that optogenetic stimulation of skeletal muscle fibres could efficiently

control muscle contraction in transgenic mice, with ChR2 expressed within the sarcolemma and T-tubules of the fibres. This optogenetic activation significantly reduced denervation atrophy, a common issue in long-term muscle disuse scenarios. A similar study by Bruegmann et al. (2015) reported successful optical contraction of skeletal muscle in transgenic mice, with tetanic force produced by optical stimulation reaching 84% of the maximal force generated by electrical stimulation. Recently, it was shown that grafting engineered muscle tissue formed from C2C12 cells expressing ChR2 can be beneficial in addressing volumetric muscle loss VML (Rousseau et al., 2023). Moreover, another study demonstrated the activation of paralyzed diaphragm muscle, where ChR2 was transfected into the muscle via AAV vectors (Benevides et al., 2022). Additionally, a study applied optogenetics to activate the tongue in mice, offering insights into respiratory physiology and potential interventions for respiratory dysfunctions (Singer et al., 2023).

1.10 Summary of Objectives

The primary aim of this thesis is to investigate novel methods for restoring function in permanently denervated skeletal muscles through 1) cell replacement therapy, which provides regenerative potential via newly introduced satellite cells, and 2) the incorporation of exogenous genes into these cells to enable optogenetic muscle activation. This research focuses on directly activating muscles via optogenetics to bypass traditional nerve stimulation pathways which could aid patients with severe injuries such as SCI, PNI, and Motor neuron diseases like ALS, where neural reconnection is absent. By advancing these approaches and employing innovative gene delivery systems, this thesis seeks to enhance strategies for functional recovery in paralyzed muscles.

Chapter 2: To develop and characterize a protocol for differentiating mouse ES cells into functional skeletal muscle fibres *in vitro*, assessing their structural, molecular, and optogenetic properties for potential applications in muscle cell replacement therapy.

Chapter 3: To evaluate the capacity of ES cell-derived myoblasts transplanted into destroyed mouse muscles, following irradiation and notexin injection, to regenerate muscle fibres, restore muscle mass, express exogenous genes (tdTomato or ChR2), and, in the case of ChR2-expressing myoblasts, to enable functional contraction through optogenetic stimulation.

Chapter 4: To characterize the anatomical and physiological properties of regenerated muscles following tdTomato-expressing myoblast transplantation (as described in Chapter 3), focusing on the capacity for innervation by endogenous motor axons and evaluating muscle contractile force to support therapeutic approaches for conditions such as DMD, VML, and PNI.

Chapter 5: To evaluate a new method for gene delivery into ES cell-derived myoblasts using ionizable LNPs, focusing on their efficiency, specificity, and safety in transferring tdTomato plasmid DNA (pDNA) into skeletal muscle cells *in vitro*.

Chapter 2: Anatomical and Physiological Characteristics of the Embryonic Stem Cell-Derived Skeletal Muscle Fibres *In Vitro*

2.1 Abstract

This study aims to develop a protocol for differentiating mouse ES cells into functional skeletal muscle cells for potential application in muscle cell replacement therapies. Mouse ES cells were successfully differentiated into mature myofibres *in vitro*, capable of surviving for extended periods and expressing skeletal muscle markers. These ES cell-derived myoblasts were engineered to express either tdTomato or ChR2, facilitating the identification or optical control of these cells post-transplantation. We used AAV to introduce the ChR2 gene into wild-type ES cell-derived myoblasts, to enhance therapeutic potential, achieving successful gene expression and functional optical responsiveness. The muscle fibres produced *in vitro* were predominantly fast-twitch fibres, as indicated by the expression of fast skeletal myosin in the absence of slow myosin expression. Additionally, the study included a developmental analysis of the differentiated muscle cells, identifying the temporal expression of myogenic markers, including Pax7, MyoD, and myogenin, revealing the progression of ES cell-derived myoblasts from quiescent to differentiated states. The maturation time was also assessed by tracking the onset of skeletal myosin and desmin expression. These findings underscore the feasibility of generating functional skeletal muscle cells from ES cells, with potential applications for transplantation into injured or denervated muscles to restore some functionality. Moreover, the use of optogenetic tools, such as ChR2, offers a novel approach to controlling muscle function post-transplantation.

2.2 Introduction

Skeletal muscle is a well-structured tissue specialized in generating force for maintaining posture, enabling movement, and facilitating breathing (Chromiak & Antonio, 2008). A distinctive characteristic of healthy adult muscle is its capability to completely restore its structure and contractile functions after routine 'wear-and-tear' and acute injuries (Sousa-Victor et al., 2022). During embryogenesis, skeletal muscle develops from the myotome. Besides generating differentiated muscle fibres at this stage, embryonic progenitor cells also create specialized muscle-forming stem cells known as satellite cells (Gros et al., 2005; C. Xu et al., 2013). In mature muscles, satellite cells are quiescent, located beneath the basal lamina, and identified by specific molecular markers, such as the paired box transcription factor 7 (Pax7) (Cosgrove & Blau, 2010; Gros et al., 2005; Mauro, 1961; Yablonka-Reuveni, 2011). Activation of these cells leads to cell division, proliferating and differentiating into new myofibres to replace damaged fibres after injury or to sustain the satellite cell pool (Dhawan & Rando, 2005; Kuang & Rudnicki, 2008; Sousa-Victor et al., 2022; Zammit, Partridge, et al., 2006). Myogenic transcription factors, including Pax7 and muscle regulatory factors (MRFs), indicate the phases of myogenic progression. For example, while Pax7-positive cells denote inactivated stem cells, the expression of MyoD alongside Pax7 indicates activated proliferating cells with two distinct destinies. Pax7/MyoD co-expressing cells will either differentiate into MyoD/Myogenin co-expressing myocytes to produce myofibres or downregulate MyoD to replenish the satellite cell pool (Day et al., 2009).

Critical motor nerve injuries, such as SCI and PNI, result in significant disabilities. These injuries disrupt neural pathways essential for motor control, leading to muscle denervation,

paralysis, atrophy, and severe dysfunction. While peripheral motor axons can regenerate after injury, CNS motor axons do not naturally regenerate (Huebner & Strittmatter, 2009). However, due to the slow regeneration rate of approximately 1 mm/ day, prolonged denervation occurs, resulting in muscle atrophy and fibrosis, reducing the possibility of successful reinnervation to only 10% (T. Gordon, 2020). Prolonged denervation renders the muscle's self-repair system incapable of restoring muscle mass and function (Wong et al., 2021). It is widely accepted in medical knowledge that muscles denervated for a year or longer cannot regenerate on their own (Seddon et al., 1943). Contrary to previous beliefs that the muscle satellite cell reserve diminishes in chronic muscle denervation, these cells appear to retain their myogenic potential and regenerative ability, capable of repopulating their niche (Wong et al., 2021). However, their failure to undergo differentiation is likely due to their migration being physically obstructed by the fibrotic tissue in the denervated muscle (Borisov et al., 2005).

Currently, there are no methods available to restore meaningful function to permanently denervated muscles. However, finding a way to restore some functionality to the muscles controlling hand movements could significantly improve the quality of life for patients suffering from permanent paralysis (Anderson, 2004). To this end, we aim to replace the denervated muscle’s cells with exogenous myoblasts expressing the ChR2 gene, which can be excited by blue light. Previously, our lab demonstrated that direct expression of ChR2 in the skeletal muscle fibres of transgenic mice causes functional muscle contraction in response to blue light photons (Magown et al., 2015).

To perform cell replacement therapy, it is necessary to generate muscle cells expressing ChR2 suitable for transplantation. In this study, we aimed to differentiate mouse ES cells

into myoblasts *in vitro*, using the method described by C. Xu et al. (2013). They examined the effects of various chemical components on myogenesis and identified six compounds that significantly enhance the differentiation of mouse satellite cells and human induced pluripotent stem cell lines (hiPSCs) (C. Xu et al., 2013). Using three of these components (basic fibroblast growth factor (bFGF), forskolin, and BIO, the GSK3β inhibitor), we successfully differentiated mouse ES cells into mature and functional myofibres, which remained viable for an extended period *in vitro*.

After validating the protocol, we required muscle cell lines carrying external genes for transplantation. Using muscle-specific promoters (Pax7 or α Human skeletal actin (HSA)), we produced ES cell-derived skeletal muscle cell lines expressing tdTomato reporter or ChR2. Both cell lines successfully differentiated into mature skeletal muscle fibres. tdTtomato-expressing myoblasts exhibited strong red fluorescence under the microscope, while ChR2-expressing myoblasts effectively contracted in response to blue light, indicating successful external gene expression in the muscle cell culture. Also, we explored an alternative method to introduce the ChR2 gene into these differentiated myoblasts. We transferred the ChR2 gene into the myotube culture through transduction with AAV-PHP.eB-CAG-ChR2-EYFP, which also resulted in successful muscle contractions in response to blue light illumination. Finally, we studied the developmental characteristics of the ES cell-derived muscle cultures at different time points by measuring the levels of muscle-specific markers (desmin and myosin) and myogenic factors (PAX7, MyoD, and myogenin). Overall, our study establishes a mouse ES cell-derived muscle culture system suitable for genetic manipulation and engraftment into host muscles *in vivo*.

2.3 Materials and Methods

2.3.1 ES Cells Passages and Embryonic Body Formation

Three different types of mouse ES cells were used in this study, including wildtype ES cells (a gift from Gregory L. Cox, The Jackson Laboratory, Bar Harbor, Maine), Pax7-tdTomato ES cells (generated in the lab), which harbor a skeletal muscle-specific pax7 promoter to induce the expression of tdTomato in mature skeletal muscles, and Ai32H1 ES cells (also generated in the lab), which carry a skeletal muscle-specific HSA promoter to induce the expression of ChR2-EYFP in mature skeletal muscle.

After quickly thawing ES cells in a 37°C water bath, they were transferred to a tube with Hanks' Balanced Salt Solution (HBSS) (Thermo Fisher Scientific). The cells were centrifuged and resuspended in ES medium, consisting of 82.5 ml Knockout DMEM (Invitrogen) with penicillin-streptomycin (Thermo Fisher Scientific), 15 ml ES Grade Fetal Bovine Serum (VWR), 1 ml Nonessential Amino Acids (NEAA), 1 ml 2-mercaptoethanol, 500 µl Hepes (Invitrogen), 10 µl Mouse Recombinant LIF (Stemcell Technologies), 10 µl Mirdametinib, and 10 µl GSK3β inhibitor (Stem Cell Technologies). These cells were plated in 5 ml ES medium on tissue culture feeder layer plates previously prepared with Mitomycin C (MTOC)-treated primary mouse embryonic fibroblasts (PMEF). The cells formed small colonies within a few days. After several passages every two days, once the ES cells had grown, ES cell medium was removed to prepare embryoid bodies, and the cells were gently rinsed with HBSS. The cells were lifted using TripLE Express enzyme (Thermo Fisher Scientific), centrifuged, and the supernatant was removed. They were resuspended in ADFNK medium, composed of 125 ml Neurobasal media (Invitrogen), 125 ml Advanced DMEM/F12 (Invitrogen), 2.85 ml 2-

mercaptoethanol (Embryomax), 2.85 ml Glutamax (Invitrogen), and 28.5 ml Knockout Serum Replacement (Invitrogen). The cells were added to gelatin-coated dishes and incubated for 30 minutes, allowing PMEFs to attach to the gelatin layer, leaving a purer population of ES cells. Non-attached cells were removed, centrifuged, and the pellets were resuspended and cultured in suspension at 37°C for two days in ADFNK medium to facilitate embryoid body formation.

2.3.2 Skeletal Muscle Differentiation

Embryonic bodies were produced and transferred two days later to STEMDiff APEL medium (Stem Cell Technologies), with 0.5 μM GSK3β inhibitor (Stem Cell Technologies), 20 μM Forskolin (Stem Cell Technologies), and 10 μg/mL bFGF (Stem Cell Technologies) in suspension culture dishes for five days. Then, 3 embryonic bodies were selected and plated in each culture well on circular, coated Thermanox coverslips, pre coated with Matrigel in the same STEMdiff medium with GSK3β inhibitor, Forskolin, and bFGF. After 3 days, once the embryonic bodies had attached to the coverslips, the medium was replaced with DMEM muscle medium (Thermo Fisher Scientific) with 2% horse serum and 1% penicillin-streptomycin (Thermo Fisher Scientific) added. The day of DMEM administration was considered as day 0. Cells were maintained in this medium for 12-15 days, with fresh medium replaced every 3 days.

2.3.3 Culture Dissociation and Replating

The DMEM medium with 10% horse serum and 1% Penicillin-Streptomycin solution were discarded. The cells were washed for 10 minutes with EDTA (Thermo Fisher Scientific), followed by the addition of 2X Trypsin EDTA and 10X DNase, after which they were triturated. The cell suspensions were centrifuged, and the resulting pellets were

resuspended in muscle medium and replated in cell culture wells containing circular coverslips pretreated with Matrigel.

2.3.4 AAV-PHP.eB-CAG-ChR2-EYFP Transduction into Cells

For transduction of AAVs carrying ChR2-EYFP genes into ES cell-derived myoblasts on day 13 post-differentiation, we first evaluated the cells to identify wells with maximum myofibre coverage and spontaneous contraction. We then dissociated (as previously described) three comparable wells (100% muscle coverage and contractile, if possible) to estimate the number of cells to be transduced from similar wells. After removing the supernatant and resuspending the pellet in 1 ml muscle medium, we counted the cells and estimated the number per well for transduction. To produce the sustained contraction pattern observed with transgenic ChR2 ES cells stimulated with blue light, a Multiplicity of Infection (MOI) of 100,000 is required. To calculate the necessary viral genome copies (GC), we multiplied the number of cells by the MOI:

Quantity of viral particles needed (GC) = estimated number of cells per well x MOI.

The titre of the AAV2 PHP.eB-CAG-ChR2-EYFP virus (Neurophotonics) was 6.3×10^{12} GC/ml (or 6.3×10^{9} GC/µl). To calculate the volume of virus needed, we used this formula:

Volume of virus needed per well (µl) = quantity of viral particles needed (GC) / titre (GC/µl).

We added the required volume of virus to each well. The next day, additional media was added without removing the existing media.

2.3.5 Light Stimulation of ChR2 Expressing Cells

Light stimulation of cells was done using fluorescent microscope (Optika microscopes) by illuminating blue light to the cells for very short fraction of time and recording the video using Optika Pro view software.

2.3.6 Cells Immunohistochemistry

Cultures were fixed for 15 minutes with 4% paraformaldehyde (PFA). Following fixation, a gentle triple rinse, each lasting 10 minutes, was performed using 1x phosphate-buffered saline (PBS). Overnight incubation at 4 °C followed with primary antibodies: mouse anti-Fast myosin IgG (1:500, Sigma-Aldrich), rabbit anti-Fast myosin IgG (1:500, Abcam), rabbit anti-desmin IgG (1:1000, Abcam), rabbit anti-MyoD1 IgG (1:1500, Proteintech), mouse anti-F5D (Myogenin) IgG1 (1:250, Developmental Studies Hybridoma Bank), mouse anti-BA-D5 IgG2b (specific to slow MHC) (1:10, Developmental Studies Hybridoma Bank), mouse anti-Pax7 IgG1 (1:250, Novusbio), and rabbit anti-GFP IgG (1:1000, Abcam). Antibodies were diluted in 1% BSA (VWR) in PBS with 0.5% PBS-Triton. After three additional PBS rinses, cultures were exposed to appropriate secondary antibodies at room temperature for 1-2 hours in the dark: Alexa Fluor 488-conjugated goat anti-mouse IgG (1:500, Invitrogen), Alexa Fluor 488-conjugated goat anti-mouse IgG1 (1:500, Invitrogen), Alexa Fluor 488-conjugated goat anti-mouse IgG2b (1:500, Invitrogen), Alexa Fluor 546-conjugated goat anti-mouse IgG (1:500, Invitrogen), Alexa Fluor 488-conjugated goat anti-rabbit (1:500, Invitrogen), and Alexa Fluor 546-conjugated goat anti-rabbit (1:500, Invitrogen). Following another triple PBS rinse, nucleus staining was performed with Hoechst 33342 (Sigma-Aldrich) at 0.1 μg/ml for 10 minutes in PBS. After the final wash, circular coverslips were placed on microscope slides

and covered with lab-made mounting medium composed of 1:2 glycerol in 1x PBS, supplemented with 0.03 mg/ml ρ-phenylenediamine.

2.3.7 Imaging

Imaging was performed using an upright fluorescent microscope (Leica Instruments), and image processing was done using Zen-Blue software (Zeiss).

The area covered by cells expressing desmin or myosin was analyzed using ImageJ software, using 20x images captured from various areas of the coverslip covered by cells. For each day 15-20 images were analysed.

For cell number counting, several 40x images were captured from various areas of the coverslip covered by cells. For each day, at least 20 images were analyzed by labelling the cells and counting the number of labels at the end.

2.3.8 Statistical Analysis

Statistical GraphPad Prism (Prism 10) software were used for the statistical analysis and graph creations. All data were expressed as the mean ± standard deviation, with statistical significance determined at $P < 0.05$. Comparison between percentage of the culture area covered by desmin and skeletal myosin expressing myoblasts/myotubes in different days were using Multiple unpaired t-test, while Multiple comparisons ANOVA test was employed for comparisons between four groups of expressing Pax7, Pax7/ MyoD, MyoD/ myogenin and myogenin in different days.

2.4 Results

2.4.1 Production of Functional Skeletal Muscle Fibres from ES Cells *in vitro*.

For muscle cell replacement therapy, the primary objective is to produce healthy and long living muscle cells *in vitro*. ES cells, sourced from the inner cell mass of the pre-implantation blastocyst, exhibit significant therapeutic potential due to their extensive proliferation and differentiation capabilities into any fully specialized cell types in the body, including skeletal muscle cells, thus making them promising candidates for cell transplantation therapy (Bhagavati & Xu, 2005).

To validate our developed cell differentiation protocol, we initially used wild-type mouse ES cells and differentiated them into skeletal muscle cells. After 3 days of differentiation and 15 days of maintenance in muscle media, these cells were dissociated and reseeded into cell culture plates pre-treated with Matrigel (Fig. 2.1A). This step was undertaken to evaluate their phenotype and survivability post-dissociation, a crucial process for preparing the cells for collection and subsequent transplantation into muscle tissue *in vivo*.

Time-course staining of these cells with skeletal muscle-specific antibodies, such as skeletal myosin and desmin, indicates that ES cell-derived myoblasts express both factors and can survive *in vitro* for a long period (Fig. 2.1B). Notably, skeletal myosin is not expressed on day 1, but its expression begins as early as day 4 (Fig. 2.1B). These cells remain viable *in vitro* in muscle media for nearly two months (results not shown). A high-magnification image of these differentiated myofibres is shown in Figure 2.1C.

2.4.2 Production of ES Cell-derived Myotubes Expressing tdTomato and ChR2

After validating the protocol, we proceeded to generate tdTomato-expressing myoblasts. Producing myoblasts expressing tdTomato is highly beneficial for distinguishing *in vitro* cultured muscle cells from endogenous muscles after *in vivo* transplantation into the host mouse's muscle. To achieve this, ES cell-derived myoblasts were produced using ES cells from Pax7Cre; tdTomato mice strain. These mice express tdTomato following the Cre-mediated excision of a floxed stop codon. As demonstrated in Figure 2.2, tdTomato-expressing cells form elongated muscle fibres *in vitro*, expressing skeletal myosin as confirmed by immunohistochemistry staining, and displaying a vivid red colouration even without the need for tdTomato antibody staining.

Furthermore, to develop muscle fibres capable of exogenous activation, which could be transplanted into denervated muscles to create optically controlled muscles, ChR2-EYFP-expressing myoblasts were produced from ES cells from HSACre; Ai32 mice strain. These transgenic mice were generated by crossing mice that possess the cre recombinase gene, driven by the HSA promoter, with Ai32 mice, which contain a LoxP-stop-LoxP-EYFP-ChR2 cassette. The engineered myoblasts were designed to express ChR2 fused with enhanced yellow fluorescent protein (EYFP), facilitating optical control. Supplementary video 2.1 (see Appendix One) shows ChR2-EYFP-expressing muscle fibres responding to blue light stimulation, indicating efficient ChR2 expression and functional optical responsiveness in these fibres.

This approach not only confirms the successful differentiation of muscle fibres but also demonstrates the potential for precise, light-controlled activation of muscle cells, offering promising insights for future therapeutic applications.

2.4.3 Transduction of ES Cells derived Myotubes with AAV-PHP.eB-CAG-ChR2-EYFP

After producing ChR2-expressing myoblasts from transgenic mice, we aimed to generate ChR2-expressing embryonic ES-derived myoblasts from wild-type mice. To achieve this, we utilized AAV, a non-enveloped virus, to introduce the ChR2-EYFP gene into the wild-type myoblasts. AAVs are well-documented for their efficiency in delivering DNA to target cells and have garnered significant attention in clinical-stage experimental therapeutic strategies. The technique of producing recombinant AAV particles, which lack viral genes and contain DNA sequences of interest, has been consistently recognized as one of the safest approaches for various gene therapy applications (Naso et al., 2017).

In particular, the AAV-PHP.eB variant, derived from AAV9, features capsid modifications that enhance its tissue penetration, making it a superior choice for transfecting the CNS and peripheral tissues (Chan et al., 2017). We selected AAV-PHP.eB-CAG-ChR2-EYFP, which has been shown to effectively infect mouse hindquarter muscle (Jiang et al., 2021), to transfect our myoblasts *in vitro*. Following the differentiation of ES cells into skeletal muscle cells, 13 days after the administration of muscle media, the muscle fibres were infected with AAV-PHP.eB-CAG-ChR2-EYFP. Figure 2.3 displays skeletal muscle fibres immunostained for EYFP, indicating efficient expression of the ChR2-EYFP conjugate upon AAV-PHP.eB-CAG-ChR2-EYFP transduction. Additionally, Video 2.2 (see Appendix One) demonstrates the contraction of these muscle fibres in response to blue light stimulation.

2.4.4 Characterization of Fibre Types in Myotubes Derived from ES Cells

To investigate the characteristics of the ES cell-derived muscle fibres we produced *in vitro*, we aimed to determine their fibre types. Mammalian skeletal muscle fibres are categorized into different types, each with distinct movement rates, responses to neural inputs, and metabolic characteristics. These fibre types are a conserved feature in vertebrate muscle. For instance, adult mouse and fish musculature exhibit a gradient of myosins, metabolic activity, innervation patterns, and various other distinguishing features. Skeletal muscle fibres are broadly classified into slow-twitch (type I) and fast-twitch (type II) categories, based on the type of myosin heavy chain (MHC) isoforms they express, which determine their contraction speed and fatigue resistance (Mukund & Subramaniam, 2020; Pette & Staron, 2000; Schiaffino & Reggiani, 2011; Talbot & Mavez, 2016).

To assess the fibre types in our ES cell-derived muscle fibres *in vitro*, we fixed and stained the fibres for both fast and slow skeletal MHCs. As shown in (Fig 2.4), all cultured muscle fibres exclusively expressed fast skeletal myosin, with no fibres expressing slow myosin. This result indicates that all the muscle fibres produced *in vitro* in our lab are fast skeletal muscle fibres, highlighting a lack of slow-twitch fibre development under the given culture conditions.

2.4.5 Developmental Characterization of ES Cell-derived Myotubes *in vitro*

In the next step, we sought to investigate the developmental characteristics of mouse ES cell-derived myoblasts *in vitro*. We examined the expression levels of various myogenic and muscle-specific factors in these cells from day 1, when they were moved to muscle media after 3 days of differentiation, until day 15, when they had grown into multinucleated muscle fibres, as shown in the graph (Fig 2.5A). Desmin, a muscle-specific

intermediate filament protein crucial for muscle formation and maintenance in both skeletal muscle and heart (Capetanaki et al., 1997; Paulin & Li, 2004), was one of the factors investigated. Another important factor examined was skeletal muscle MHC, a fundamental component of the sarcomere structure and muscle contraction. Deficiencies and mutations in genes encoding skeletal muscle MHC isotypes induce atrophic changes in skeletal muscle (Hitachi et al., 2023). Changes in desmin and Skeletal myosin expression over time are illustrated in (Fig 2.5 B, C). Desmin-positive cells were observed from day 1, whereas myosin expression began on day 5. As shown in (Fig 2.5 C), the percentage of the area covered by desmin-positive cells on days 1, 3, and 5 (7.33% ± 3.0, 35.23% ± 5.8, and 37.57% ± 14.2, respectively) was significantly higher than the area covered by myosin-positive cells, which remained at 0% on days 1 and 3, and only reached 4.31% ± 4.9 on day 5 ($P=0.0019$, $P<0.0001$, and $P=0.0015$, respectively). However, by days 10, 13, and 15, myosin expression increased, bridging this initial lag (59.59% ± 10.7, 85.69% ± 3.4, and 88.64% ± 4.2, respectively), showing no significant difference compared to desmin expression levels (62.13% ± 13.0, 85.57% ± 4.05, and 88.21% ± 4.0, respectively) ($P=0.7210$, $P=0.9606$, and $P=0.8592$, respectively).

Satellite cells and their progeny exhibit temporal expression of transcription factors that correspond to various stages of myogenic progression. These factors include the Pax7 and the MRFs such as MyoD and myogenin (Day et al., 2009; Smith et al., 1993; Yablonka-Reuveni & Rivera, 1994). Cells expressing only Pax7 represent quiescent satellite cells (Singh & Dilworth, 2013; Zammit, Relaix, et al., 2006), while Pax7/ MyoD co-expressing cells are activated, proliferating satellite cells. These cells proliferate and divide to produce a pool of muscle precursor cells that either downregulate MyoD and self-renew as Pax7-

positive cells or differentiate and eventually fuse to form myofibres. MyoD/ myogenin co-expressing or only myogenin expressing cells are differentiating myocytes (Day et al., 2009; Eftimie et al., 1991; Miner & Wold, 1991). Indeed, MyoD directly activates genes that promote cell cycle progression, resulting in myoblast proliferation, while myogenin exhibits antiproliferative effects by activating genes that inhibit the cell proliferation machinery, leading to cell cycle exit and promoting myoblast differentiation into mature muscle fibres (Singh & Dilworth, 2013).

To determine the pattern of Pax7, MyoD, and myogenin expression within the ES cell-derived myogenic cell culture, we immunostained them on different days (day 1, 5, 10, and 15). Examples of this staining on day 1 and day 15 are shown in Figure 2.5 D. As shown in Figure 2.5 E, on day 1 after differentiation, there were only Pax7 positive cells in the culture, indicating all the myogenic cells were in the quiescent stage. There was a significant difference between the number of Pax7 expressing cells (42.19% ±18.9) and Pax7/MyoD co-expressing, MyoD/myogenin co-expressing, and only myogenin positive cells (0%, P= 0.0002). On day 5, cells co-expressing Pax7/MyoD had the highest number in the culture, accounting for 27.37% ± 9.3 of the total number of cells counted based on Hoechst staining. This indicates that most cells had entered the activated phase. The number of Pax7/MyoD positive cells was significantly higher than the number of myogenin positive cells, which was only 2.81% ± 5.6 (P= 0.0089). The numbers of Pax7 positive and MyoD/myogenin co-expressing cells were 19.35% ± 10.4 and 23.86% ± 22.9 of the total cell numbers, respectively, with no significant difference between them and Pax7/MyoD co-expressing cells. On day 10, the number of differentiated cells MyoD/myogenin co-expressing was the highest at 36.49% ± 5.3 of total cells, significantly

higher than Pax7 positive (12.41% ± 2.3), Pax7/MyoD positive (24.00% ± 6.4), and myogenin positive (10.64% ± 2.5) cells (P= 0.0001, P= 0.0451, and P< 0.0001, respectively), indicating that most cells were in the differentiation phase. Finally, on day 15, MyoD/myogenin positive cells again had the highest number in the culture (35.14% ± 5.1), significantly more than Pax7 positive (14.7% ± 5.2), Pax7/MyoD positive (24.03% ± 5.0), and myogenin positive (21.28% ± 5.5) cells (P=0.0042, P= 0.0443, P= 0.0184, respectively).

In summary, initially only quiescent satellite cells were present in the culture, but by day 5, most had entered the activated stage to differentiate into long multinucleated muscle fibres or reproduce Pax7 positive muscle satellite cells. By days 10 and 15, most cells were in the differentiation phase, expressing MyoD/myogenin or fully mature multinucleated fibres downregulated MyoD and expressing only myogenin.

2.5 Discussion

This study aimed to develop and validate a protocol for differentiating mouse ES cells into functional skeletal muscle cells that express external genes, particularly ChR2, for potential use in muscle cell replacement therapies. The primary goal was to generate viable skeletal muscle cells *in vitro* that could be transplanted into denervated muscles or injured muscles with impaired regenerative capabilities. These cells would potentially regenerate muscle tissue through engraftment and development of the transplanted differentiated muscle cells and could be used to activate denervated muscles optically, thereby restoring some level of function to these muscles.

The results effectively demonstrated that the ES cells were successfully differentiated into myoblasts, expressing key muscle-specific markers such as skeletal myosin and desmin, with these cells maintaining viability *in vitro* for up to two months. Furthermore, the study generated muscle fibres expressing the tdTomato reporter gene and the optogenetic tool ChR2. The latter enabled muscle contractions in response to blue light, demonstrating the successful functional integration of the introduced gene. Myofibres expressing tdTomato exhibited a strong red fluorescence under the microscope, which remained stable during immunostaining, eliminating the need for an anti-tdTomato antibody. ChR2-expressing myofibres, as shown in the video, strongly contracted upon blue light stimulation. Additionally, the study explored the use of an AAV as an alternative way to transduce the ChR2 gene into wild-type ES cell-derived myoblasts, successfully resulting in muscle fibres that could also be optically stimulated. We found that all the muscle fibres produced *in vitro* were fast-twitch fibres, as indicated by the exclusive expression of fast skeletal myosin in the absence of slow myosin expression. The developmental characterization of the ES cell-derived myotubes revealed the temporal expression patterns of key myogenic markers, including Pax7, MyoD, and myogenin, plus muscle markers desmin and myosin indicated a well-organized progression of myogenesis, from quiescent satellite cells to differentiated myotubes. This comprehensive set of results underscores our success in generating ES cell-derived muscle cultures that are both functionally active and suitable for potential therapeutic applications.

In a study by C. Xu et al. (2013), researchers utilized a zebrafish embryo culture system to screen 2,400 chemicals for their impact on myogenesis. They identified six compounds that significantly enhanced muscle development, with forskolin being notably effective in

promoting this process. The study further demonstrated that forskolin enhances the proliferation and differentiation of mouse satellite cells *in vitro*. Forskolin is an adenylyl cyclase (cAMP) activator, and it is shown that enhancing cAMP signaling with an activated version of cAMP response element binding protein (CREB) leads to increased proliferation of primary myoblasts *in vitro* (Stewart et al., 2011). The researchers also showed that hiPSC-derived muscle progenitors treated with a chemical cocktail, including forskolin, bFGF, and BIO, could induce myogenesis. These cells were able to engraft and contribute to muscle regeneration in immune-compromised NSG mice, as evidenced by the expression of the human δ-Sarcoglycan protein. In our study, we also employed the same triple-component cocktail used by C. Xu et al. (2013) to differentiate mouse ES cells into skeletal muscle fibres. Remarkably, all three mouse ES cell lines successfully differentiated into multinucleated skeletal muscle fibres. Notably, our cultures exhibited a faster maturation rate compared to the C. Xu et al. (2013) study. While we observed mature skeletal fibres covering the whole culture plate surface and expressing desmin and skeletal myosin as early as day 13, Xu et al. reported that myosin expression starts at day 36. Furthermore, our cultures showed the presence of both myosin and myogenin, key late myogenic markers, starting on day 5. This suggests that our modified protocol is highly effective for differentiating mouse ES cells, achieving a much faster maturation timeline.

The fundamental unit of adult skeletal muscle is the myofibre, a highly specialized syncytium designed to generate force through contraction. Myofibres are maintained by numerous post-mitotic myonuclei and are effectively repaired and regenerated by satellite cells (Mauro, 1961; Zammit, Partridge, et al., 2006). The formation of new myofibres primarily relies on satellite cells, which provide new myonuclei (Moss & Leblond, 1971)

before entering a quiescent state in fully matured muscle (Schultz et al., 1978). Despite this dormancy, satellite cells can still proliferate and differentiate when necessary, whether for routine myonuclear turnover or in response to the less frequent demands of myofibre hypertrophy and muscle repair (Bischoff, 1986; Schmalbruch & Lewis, 2000; M. Snow, 1978; M. H. Snow, 1977). All satellite cells uniformly express the Pax7, which is essential for their maintenance and the regeneration of skeletal muscle during the quiescent state, (Lepper et al., 2009; Seale et al., 2000; Von Maltzahn et al., 2013). Pax7 is crucial for myogenesis and satellite cell function. The deletion of Pax7 in primary myoblasts and satellite cells results in growth arrest and a decrease in the expression of MRFs (Kawabe et al., 2012; McKinnell et al., 2008). The limited regeneration observed in adult muscle lacking Pax7 is likely due to the premature differentiation of committed satellite cells without their usual proliferation. Furthermore, without Pax7, satellite cells lose their ability to self-renew, ultimately leading to their depletion through terminal differentiation (Von Maltzahn et al., 2014). Our results showed that differentiated mouse ES cells highly express Pax7, a marker for skeletal muscle differentiation, from day 1 after differentiation. Upon activation, satellite cells express another transcription factor, MyoD, from the MRF group, which is crucial for myogenic differentiation. The co-expression of Pax7 and MyoD indicates activated satellite cells (Olguin & Olwin, 2004; Schmidt et al., 2019; Zammit, Partridge, et al., 2006). At this stage, many activated satellite cells proceed to proliferate, reduce Pax7 expression, and begin differentiation. In contrast, another group of proliferating cells continues to express Pax7 while losing MyoD expression, subsequently exiting the cell cycle and halting immediate myogenic differentiation, reverting to a quiescent state to preserve the satellite cell pool (Day et al., 2009; Nagata et al., 2006; Zammit et al., 2004). On day 5, we observed the highest rate of myogenic cells co-

expressing Pax7 and MyoD, and these cells were still present on days 10 and 15, indicating that satellite cells retain the potential to become activated and follow either of fates. As myogenesis progresses, myogenin, another MRF family member, co-expresses with MyoD after Pax7 is downregulated. Myogenin mediates terminal differentiation, a process accompanied by the downregulation of MyoD expression (Hernández-Hernández et al., 2017; Schmidt et al., 2019; Von Maltzahn et al., 2014). Interestingly, myogenin-null mice cannot survive and die at birth due to severe muscle defects (Comai & Tajbakhsh, 2014; Hasty et al., 1993; Nabeshlma et al., 1993; Venuti et al., 1995). While MyoD-null mutants can survive, a significant number do not make it past birth, with survival rates varying depending on the genetic background of the mice (Comai & Tajbakhsh, 2014; Zammit, 2017). In our results, we observed that cells co-expressing MyoD and myogenin were most abundant on days 10 and 15, and myogenin-only expressing cells, representing mature myofibres, were at their highest level on day 15. This indicates that skeletal muscles are mostly mature by these days, although some cells are still in the initial and myogenic phases.

Skeletal muscle is defined by its distinct fibres' architecture, where the precise arrangement of muscle fibres is crucial for enabling a broad range of functional capabilities. The presence of different fibre types contributes to the heterogeneous nature of the tissue. Muscle fibres can be categorized based on their structural and functional properties (Pette & Staron, 1990). According to MHC isoforms, muscle fibres fall into two main groups: slow-twitch (Type I) and fast-twitch (Type II) fibres. Fast-twitch fibres are further subdivided into three subgroups: Type II A, II X (sometimes referred to as IID), and II B (Pette & Staron, 2000). However, in human muscles, Type IIB fast-twitch fibres

are absent (Talbot & Mavez, 2016). Slow fibres are red, fatigue-resistant fibres with high oxidative and low glycolytic capacity. Among the fast-twitch fibres, Type IIA fibres exhibit high myosin ATPase activity, along with both high oxidative and glycolytic capacities, making them relatively fatigue-resistant. Type IIB fibres also have high myosin ATPase activity but low oxidative and high glycolytic capacity, leading to rapid fatigue (Herbison et al., 1982). Type IIX fibres are intermediate, contracting faster than Type IIA but slower than Type IIB, and primarily rely on glycolytic capacity (Talbot & Mavez, 2016). Most muscle fibres contain a single type of myosin isoform and are therefore classified as pure fibres. However, some fibres contain two different myosin isoforms, such as Type I and Type IIA, Type IIA and IIX, or IIX and IIB. These are known as hybrid fibres (Augusto et al., 2004; Pette & Staron, 2000). During embryogenesis, the first postmitotic skeletal muscle cells express two types of MHCs: slow Type I and embryonic myosin. Later in fetal development, fast myosins begin to be expressed, but in adult muscle fibres, either type (slow or fast) can be expressed (Chal & Pourquié, 2017).

Interestingly, our ES cell differentiated myofibres all exhibited fast-twitch characteristics, expressing only fast myosin. Feldman & Stockdale (1991) conducted an *in vitro* study of satellite cells isolated from two types of bird muscles—the pectoralis major (PM, a fast-twitch muscle) and the anterior latissimus dorsi (ALD, a slow-twitch muscle)—to determine whether they would produce fast, slow, or hybrid muscle fibres when cultured without nerve input or specific external signals. They observed that satellite cells from the PM produced only fast-twitch fibres, while those from the ALD produced up to 25% hybrid fibres (expressing both fast and slow MHC isoforms), with the remaining fibres being fast-twitch. This suggests that the culture environment may influence muscle cells

to express fast myosin types. We did not distinguish the subtypes of these fast-twitch myofibres, which could be investigated in future studies.

Muscle fibres are highly adaptable and can modify their characteristics in response to various conditions, such as changes in neuromuscular activity, mechanical stress, hormonal fluctuations (particularly thyroid hormones), and aging. These adaptations often involve shifts in MHC isoform expression, typically following a pattern of reversible transitions between fast-twitch and slow-twitch phenotypes depending on the stimuli (Pette & Staron, 2000). This suggests that these cells might convert slow fibres in response to increased activity or co-culturing with motoneurons which should be investigated in future studies.

In conclusion, this study establishes a reliable, modified method for differentiating ES cells into functional skeletal muscle fibres capable of expressing external genes and responding to optical stimuli. The findings pave the way for future research into the therapeutic potential of these cells, particularly in muscle regeneration and optogenetic control of muscle activity. However, further research is needed to optimize culture conditions to produce a more diverse range of muscle fibre types and fully explore the therapeutic potential of these ES cell-derived muscle fibres *in vivo*.

2.6 Figures

Figure 2.1 Mouse ES cell differentiation into myoblasts/myotubes produce functional muscle fibres *in vitro.* A) Schematic illustration of the skeletal muscle differentiation protocol. B) Myoblasts/myotubes cultures, after dissociation, immunostained for desmin (red) and skeletal myosin (green), show differentiated myofibres 1, 4, 8, 14, 26 and 36 days *in vitro*. Scale bar =100 μm C) A high-resolution image shows skeletal myosin expression in ES cell-derived myofibres after 36 days *in vitro.* Scale bar =20 μm

A)

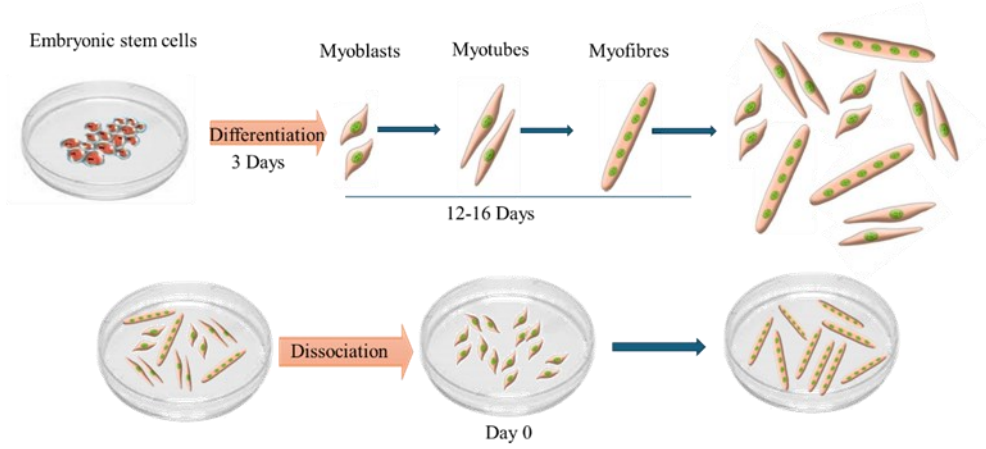
Embryonic stem cells
Myoblasts
Myotubes
Myofibres
Differentiation
3 Days
12-16 Days
Dissociation
Day 0

B)

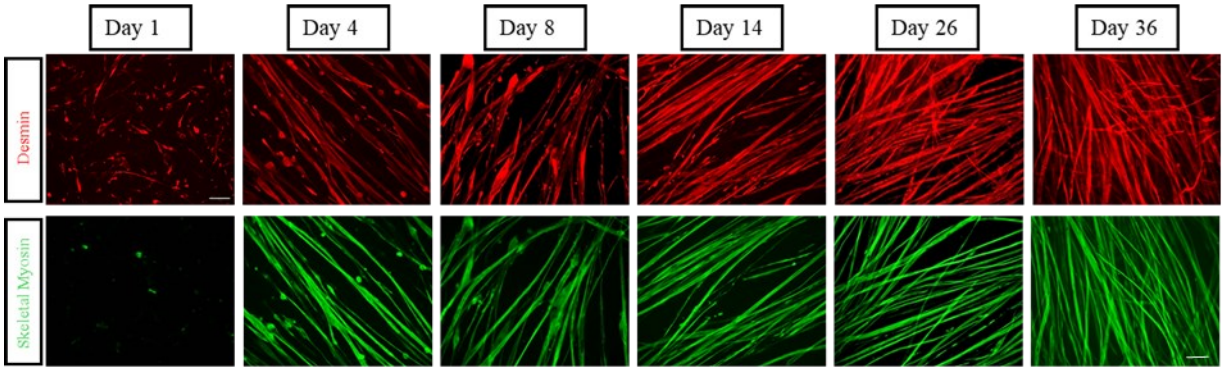
Day 1
Day 4
Day 8
Day 14
Day 26
Day 36
Desmin
Skeletal Myosin

C)

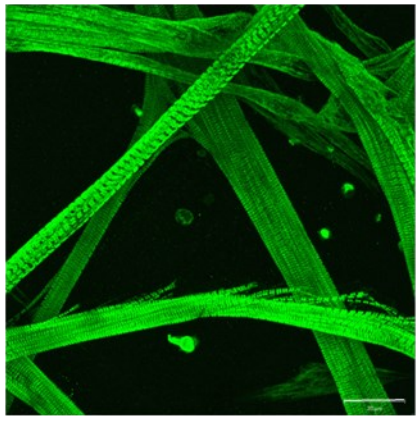

Figure 2.2. Generation of tdTomato and ChR2 expressing myotubes from mouse ES Cells. ES cell-derived myoblast/ myotube culture, expressing tdTomato (red) and immunostained for skeletal myosin (green) and Hoechst (purple). Scale bar =100 μm

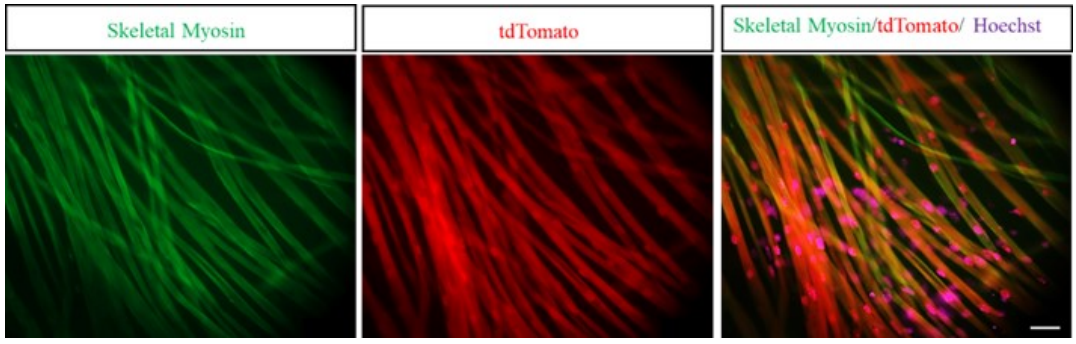
Skeletal Myosin
tdTomato
Skeletal Myosin/tdTomato/ Hoechst

Figure 2.3. Introduction of AAV-PHP.eB-CAG-ChR2-EYFP into ES cell-derived myotubes. ES cell-derived myotube culture expressing EYFP, the fused fluorescent reporter of ChR2, through transduction with AAV-PHP.eB-CAG-ChR2-EYFP vectors. Scale bar =100 μm

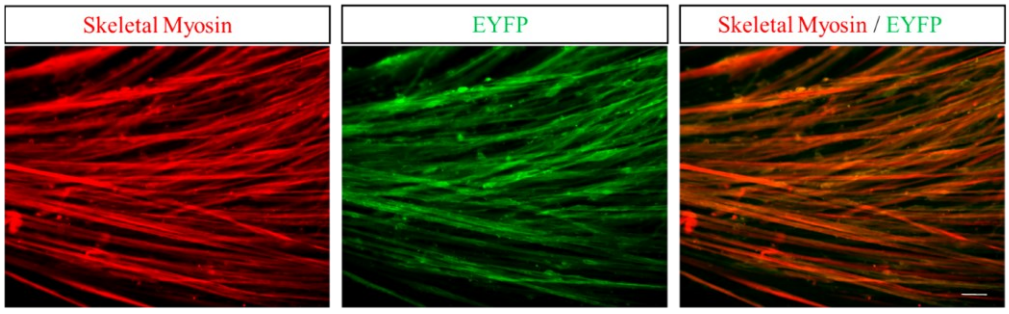
Skeletal Myosin
EYFP
Skeletal Myosin / EYFP

Figure 2.4. ES derived myotubes are fast-twitch fibres. ES cell derived myotube culture, immunostained for fast (red) and slow (green) myosin shows that *in vitro* cultured fibres are fast-twitch fibres. Scale bar =100 μm

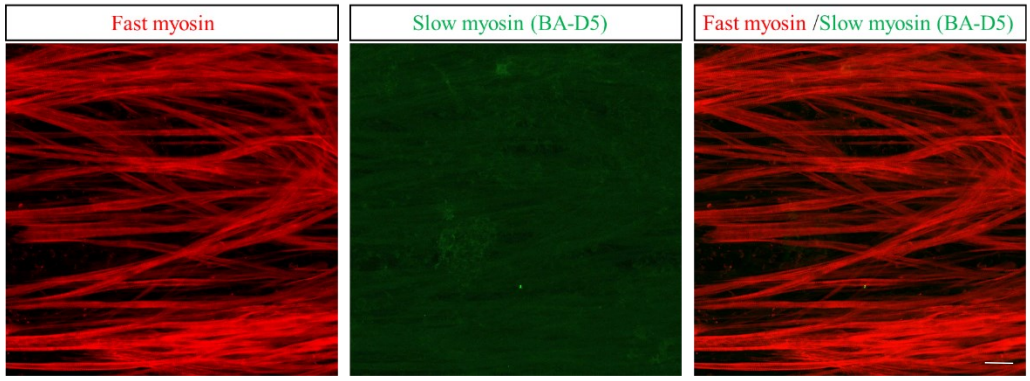
Fast myosin
Slow myosin (BA-D5)
Fast myosin /Slow myosin (BA-D5)

Figure 2.5. Developmental analysis of ES cell-derived myoblasts/ myotubes. **A)** Schematic illustration of the timeline of the developmental analysis **B)** ES cell-derived myoblasts/ myotubes cultures immunostained for desmin (red) and skeletal myosin on days 1, 3, 5, 10, 13, and 15 after differentiation. Scale bar=100 μm **C)** Mean (± SD) percentage of the culture area covered by desmin and skeletal myosin expressing myoblasts/myotubes. (*P= 0.0019 day 1, *P = 0.0000 day 3 and *P = 0.0015 day 5 after differentiation; multiple unpaired t-test). **D)** ES cell-derived myoblasts/ myotubes cultures immunostained for Pax7 (green), Myo D (red), Hoechst (gray) and Myogenin (green) on days 1 and 15 after differentiation. Scale bar=50 μm **E)** Mean (± SD) percentage of the total cell numbers in the myoblasts/ myotubes culture expressing pax7, Pax7/ MyoD, MyoD/ myogenin and myogenin on days 1, 5, 10 and 15 after differentiation. Day 1 (*** P = 0.0002), day 5 (** P = 0.0089), day 10 (****P<0.0001, ***P= 0.0001 and *P= 0.0451 Pax7/ MyoD vs MyoD/ myogenin and *P= 0.0266 Pax7/ MyoD vs myogenin) and day 15 (**P=0.0042, *P= 0.0443 Pax7/ MyoD vs MyoD/ myogenin and *P= 0.0184 Pax7/ MyoD vs myogenin; multiple comparisons ANOVA test)

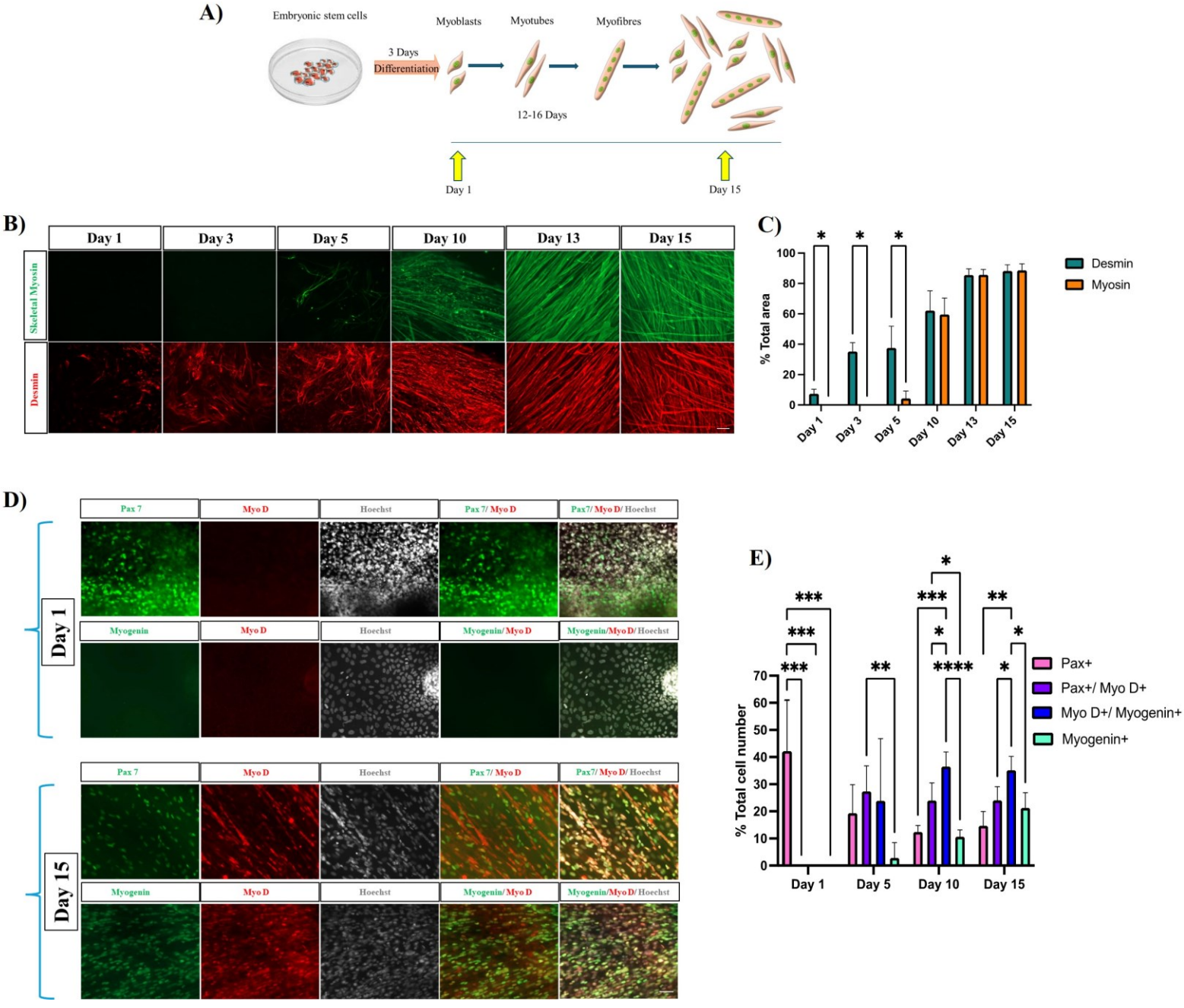
A)
Embryonic stem cells
3 Days
Differentiation
Myoblasts
Myotubes
Myofibres
12-16 Days
Day 1
Day 15
B)
Day 1
Day 3
Day 5
Day 10
Day 13
Day 15
Skeletal Myosin
Desmin
C)
% Total area
Desmin
Myosin
D)
Pax 7
Myo D
Hoechst
Pax 7/ Myo D
Pax7/ Myo D/ Hoechst
Day 1
Myogenin
Myogenin/ Myo D
Myogenin/Myo D/ Hoechst
Day 15
E)
% Total cell number
Pax+
Pax+/ Myo D+
Myo D+/ Myogenin+
Myogenin+

Chapter 3: Anatomy and Function of Grafted Embryonic Stem Cell-Derived Myoblasts into the Irradiated/ Notexin Injected Muscles

3.1 Abstract

SCIs, PNIs, and motoneuron diseases such as Amyotrophic Lateral Sclerosis (ALS) cause permanent paralysis when the affected skeletal muscles are completely and permanently denervated due to motoneuron death or muscle atrophy. Even with advances in neuroprosthetics, achieving functional movement of completely denervated muscles remains extremely difficult because non-innervated muscles cannot be activated via electrical stimulation. To address this issue, previous work in our lab demonstrated that muscle function could be activated through blue light stimulation rather than neural stimulation in transgenic mice expressing ChR2. In this study, we explored innovative strategies to express genes in skeletal muscles without relying on transgenic technology, aiming to restore muscle function using optogenetic techniques. For this purpose, shank muscles in adult mice were subjected to a high dose of gamma irradiation followed by notexin injection into the soleus muscle. This procedure kills all the soleus muscle fibres and resident satellite cells. Later, the injured muscles were injected with mouse ES cell-derived myoblasts expressing a gene of our choice. Our results showed that transplanted tdTomato-expressing myoblasts, used as an indicator for cell engraftment, survived the transplant procedure, fused to form multinucleated muscle fibres, and restored muscle mass and whole muscle CSA. Interestingly, the transplanted soleus muscles contained significantly more muscle fibres compared to non-operated muscles, but the fibre size was significantly smaller than normal. Degenerating muscles transplanted with ChR2-EYFP expressing ES cell-derived myoblasts were also completely repopulated with exogenous muscle fibres. As a result, optical stimulation of the transplanted muscles produced the same contractile forces as direct neural stimulation, and the force could be controlled by varying light intensity and duration. Additionally, transplanting ES cell-derived myoblasts transduced with AAV-PHP.eB-CAG-ChR2-EYFP facilitated muscle contraction in response to blue light. Overall, this study demonstrates that regenerated muscles *in vivo* through ChR2-expressing ES cell-derived myoblast engraftment could produce optical force and restore muscle function without the need for nerve stimulation.

3.2 Introduction

SCIs and PNIs are serious medical issues causing functional disabilities. These injuries disrupt the neural pathways essential for motor control, leading to muscle atrophy and loss of function (Redondo-Castro & Navarro, 2013; Weng et al., 2018). SCI is particularly debilitating, causing the loss of central control over peripheral nerves below the injury site and profound sensory, motor, and autonomic dysfunction (Gorgey & Dudley, 2007; X. Xu et al., 2023). This frequently manifests as permanent muscle paralysis and severe immobilization due to the apoptosis of some motoneurons, subsequent skeletal muscle denervation, extensive atrophy, and fibrous tissue formation (X. Xu et al., 2023). Motor axons in PNIs, unlike the ones in the CNS, can regenerate following proximal nerve injuries such as BPIs (Fu & Gordon, 1997; Gaudet et al., 2011; T. Gordon, 2020; T. Gordon & Borschel, 2017; Lieberman, 1971). However, the slow axon regeneration rate (approximately 1 mm per day in humans) means that it takes more than a year for the regenerating nerves to reach the target muscles. By that time, the muscles will mostly be atrophied and replaced by fat. This prolonged denervation has a destructive, irreversible effect on the muscles, reducing functional recovery by up to 90% (Fu & Gordon, 1995).

In both scenarios, paralysis and loss of function dramatically limit mobility and essential movements in patients. While the ultimate goal for treating paralysis is a complete cure, achieving partial improvements may be a more practical approach to immediately enhancing the quality of life (Anderson, 2004; Collinger et al., 2013). Surveys indicate that regaining hand movement and grasping function is the highest priority for quadriplegic patients. Thus, finding ways to restore meaningful function to muscle groups,

like those controlling hand movement, can greatly enhance the life quality and offer a degree of independence in these patients (Anderson, 2004).

Previous strategies aimed at restoring hand muscle functionality, such as neuroprosthetics that combine orthoses (non-surgical, wearable devices) with electrical stimulation to activate peripheral nerves innervating paralyzed muscles, have not been very successful. These devices rely on the stimulation of peripheral nerves that still innervate the paralyzed muscles (Prochazka et al., 2001). However, in SCI and PNIs, muscles are often permanently denervated, leaving no nerves available for stimulation (C. K. Thomas et al., 1997). Another promising strategy is transplanting MNs, which can restore some motor function by reinnervating the muscles (Yohn et al., 2008). It has been shown that transplanting MNs expressing ChR2 after reinnervation can produce some contractile force (Bryson et al., 2014). But again, this approach is not helpful when the muscle is atrophied due to late reinnervation, and axons need healthy muscle fibres to form NMJs (Fu & Gordon, 1995).

A possible strategy to restore meaningful function to completely and permanently denervated muscles is to replace the endogenous muscle fibres with those that can be optically activated through ChR2 expression. In previous studies in our lab, it was shown that transgenic expression of ChR2 directly into skeletal muscle fibres enables functional muscle contraction in response to blue light illumination and chronic activation of denervated muscles, reduces muscle atrophy (Magown et al., 2015).

Here, we developed novel approach to express genes in denervated skeletal muscles without relying on transgenic technology. In this study, the soleus muscles in mice were

irradiated to prevent native fibre regeneration after injury and subsequently destroyed via injection of notexin, a venom from the Australian tiger snake, or destroyed through notexin injection alone, before injecting ES cell-derived muscle fibres (i.e., satellite cells) into the remnants of the soleus muscles *in vivo*. Initially, transplanting tdTomato-expressing myoblasts into the injured muscles served as an indicator of cell engraftment and muscle regeneration with exogenous myoblasts. This revealed the formation of muscle fibres from ES cell-derived myoblasts in the irradiated/notexin-injected muscles, while only a few transplanted cells survived in the non-irradiated/notexin-injected muscles, as the native satellite cells regenerated muscle fibres, and there was no fusion between the transplanted and endogenous fibres. Interestingly, the muscles transplanted with tdTomato-expressing myoblasts exhibited elongated yet smaller muscle fibre size, but a larger muscle mass compared to the control muscles in the contralateral leg.

The ultimate goal of this study was to replace endogenous muscle fibres with exogenous muscle fibres expressing ChR2. Transplanting ChR2-expressing ES cell-derived myoblasts into the degenerating muscles successfully repopulated the muscle with exogenous fibres. As a result, optical stimulation of the transplanted muscles produced the same contractile forces as direct neural stimulation. Finally, we examined transplanting ES cell-derived myoblasts transduced with AAV-PHP.eB-CAG-ChR2-EYFP into the degenerating muscle, which led to muscle contraction upon optical stimulation, though producing lower force compared to nerve stimulation. Overall, this study presents a novel promising method to activate denervated muscles without the need to stimulate the nerves.

3.3 Materials and Methods

3.3.1 Mice

In this study, male and female C57BL/6J mice, weighing between 25 and 30 grams and sourced from Charles River Laboratories, were utilized. These mice were accommodated at the Carleton animal care facility within Dalhousie University, where they were maintained under a controlled environment featuring a 12-hour light/12-hour dark cycle having unlimited access to food and drink.

3.3.2 Gamma Radiation

Animals underwent anesthesia through an intraperitoneal injection consisting of Ketamine (117 mg/kg) and Xylazine (13 mg/kg). Then animals were carefully positioned within a lead shield that was specifically designed with a small opening. This opening allowed only one leg to extend outside the container, ensuring that the rest of the animal's body was fully protected and immobilized. Then the exposed leg was securely fastened with tape to prevent any movement during the procedure.

This setup was subsequently placed in the Gamma Cell 3000 Elan cesium-137 irradiator. The animals were then subjected to a single dose of 18 Gy, meticulously administered to the exposed shank. At the end of the session, 0.4 ml of injectable 0.9% Sodium Chloride was subcutaneously injected into the animals to prevent dehydration. The mice cages were placed on a heating pad to minimize pain, and clear H_2O hydrogel was provided as an additional source of hydration

3.3.3 Myoblasts Preparation for the Transplantation

The muscle media (DMEM supplemented with 10% horse serum and 1% Penicillin-Streptomycin solution) for 15-day-old ES cell-derived myoblast cultures were removed. After a 10-minute wash with EDTA (Gibco), 2X Trypsin EDTA and 10X DNase were added, and the cells were triturated. The cell suspensions were then centrifuged, and the resulting cell pellets were resuspended in 1X DNase and kept on ice for transplantation.

3.3.4 Surgeries

All surgeries were conducted in aseptic condition in compliance with the guidelines approved by the Dalhousie University Animal Care Committee, aligning with the principles set forth by the Canadian Council on Animal Care.

The day after leg irradiation mice underwent anesthesia using a mix of isoflurane and oxygen. A precise incision was made on the posterior aspect of the lower hindlimb to access the soleus muscle in mice. The gastrocnemius muscle was carefully retracted to expose the soleus muscle, into which 3µl of notexin (Notechis scutatus scutatus, Sigma) with a concentration of 1.5µg/ µl was injected at various points along the muscle. Subsequently, the area surrounding the soleus muscle was gently cleansed using a 0.9% Sodium Chloride injection solution, ensuring that any excess fluids were absorbed with cotton-tipped applicators. The incision was then sutured closed to facilitate proper healing.

For the cell transplantation process, the sutures from the previously made incision were carefully removed two days after the notexin injection injury. Following this, the gastrocnemius muscle was retracted again, and 5 µl of myoblast suspension, with a concentration of 1×10^5 cells/µl, was administered at multiple sites along the injured soleus

Immediately after each surgery and the following day, 5 mg/kg of Meloxicam to minimize pain and inflammation, and 0.4 ml of injectable 0.9% Sodium Chloride to prevent the animal's dehydration, were injected. Also, to support cell transplantation and minimize the risk of rejection, the mice were administered a daily dose of cyclosporine (NOVARTIS) at a dosage of 10 mg/kg. This subcutaneous injection began one day before the cell implantation and continued daily until the end of the experiment.

3.3.5 *Ex vivo* Soleus Muscle Isometric Tension

Initially, a mixture of isoflurane and oxygen was used to anesthetize the mice. The soleus muscle, along with its innervating nerve, was promptly dissected and transferred into a recording chamber coated with Sylgard (Dow Corning), continuously supplied with oxygenated Tyrode's solution. This solution consisted of 125 mM NaCl, 24 mM $NaHCO_3$, 5.37 mM KCl, 1 mM $MgCl_2$, 1.8 mM $CaCl_2$, and 27.75 mM dextrose. The muscle's proximal tendon was securely fixed, and a thin thread was knotted to the muscle's distal tendon and hooked to a force transducer (FT 03; Grass Technologies).

A glass suction electrode with a fine tip was used to apply electrical current to the muscle's innervated nerve. This current was generated using an S88 stimulator (Grass Technologies), which was electrically isolated from the ground using a stimulus isolation unit (PSIU6; Grass Technologies). The length of the muscle was adjusted to achieve maximum isometric contraction. Neural twitch forces were recorded for 2.5 ms using a Digidata 1322A analog-to-digital board and AxoScope version 10.2 software (Molecular Devices).

Optical stimulation was executed using a blue (470 nm) Rebel Star O Drop-in LED by Luxeon Star (Quadica Development Inc.), positioned immediately above the muscle. The LED's current and voltage were regulated by a variable DC power supply (Micronta), which was linked to a solid-state relay and activated by the S88 stimulator. Optical twitch forces were recorded in varying durations of 1 ms to 500 ms.

3.3.6 Intracellular Electrophysiology of Myofibres

After isometric tension measurement, muscles were pre-incubated for 60 minutes in an oxygenated Tyrode solution containing 5μM μ-conotoxin (μCTX) GIIIB (Alomone Labs, Jerusalem, Israel) to inhibit muscle spontaneous contractions. Muscles were then transferred to a Sylgard-coated recording chamber, pinned and perfused with μCTX-free oxygenated Tyrode solution for the duration of the recording.

Optical stimulation was achieved with blue, fluorescent light from Zeiss Examiner D.1 microscope triggered through a Grass S88 stimulator and controlled with SlideBook6 software. Muscle fibres were stimulated by blue light for varying durations of 1 to 1000 ms with the natural density filter set to 75, and to varying intensity by applying natural density filters from 1 to 250 for a set, 50 ms duration. Responses to light stimulation were monitored by MultiClap 700B amplifier, digitized with Digidata 1440A, and processed with Clapex 10.3 (Molecular Devices) software. Collected data were analyzed with the MiniAnalysis (SynaptoSoft, Decatur, GA) program.

3.3.7 Muscle Immunohistochemistry and Histology

After measuring the muscles mass, they were affixed at their physiological length in cryomolds using insect pins. Before sectioning, the muscles were subjected to imaging

under the microscope to check for red or green fluorescence. The muscles were then submerged in a mixture of 20% sucrose (Fisher Chemical)/ phosphate buffered saline (PBS) and tissue freezing medium O.C.T. Compound (Tissue Tek) in a 1:2 ratio. Following this preparation, the muscles were rapidly frozen in a 2-methylbutane (Sigma-Aldrich) bath that had been cooled with liquid nitrogen. The frozen muscles were then preserved at -80 °C for at least 24 hours before sectioning.

For cross-sectioning, the muscles were sliced using a cryostat (Leica) to a thickness of 20 μm and then mounted onto microscope slides. The slides were subsequently fixed with 4% PFA for 15-20 minutes, followed by three rinses with PBS. The sections were incubated with antibodies in 1% BSA (VWR) in PBS plus 0.5% PBS-Triton solution. Overnight, the sections were incubated with Wheat Germ Agglutinin (WGA) conjugated to Alexa Fluor 488 antibody (1:1000, Thermo Fisher Scientific) at room temperature. After three washes with PBS, 0.1 μg/ml Hoechst 33342 (Sigma-Aldrich) in PBS to stain nuclei was administered to the slides for 10 minutes and washed once more with PBS. Finally, to preserve the tissue and prevent fading, slides were mounted using a mounting solution containing 50% glycerol/ PBS and 0.03 mg/ ml ρ-Phenylenediamine.

For muscle teasing, the muscles were pinned at their physiological length and fixed in 4% PFA for 20 minutes. The samples were then rinsed three times in PBS and permeabilized with methanol at -20 °C for 6 minutes. Following another three washes with PBS, the muscles were firmly affixed with insect pins in a Sylgard-coated dish submerged in PBS for examination under a dissecting microscope. One tendon was detached to allow the muscle fibres to be delicately teased into individual fibres using forceps.

The tissues were not stained for tdTomato, and the red fluorescence observed in the images is due to the natural fluorescence of tdTomato-expressing muscles.

For the Hematoxylin and Eosin (H & E) staining of the muscle cross-section slides, the process began with fixation using 4% PFA for 15 minutes. Following this, the slides were dipped into a Xylene bath four times to clear the tissue. Next, they were sequentially immersed in three baths of 100% ethanol, followed by three baths of 95% ethanol, and once in 70% ethanol to dehydrate the tissue. After dehydration, the slides were rinsed with running water and then inserted into Harris Hematoxylin stain for 2 minutes to stain the nuclei. Another wash with running water followed, after which the slides were dipped into Scott's H_2O solution, rinsed again, quickly dipped into 0.2% nitric acid, and immediately rinsed once more. Before staining with Eosin Y, the slides underwent another dip in Scott's H_2O and a water rinse. The slides were then dipped quickly 20 times into the Eosin Y stain bath to stain the cytoplasm. This was followed by sequential dipping twice in 70% ethanol, twice in 95% ethanol, and twice in 100% ethanol for dehydration. Finally, the slides were dipped four times in Xylene to clear the tissue, then left to dry under a fume hood before being mounted.

3.3.8 Imaging

For imaging purposes, either an upright microscope (Leica Instruments) equipped with Zen-Blue software (Zeiss) or a laser scanning confocal microscope (Zeiss LSM 880) using Zen-Black software (Zeiss) was utilized. The Z stacks acquired by the confocal microscope were processed into the final images using Fiji (ImageJ) software.

3.3.9 Myofibre Number Quantification

Using the Zen-Blue software, the CSAs of the entire muscle and individual myofibres stained with WGA and Hoechst were measured. For each examined muscle, at least 10 CSAs of the whole muscle and 50 CSAs of individual myofibres were assessed. To quantify the number of myofibres in each muscle, the ratio of the average whole muscle CSA to the average muscle fibre CSA was calculated.

3.3.10 Statistical Analysis

Statistical analysis and graph creation were performed using GraphPad Prism (Prism 10) software. All results were presented as the mean ± standard deviation and were considered statistically significant at $P < 0.05$. T-tests were conducted for comparisons between two groups, while ANOVA tests were used to compare means across more than two groups.

3.4 Results

3.4.1 Lack of Fusion between tdTomato-Expressing ES Cell-Derived Myoblasts and Endogenous Myoblasts *in vivo*

To investigate if transplanted tdTomato-expressing myoblasts are capable of fusing with endogenous myoblasts to form a chimeric regenerated muscle, notexin was first injected into the host muscle. This venom degrades muscle fibres and induces a necrotic response in the muscle without damaging muscle satellite cells, so triggers and facilitates rapid muscle regeneration (Dux et al., 1993; Huard et al., 1994; Vilquin et al., 1995). Two days after the injury, ES derived myoblasts were injected into the damaged muscle (n=4). One month following the injury and myoblast transplantation, the muscles had completely regenerated and appeared healthy, as shown in (Fig 3.1A). These regenerated muscles

showed no difference in size post-regeneration compared to unoperated control muscles. There were no significant differences in wet muscle weight (15.05 ± 3.3 mg for unoperated vs. 18.18 ± 3.0 mg for notexin/transplanted), the ratio of wet muscle weight to body weight (0.46 ± 0.09 for unoperated vs. 0.56 ± 0.06 for notexin/transplanted), or muscle CSA (1.58 ± 0.06 mm² for unoperated vs. 1.68 ± 0.09 mm² for notexin/transplanted) (P=0.2199, P=0.1493, and P=0.0546, respectively) (Fig. 3.1B-D). Fluorescent microscopy of the muscle before being subjected to the cross sectioning, revealed no red fluorescence, indicating an absence of tdTomato expression (Fig 3.1E). Examination of the muscle CSA showed that the muscle fibres were indeed regenerated, as evidenced by the presence of central nuclei (visualized in blue using Hoechst staining)—a hallmark of muscle regeneration known for over 50 years (Fig 3.1F). In studies using animal models with induced injuries like toxin injections, researchers observed patterns of centrally located nuclei within fibres of small diameter, reminiscent of embryonic stages. This observation supports the notion that muscle fibre regeneration mirrors the original development process of fibres, with nuclei eventually migrating towards the periphery of the fibre during the regeneration phase and fibre maturation (Meyer, 2018). However, no red fibres were detected in the regenerated muscle cross-sections, and only a small number of single red cells with nuclei located between endogenous muscle fibres were identified, which might represent single transplanted myoblasts that survived without fusing into the host muscle myoblasts (Arrows) (Fig 3.1F). There was no significant difference in muscle fibre CSA between unoperated and non-fluorescent regenerated fibres (2237 ± 699 μm² and 2339 ± 1101 μm², respectively; P=0.6827), nor in the total number of muscle fibres (663.6 ± 145 vs. 785.1 ± 170, respectively; P=0.4245). However, the red single cells exhibited a 12-times smaller fibre CSA (184.1 ± 85 μm^2, $P < 0.0001$) and a significantly lower number

(Average = 20.3 ± 5.7 cells per CSA, $P < 0.0001$) compared to non-fluorescent control and regenerated fibres (Fig 3.1G, H). All these data suggest that *in vitro* cultured myoblasts were generally unable to engraft and fuse with the endogenous myoblasts during regeneration, so mostly die off, with a few surviving as single muscle cells rather than fusing and forming hybrid myofibres.

3.4.2 Gamma Radiation and Subsequent Notexin Injection Impede Muscle Fibre Regeneration by Destroying Endogenous Satellite Cells

To address the issue of endogenous satellite cells' activation suppressing the growth of transplanted cells in the host muscle, we opted to inactivate the native satellite cells by irradiating the mouse leg. Previous studies have shown that inhibiting the proliferation of endogenous myogenic cells can enhance the engraftment of exogenous muscle cells into pre-injured muscle (Huard et al., 1994; Vilquin et al., 1995; Wernig et al., 2000).

In our experiment, one leg of each mouse was exposed to 18 Gy of gamma radiation, followed 24 hours later by an injection of notexin (n=4). 30 days after the radiation and notexin-induced injury, the extracted muscle appeared markedly thinner and paler compared to the unoperated control muscle from the contralateral leg, with no signs of regeneration observed (Fig 3.2A). H&E staining of muscle cross-sections revealed the absence of muscle fibres in the irradiated and notexin-injected muscle, with only mononuclear cells present, likely phagocytes and muscle-derived cells as suggested by Dux et al. (1993) (Fig 3.2B). As anticipated, the irradiated-notexin-injected soleus muscles showed significant weight loss compared to the unoperated soleus muscles one-month post-injury. Specifically, wet muscle weight was reduced (unoperated: 12.5 ± 1.7 mg vs. irradiated-notexin-injected: 7.05 ± 2.2 mg; P=0.0090), as was the muscle weight-to-body

weight ratio (unoperated: 0.61± 0.11 vs. irradiated-notexin-injected: 0.34 ± 0.11; P=0.0157) (Fig. 3.2C, D). These results suggest that irradiation prior to notexin-induced injury can effectively suppress the activation and proliferation of original satellite cells and muscle regeneration post-injury.

3.4.3 Engraftment and Muscle Fibre Formation of tdTomato-Expressing ES Cell-Derived Myoblasts in Irradiated/Notexin-Injected Muscles

To investigate whether inhibiting endogenous myogenesis could enhance the engraftment of transplanted myoblasts into injured muscle, $5x10^5$ tdTomato-expressing myoblasts were injected into the damaged soleus muscle 48 hours following notexin injection (n=7). One-month post-transplantation, the soleus muscles were extracted and assessed. The operated muscles appeared regenerated and healthy and were notably larger in size compared to the unoperated muscles (Fig 3.3A). Fluorescent microscopy revealed extensive red fluorescence in these regenerated muscles, indicating successful regeneration with tdTomato-expressing myoblasts (Fig 3.3B). Detailed examination of one of these muscles, which was teased apart, showed tangled and individual tdTomato-expressing muscle fibres from a transplanted soleus muscle (Fig 3.3C, D). The transplanted muscles demonstrated a statistically significant increase in wet weight (unoperated: 15.22 ± 3.2 mg vs. transplanted: 24.4 ± 5.9 mg; P=0.0221), as well as an increase in muscle weight relative to body weight (unoperated: 0.46 ± 0.06 vs. transplanted: 0.99 ± 0.2; P=0.0442). Additionally, the transplanted muscles exhibited a considerably larger muscle CSA only covered by red cells (unoperated: 1.53 ± 0.09 mm^2 vs. transplanted: 1.765 ± 0.19 mm^2; P= 0.0207). These findings underscore a robust enhancement in both the mass and structural dimensions of the transplanted soleus muscles following transplantation (Fig 3.3E-G).

Collectively, these results demonstrate the successful *in vivo* engraftment of ES-cell-derived myoblasts into the mouse soleus muscle after irradiation and notexin injection.

3.4.4 tdTomato Expressing Myoblasts Increase Muscle Mass with Red Fluorescent Fibres Smaller in Size but Higher in Number Compared to the Unoperated Muscle Fibres

Cross sections of the regenerated muscles displayed a predominance of red fluorescent fibres throughout most of the transplanted soleus muscle, while no red fibres were observed in the cross sections of the unoperated muscles (n=3) (Fig 3.4A). The average CSA of the transplanted muscles, predominantly consisting of tdTomato-expressing red fibres, covered 78.6% ± 13.6 of the total muscle CSA (Fig 3.4B). A notable observation was made when comparing the sizes of muscle fibres between the transplanted and unoperated muscles; there was a substantial difference in fibre sizes. Specifically, the CSA of tdTomato-expressing fibres was 4.6 times smaller than the unoperated muscle fibres (unoperated: 2237 ± 699 μm^2 vs. transplanted: 480.4 ± 259 μm^2; $P<0.0001$) (Fig 3.4C, D). The distribution of muscle area sizes is detailed in Figure 3.4E. On the other hand, the number of red fluorescent fibres in the CSA of the transplanted muscles was 5.5 times higher than in the unoperated muscles (unoperated: 663.6 ± 145 vs. transplanted: 3676 ± 637; $P<0.0001$) (Fig 3.4F). Overall, these results indicate that although the red muscle fibres are significantly smaller in size than those in the unoperated muscles, there is a higher number of these fibres present within the transplanted muscles, which contributes to an increased overall muscle mass in the regenerated tissues.

3.4.5 Engraftment of ChR2-EYFP Expressing Myoblasts into Irradiated and Notexin-Injected Soleus Muscles

Following the successful transplantation of tdTomato-expressing myoblasts into irradiated/notexin-injected soleus muscles, which resulted in muscle regeneration with exogenous cells, we investigated the transplantation of ChR2-EYFP expressing myoblasts with the aim of creating light-activated muscles (n=6). The muscles were extracted between one- and two-months post-cell injection. The transplanted muscles appeared regenerated and displayed similar weight and colour compared to unoperated muscles (Fig 3.5A). Fluorescent microscopy revealed the presence of ChR2-EYFP expressing fibres, indicated by green fluorescence in the transplanted muscles (Fig 3.5B). Interestingly, unlike the tdTomato-expressing muscles, there was no significant difference in wet muscle weight between transplanted and unoperated muscles (unoperated: 16.25 ± 1.8 mg vs. transplanted: 15.20 ± 4.9 mg; P=0.6506). Similarly, the muscle weight-to-body weight ratio showed no significant difference (unoperated: 0.43 ± 0.05 vs. transplanted: 0.39 ± 0.1; P=0.5052) (Fig 3.5C, D). This discrepancy might be attributed to the difference in the cell lines and qualities of the ES-cell-derived myoblasts expressing tdTomato and ChR2-EYFP. These results demonstrate that ChR2-EYFP-expressing myoblasts, similarly to tdTomato-expressing cells, are capable of regenerating the irradiated/notexin-injected muscles, thereby imparting new exogenous characteristics to them.

3.4.6 Contractile Responses in ChR2- EYFP Expressing Muscle Fibres: Effects of Optical Stimulation Intensity and Duration

ChR2 functions as a light-sensitive ion channel that activates under blue light exposure at approximately 470 nm, inducing the isomerization of all-trans-retinal to 13-cis-retinal

within the channel. This molecular change leads to the opening of the channel pore, allowing cations, predominantly protons, to flow down their electrochemical gradient across the cell membrane, resulting in cell depolarization. If the depolarization reaches a sufficient level, it can trigger an action potential (Yang et al., 2019). To investigate if muscles regenerated with ChR2-EYFP expressing cells could contract in response to blue light stimulation independently of neural inputs, soleus muscles were isolated and connected to a force inducer. Positioned closely, a 470 nm LED light inducer stimulated the muscles at various light intensities and durations (n=6). Figure 3.6A depicts the positioning of a blue LED light closely directed toward the muscle and activating the ChR2-expressing muscle fibres. Successful muscle contraction in response to light illumination is documented in Supplementary Video 3.1 (see Appendix Two). The graph in Figure 3.6B displays muscle twitch forces in response to nerve stimulation (pink) and 1, 10, and 100 ms optical stimulations at 24mV light intensity.

Previous research in our lab demonstrated that in transgenic Sim1-Ai32 mice, where ChR2-EYFP is expressed in skeletal muscle fibres, optical stimulations longer than 5 ms do not synchronously depolarize all myofibres. Myofibres closer to the light source depolarize earlier than those further away, resulting in smaller but prolonged EMG measurements (Magown et al., 2015). Additionally, the gradation in force is attributed to an increase in the number of muscle fibres activated and the contractile strength of each fibre (Henneman et al., 1965b). This information suggests that the deflections observed in 10 ms and 100 ms stimulations (indicated by asterisks) could be due to the delayed activations of certain myofibre groups.

We also discovered that muscle contractile forces vary with different light pulse durations and intensities. A comparison of neural muscle twitch forces (9.88 ± 4.2 mN) versus optical muscle twitch forces at durations of 1 ms (1.08 ± 0.4 mN), 5 ms (4.23 ± 3.8 mN), 10 ms (6.36 ± 3.8 mN), 20 ms (8.15 ± 3.9 mN), 50 ms (10.57 ± 5.7 mN), 100 ms (11.03 ± 6.08 mN), 200 ms (10.8 ± 5.1 mN), and 500 ms (9.32 ± 4.3 mN) with 24 mV light pulses is shown in Figure 3.6C; ($P=0.0154$, $P= 0.2100$, $P=0.6776$, $P=0.9879$, $P>0.9999$, $P=0.9998$, $P>0.9999$, $P>0.9999$, respectively). Twitch forces induced for 50 ms and longer, produced contractile forces nearly equivalent but higher to those generated by neural stimulation. As depicted in Figure 3.6D, increasing the light intensity with a 50 ms stimulation time caused a rise in muscle contractile force.

Further investigation into the electrical properties of single ChR2-EYFP expressing myofibres revealed that myofibre depolarization increases with light intensity up to a certain point and then plateaus. There is significant variability in depolarization among different fibres, potentially caused by varied levels of ChR2 expression across myofibres or inconsistencies in light penetration and delivery across the muscle, which means muscles in deeper positions may receive less stimulation (Fig 3.6E). The average myofibres depolarization change with increasing light intensity is presented in Figure 3.6F. Also, the duration and magnitude of depolarization achieved by increasing stimulation length at constant light intensity is shown in Figure 3.6G, H. Notably, while the duration of depolarization increases with longer light stimulation periods, the amplitude of depolarization remains unchanged (Fig 3.6G, H). One possible reason is that even with a 1ms stimulation duration, myofibres reach their maximum depolarization capacity, making longer stimulation periods ineffective in increasing the depolarization magnitude.

When comparing the depolarization magnitudes of individual myofibres in response to increased light intensity (Fig. 3.6E), we observe that the maximum depolarization is similar to what is achieved with a 1 ms stimulation. Another possible explanation for this phenomenon is the ChR2-mediated depolarization block, as described by Herman et al. (2014). In this context, extended light exposure silences, rather than activates, neurons expressing ChR2. This response to optogenetic stimulation varies among neuronal subtypes and is attributed to ChR2's nature as a cation-permeable membrane channel, which permits excessive cation influx, resulting in prolonged membrane depolarization in targeted neurons.

3.4.7 Optical Stimulation of Transplanted Muscles Expressing ChR2 via AAV-PHP.eB-CAG-ChR2-EYFP Transduction.

Recombinant adeno-associated viruses (rAAVs) are recognized as safe and have been extensively employed in both clinical trials and preclinical studies for gene therapy (Jiang et al., 2021; L. Li et al., 2023). The AAV-PHP.eB variant, derived from AAV9, exhibits enhanced penetration capabilities into the CNS and peripheral tissues, surpassing its progenitor serotype. These improvements are attributed to capsid modifications that enhance its ability to cross biological barriers such as the blood-brain barrier and muscle cell membranes (Chan et al., 2017). Although this AAV variant is primarily established for CNS transduction, recent findings by Jiang et al. (2021) indicate its efficient infection capabilities in mouse hindquarter muscle. In this experiment, we used AAV-PHP.eB vectors carrying the ChR2-EYFP gene to enable ChR2 expression in the muscle cells used for transplantation.

AAV-PHP.eB-CAG-ChR2-EYFP vectors were applied two days before transplantation to the myofibre culture *in vitro*. These myofibres were dissociated, turned into myoblasts, and transplanted into irradiated/notexin-injected mouse soleus muscles. Transplanted muscles were extracted one to two months after transplantation (n=3). Examination of the contractile force of these muscles under blue light stimulation demonstrated effective contraction, as shown in Supplementary Video 3.2 (see Appendix Two), although twitch force was slightly lower than that produced by neural stimulation (Fig. 3.7A). This reduction in force was particularly notable at shorter stimulation durations of 1 ms (0 mN), 5 ms (0.33 ± 0.5 mN), and 10 ms (4.03 ± 1.7 mN) compared to neural stimulation (15.87 ± 8.46 mN; P=0.0020, P=0.0024, P=0.0224, respectively). However, no significant differences in contraction force were observed between neural and light-evoked contractions at durations of 20 ms to 500 ms (20 ms: 7.56 ± 3.9 mN, P=0.1572; 50 ms: 9.9 ± 4.0 mN, P=0.4184; 100 ms: 9.53 ± 3.8 mN, P=0.3557; 200 ms: 9.56 ± 4.5 mN, P=0.4636; 500 ms: 9.5 ± 4.9 mN, P=0.4239) (Fig. 3.7B). Also, at a stimulation time of 50 ms, increasing the light intensity enhanced the muscle contractile force (Fig 3.7C). The lower force compared to neural stimulation could be due to incomplete infection of the muscle cells by the AAV vectors or dilution of the vectors during cell division and muscle fibre formation which should be investigated later. Overall, transduction of ES-cell-derived myoblasts with AAV-PHP.eB-CAG-ChR2-EYFP followed by their transplantation into injured muscles enabled successful muscle contraction in response to blue light illumination, in the absence of neural stimulation.

3.5 Discussion

Skeletal muscle functions are necessary for all movements, posture and breathing (Chromiak & Antonio, 2008), Therefore, losing them can significantly affect the quality of life and cause strong disabilities in people. SCIs and motor neuron diseases such as ALS often lead to muscle denervation, atrophy, and severe dysfunction due to the inability of CNS motor axons to regenerate naturally. On the other side, although in PNI such as brachial plexus injury motor axons can regenerate, albeit slowly, resulting in prolonged denervation and muscle fibrosis, which significantly hinders functional recovery (T. Gordon, 2020). Given these challenges, novel strategies are essential for improving patients' lives.

This study aimed to explore the innovative potential of restoring muscle function in completely denervated muscles by leveraging optogenetic technology and ES cell-derived muscle fibres. Specifically, the goal was to develop a technique for expressing ChR2 in muscle fibres to enable functional contraction upon blue light stimulation, providing a potential solution to restore function in selected groups of muscles where nerve regeneration and muscle reinnervation fall short.

Our initial experiments demonstrated that tdTomato-expressing ES cell-derived myoblasts injected into only notexin-injured muscles did not fuse with endogenous myoblasts to form chimeric regenerated muscle. Although the muscles regenerated and appeared healthy, the lack of red fluorescence indicated the absence of tdTomato expression. This suggests that the survival of endogenous satellite cells following induced muscle injury drives muscle regeneration through their activation and proliferation, and the endogenous muscle cells do not integrate with the transplanted tdTomato-expressing myoblasts. Some of the

transplanted myoblasts survived only as individual cells rather than integrating into host muscle fibres. All these findings indicate that *in vitro* cultured myoblasts generally fail to integrate and merge with endogenous myoblasts during the regeneration process. Instead of fusing and forming hybrid myofibres, most of the transplanted myoblasts die, with only a few surviving as isolated muscle cells.

To address the suppression of transplanted cells by endogenous satellite cells, we employed gamma radiation followed by notexin injection to inactivate native satellite cells before damaging the endogenous muscle fibres. This approach significantly inhibited muscle regeneration, as evidenced by the absence of muscle fibres and the presence of only mononuclear cells in irradiated and notexin-injected muscles. The transplantation of tdTomato-expressing myoblasts into irradiated/notexin-injected muscles resulted in successful muscle regeneration. These regenerated muscles displayed extensive red fluorescence, indicating the formation of muscle fibres from the transplanted cells and demonstrating robust engraftment. These findings suggest that preconditioning the muscle environment can enhance the integration of exogenous cells. These muscles exhibited a notable increase in muscle mass and CSA, with red fluorescent fibres predominantly covering the muscle tissue. Although these fibres were smaller than those in unoperated muscles, their higher number contributed to increased overall muscle mass.

ChR2-EYFP-expressing myoblasts also successfully regenerated muscle fibres in irradiated/ notexin-injected muscles, enabling optical control of muscle contractions through blue light stimulation. The generated contractile forces varied in response to different light intensities and durations, achieving forces nearly equivalent to the force produced by neural stimulation at the highest light pulse intensity (24 mv) and 50, 100 or

200 ms duration. Indeed, by applying single light pulses with varying durations and intensities, we observed that twitch forces increased with both higher light intensities and longer pulse durations to the certain point. This likely occurs due to the activation of more muscle fibres, as higher intensities and longer stimulation periods can recruit deeper fibres, indicating that muscle force can be controlled by adjusting light parameters. However, durations longer than 200 ms did not further increase the force, possibly because all fibres were already activated within 50 to 200 ms. This is in agreement with the results of Magown et al. (2015) and Bruegmann et al. (2015) from transgenic mice, where an increase in light intensity and duration is accompanied by larger depolarizations. Further investigation into the electrical properties of single ChR2-EYFP expressing myofibres revealed variability in depolarization magnitude among different fibres but reserving almost the same pattern, potentially caused by varied levels of ChR2 expression across myofibres or inconsistencies in light penetration and delivery across the muscle.

AAVs have been widely used in clinical trials and preclinical studies for gene therapy due to their safety and efficiency in gene delivery (Jiang et al., 2021; L. Li et al., 2023). Therefore, utilizing AAVs represents a promising and safe method for introducing the ChR2 gene into skeletal muscle fibres in humans, offering a reliable approach for potential therapeutic applications in future. The AAV-PHP.eB variant, derived from AAV9, exhibits enhanced penetration capabilities into the CNS and peripheral tissues (Chan et al., 2017). Additionally, Jiang et al. (2021), demonstrated its efficacy in delivering genes of interest into muscle fibres. Transducing ES-cell-derived myoblasts with AAV-PHP.eB-CAG-ChR2-EYFP and subsequently transplanting them into injured muscles facilitated muscle contraction in response to blue light illumination. Once again, increasing light

intensity and duration resulted in greater muscle force, with the maximum effective duration being 50 ms. The force produced by AAV-transduced muscles was slightly lower compared to neural stimulation, though this difference was not significant at longer light pulse durations (≥ 20 ms). This reduction in force could be attributed to several factors, including the possible dilution of vectors following myoblast division, incomplete infection of all muscle fibres by the vectors, or the tendency of AAVs to transfect satellite cells less efficiently than mature myofibres. These possibilities should be explored further in future studies. Despite this, the successful optical contraction demonstrates the potential of this approach for restoring muscle function in cases of severe nerve injury, bringing us closer to the possibility of clinical trials.

In recent years, optogenetic techniques have become increasingly significant in fundamental research, particularly within neuroscience (Gundelach et al., 2020) Numerous methods with potential future clinical applications have been identified, such as brain implants for treating Parkinson's disease (Gradinaru et al., 2009) and epilepsy (Paz & Huguenard, 2014), peripheral nerve stimulation to alleviate chronic pain (S. M. Iyer et al., 2014), methods to restore urinary bladder function (Mickle et al., 2019) and even optical stimulation of the cochlea (Jeschke & Moser, 2015).

However, while optogenetics has been widely used to activate different types of neurons, only a limited number of studies have explored muscle activation through ChR2 expression. Muscle optogenetic activation has been attempted both indirectly and directly. Indirect stimulation, which involves expressing ChR2 in the peripheral motoneurons innervating muscles, offers a promising alternative to electrical stimulation for specific therapeutic applications. This method leverages precise control over motor neuron

activation to reduce side effects and enhance performance (Gundelach et al., 2020). One significant limitation of electrical stimulation, for muscle control is its tendency to activate large, easily fatigable MUs before smaller, more endurance-capable ones, even at the lowest intensity settings. This recruitment pattern is the reverse of what naturally occurs in the body, where smaller units are engaged first. Optogenetic activation of small motoneurons can induce muscle contraction and maintain the physiological recruitment order of MUs (Llewellyn et al., 2010). Other examples of indirect optical muscle activation include restoring diaphragm electromyographic (EMG) activity following a SCI (Alilain et al., 2008) and controlling the ankle joint position through optical stimulation of peripheral nerves in the lower limb (Srinivasan et al., 2018).

Electrical stimulation or indirect optical activation of muscle fibres are ineffective when the fibres are completely denervated. Stimulating denervated muscles electrically requires much higher currents to induce contractions compared to neural stimulation. These high currents can lead to issues such as electrode corrosion, tissue damage, discomfort, and unintended stimulation of neighboring muscles (Plenk, 2011). In the case of optical activation of peripheral motor neurons, transplanting motoneurons expressing ChR2 to restore muscle function after injury is only feasible after the body's natural recovery process, which can take several months in humans (Calancie et al., 2004). This delay poses a significant challenge for motor neuron transplantation because prolonged axotomy or muscle denervation severely hinders motor axon regeneration and reinnervation of muscle fibres. Consequently, while motor neuron transplantation therapies derived from pluripotent cells show promise, these practical limitations may impede their clinical application (Fu & Gordon, 1995; Gutmann, 1948).

A very limited number of studies have explored direct optical activation of muscles, mostly focusing on cardiac muscle stimulation with potential applications for treating cardiac arrhythmias (Bruegmann et al., 2010; Crocini et al., 2016; Nyns, Poelma, Volkers, Bart, et al., 2019; Scardigli et al., 2018; Zaglia et al., 2015). The initial demonstration of direct optogenetic stimulation in skeletal muscles was achieved in Caenorhabditis elegans nematodes, which expressed ChR2 in their body wall and egg-laying muscles (Nagel et al., 2005). The first optical stimulation of skeletal muscle in mammals was conducted *in vitro* using immortalized myoblasts derived from mice (C2C12 cells), resulting in cell contraction (Asano et al., 2012). Later, expressing ChR2 in skeletal muscle was accomplished in transgenic mice by Magown et al. (2015) and Bruegmann et al. (2015). In both models, ChR2 was expressed across all skeletal muscles, specifically located at the sarcolemma and within the t-tubular system. The presence in the t-tubular system is crucial for efficient excitation–contraction coupling. This localization is significant because it is at the triadic junctions where L-type Ca^{2+} channels detect depolarization and trigger the release of Ca^{2+} from intracellular stores by directly opening ryanodine receptors type 1 (van Bremen et al., 2017). In addition to direct optical activation of skeletal muscles, Magown et al. (2015) demonstrated that daily light activation of chronically denervated muscles significantly attenuated muscle atrophy. In a recent study by Rousseau et al. (2023), engineered muscle tissue fabricated from ChR2-expressing C2C12 cells was engrafted into the TA muscle to help with VML. Another study of skeletal muscle activation via photostimulation involved diaphragm muscles, where direct injection of AAV9-CAG-ChR2 conducted by Benevides et al. (2022) caused EMG activity in paralyzed muscles and facilitated breathing.

Our study builds on the work of Magown et al. (2015) conducted previously in our lab, highlighting the potential of the optogenetic approach as a novel method for controlling skeletal muscle function and potentially bypassing the need for neural inputs in transgenic animals. In this study, we take a step closer to the ultimate goal of clinical application of optical activation of skeletal muscles by demonstrating successful direct activation of mouse skeletal muscles through the introduction of the ChR2 gene via transplantation of exogenous muscle cells. The feasibility of this method was validated using both transgenic ChR2-expressing cells and AAV-mediated transduction. Our results are consistent with previous findings, indicating that skeletal muscles expressing ChR2 in non-transgenic mice through cell engraftment can achieve functional contraction when optically activated. Additionally, muscle activation can be controlled by varying the light intensity and duration.

In summary, this study illustrates that the optogenetic approach offers an innovative method for controlling muscle function, potentially avoiding the need to neural stimulation. This advancement could significantly enhance the quality of life and slightly improve the level of independence for individuals living with paralysis.

3.6 Figures

Figure 3.1. tdTomato-expressing ES cell-derived myoblasts do not fuse with the endogenous myoblasts *in vivo*. A) Representative image of an unoperated soleus muscle alongside a soleus muscle transplanted with tdTomato expressing myoblasts following notexin injection injury, observed 30 days post-transplantation. B) Mean (± SD) wet weight values (P=0.2199), C) Muscle weight/body weight (P=0.1493) and D) CSA (P=0.0546) of the unoperated soleus and notexin injected/ tdTomato expressing myoblasts transplanted soleus muscle 30 days after transplantation (Welch's t-test). E) Representative bright-field and red fluorescent images of unoperated and notexin injected/ tdTomato expressing myoblasts transplanted soleus muscles. Scale bar = 1000 μm. F) Representative cross-sections of unoperated and notexin injected/ transplanted soleus muscles show that regeneration in injured muscles occurs only through the recruitment of endogenous myoblasts and tdTomato expressing myoblasts fail to integrate with these regenerating fibres. A limited number of red myoblasts are survived among the regenerated muscle fibres, discernible by arrows. Scale bar = 50 μm. G) Quantification of the Mean (± SD) cross-sectional muscle fibre areas and H) muscle fibre numbers in a single cross-section in unoperated and tdTomato transplanted soleus 30 days after notexin injection and transplantation. **** $P < 0.0001$ (Ordinary One-way ANOVA test).

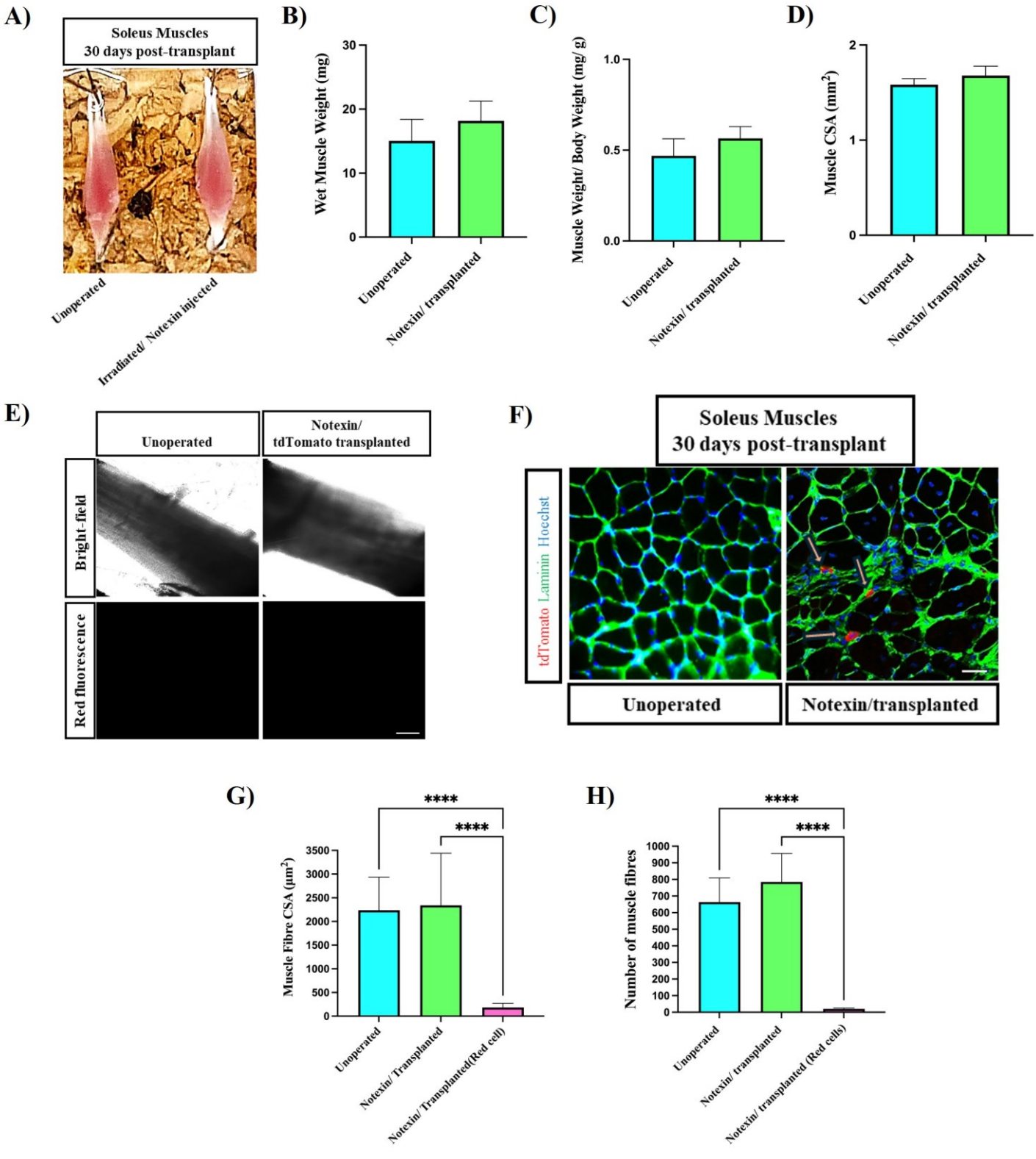
A)
Soleus Muscles
30 days post-transplant
Unoperated
Irradiated/ Notexin injected
B)
Wet Muscle Weight (mg)
30
20
10
0
Unoperated
Notexin/ transplanted
C)
Muscle Weight/ Body Weight (mg/ g)
1.0
0.5
0.0
Unoperated
Notexin/ transplanted
D)
Muscle CSA (mm2)
2
1
0
Unoperated
Notexin/ transplanted
E)
Unoperated
Notexin/
tdTomato transplanted
Bright-field
Red fluorescence
F)
Soleus Muscles
30 days post-transplant
tdTomato Laminin Hoechst
Unoperated
Notexin/transplanted
G)
****
****
Muscle Fibre CSA (µm2)
3500
3000
2500
2000
1500
1000
500
0
Unoperated
Notexin/ Transplanted
Notexin/ Transplanted(Red cell)
H)
****
****
Number of muscle fibres
1000
900
800
700
600
500
400
300
200
100
0
Unoperated
Notexin/ transplanted
Notexin/ transplanted (Red cells)

Figure 3.2. Gamma radiation, followed by notexin injection, kills endogenous satellite cells, and prevents muscle fibre regeneration. A) Representative image of soleus muscles 30 days post-injury (i.e. after irradiation and venom injection). B) Representative cross-sections of unoperated and irradiated/notexin-injected soleus muscles stained with H&E, 30 days post-injury. Scale bar = 50 μm. C) Mean (± SD) wet weight and D) muscle weight/body weight from unoperated and irradiated/notexin injected soleus muscles 30 days post-injury. ** $p < 0.01$ and *$P < 0.05$ (Welch's t-test).

A)

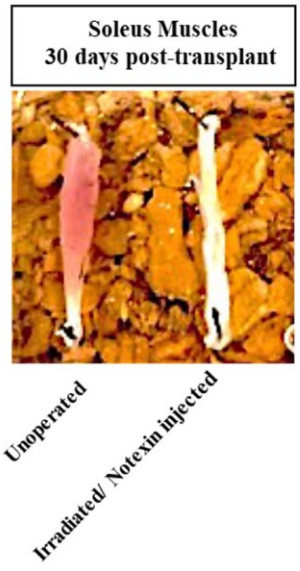
Soleus Muscles
30 days post-transplant
Unoperated
Irradiated/ Notexin injected

B)

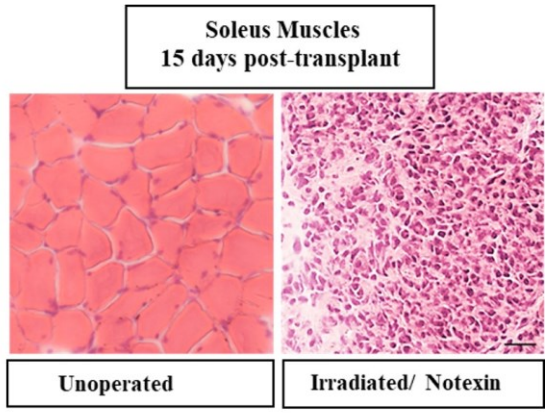
Soleus Muscles
15 days post-transplant
Unoperated
Irradiated/ Notexin

C)

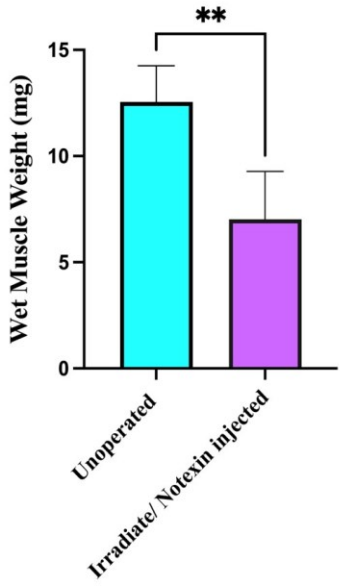
**
Wet Muscle Weight (mg)
15
10
5
0
Unoperated
Irradiate/ Notexin injected

D)

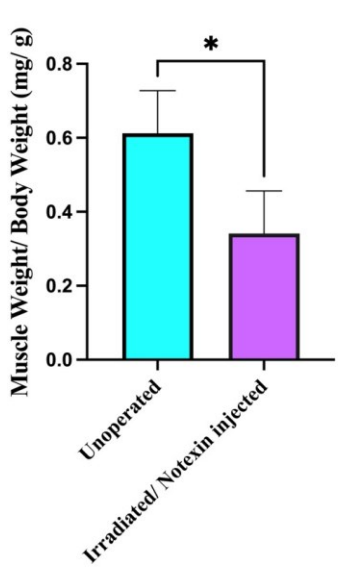
*
Muscle Weight/ Body Weight (mg/ g)
0.8
0.6
0.4
0.2
0.0
Unoperated
Irradiated/ Notexin injected

Figure 3.3. tdTomato expressing ES cell-derived myoblasts engraft and form muscle fibres when transplanted into irradiated/notexin-injected muscles. A) Representative image of an unoperated soleus muscle alongside a soleus muscle that underwent transplantation with tdTomato expressing myoblasts following irradiation and notexin injection, observed 30 days post-transplant. B) Representative bright-field and red fluorescent images comparing unoperated soleus muscles with transplanted soleus muscle with tdTomato-expressing myoblasts following irradiation and notexin injection. Scale bar = 500 μm. C) A group of red fluorescent muscle fibres (Scale bar = 500 μm) and D) single tdTomato expressing muscle fibres (Scale bar = 50 μm) teased from a transplanted soleus muscle show tdTomato expression along their entire length. E) Mean (± SD) wet weight values, F) muscle weight/body weight ratio, and G) CSA measurements of both unoperated soleus muscles and those transplanted with tdTomato-expressing myoblasts after irradiation and notexin injection, assessed 30 days post-transplantation. * $p < 0.05$ (Welch's t-test).

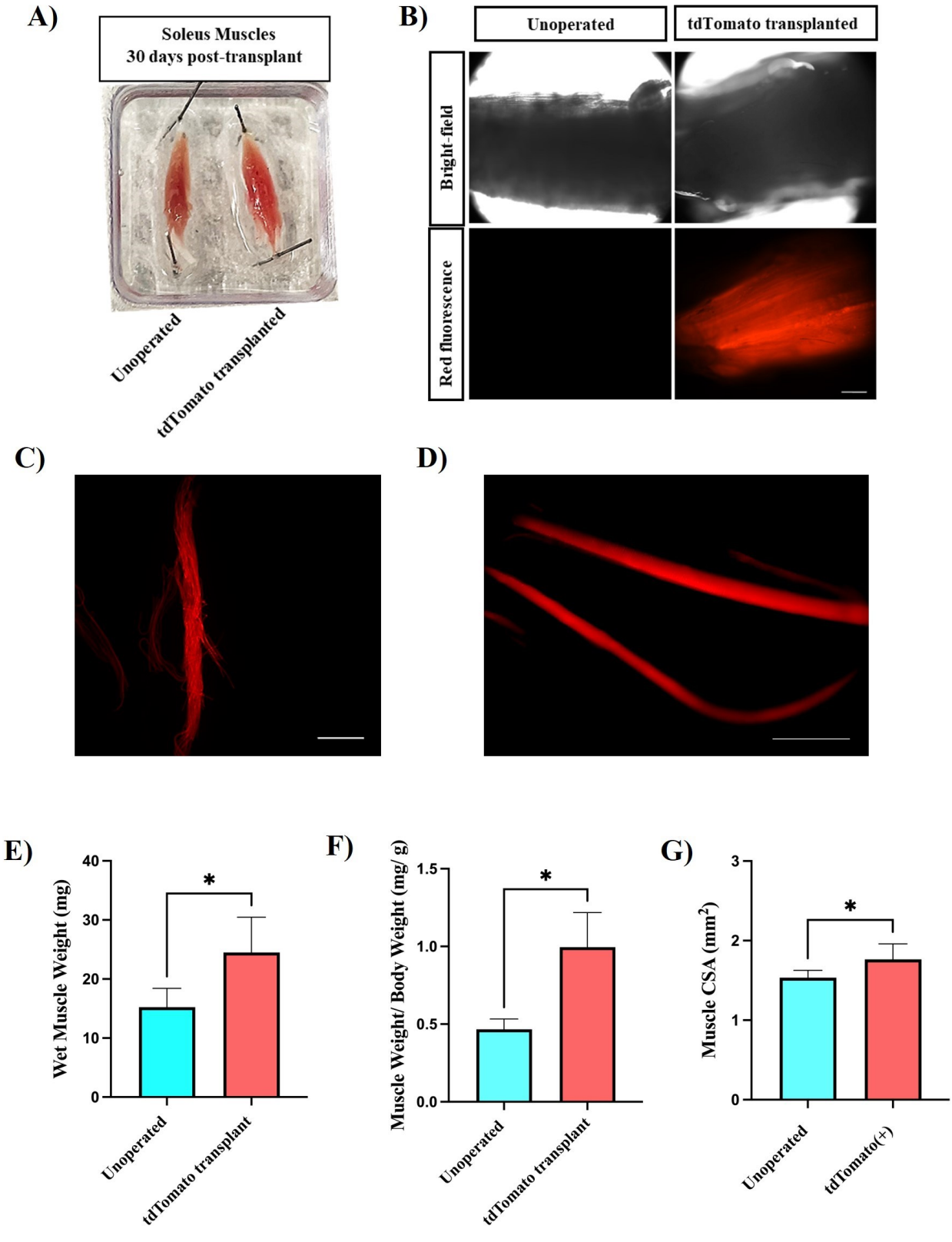
A)
Soleus Muscles
30 days post-transplant
Unoperated
tdTomato transplanted
B)
Unoperated
tdTomato transplanted
Bright-field
Red fluorescence
C)
D)
E)
Wet Muscle Weight (mg)
40
30
20
10
0
*
Unoperated
tdTomato transplant
F)
Muscle Weight/ Body Weight (mg/ g)
1.5
1.0
0.5
0.0
*
Unoperated
tdTomato transplant
G)
Muscle CSA (mm2)
3
2
1
0
*
Unoperated
tdTomato(+)

Figure 3.4. tdTomato expressing myoblasts form elongated, but small muscle fibres, when transplanted into irradiated/notexin-injected soleus muscles. A) Florescent image of a cross-section from tdTomato expressing myoblasts transplanted soleus 30 days after transplant. Scale bar = 500 μm. B) Mean (± SD) CSA of tdTomato- and tdTomato+ fibres in a single muscle cross-section. **** $P < 0.0001$ (Welch's t-test). C) Representative cross-sections of unoperated and transplanted soleus muscles show that tdTomato-expressing fibres exhibit a smaller size, but a greater abundance compared to control fibres. Scale bar = 500 μm. D) Quantification of the mean (± SD) cross-sectional muscle fibre areas in unoperated and transplanted soleus 30 days post-transplantation. **** $P < 0.0001$ (Welch's t-test). E) Frequency distribution of muscle fibre CSA of unoperated and tdTomato expressing myoblasts transplanted soleus 30 days post-transplantation. F) Quantification of the mean (± SD) muscle fibre numbers in a single cross-section in unoperated and tdTomato expressing myoblasts transplanted soleus 30 days post-transplantation. **** $P < 0.0001$ (Welch's t-test).

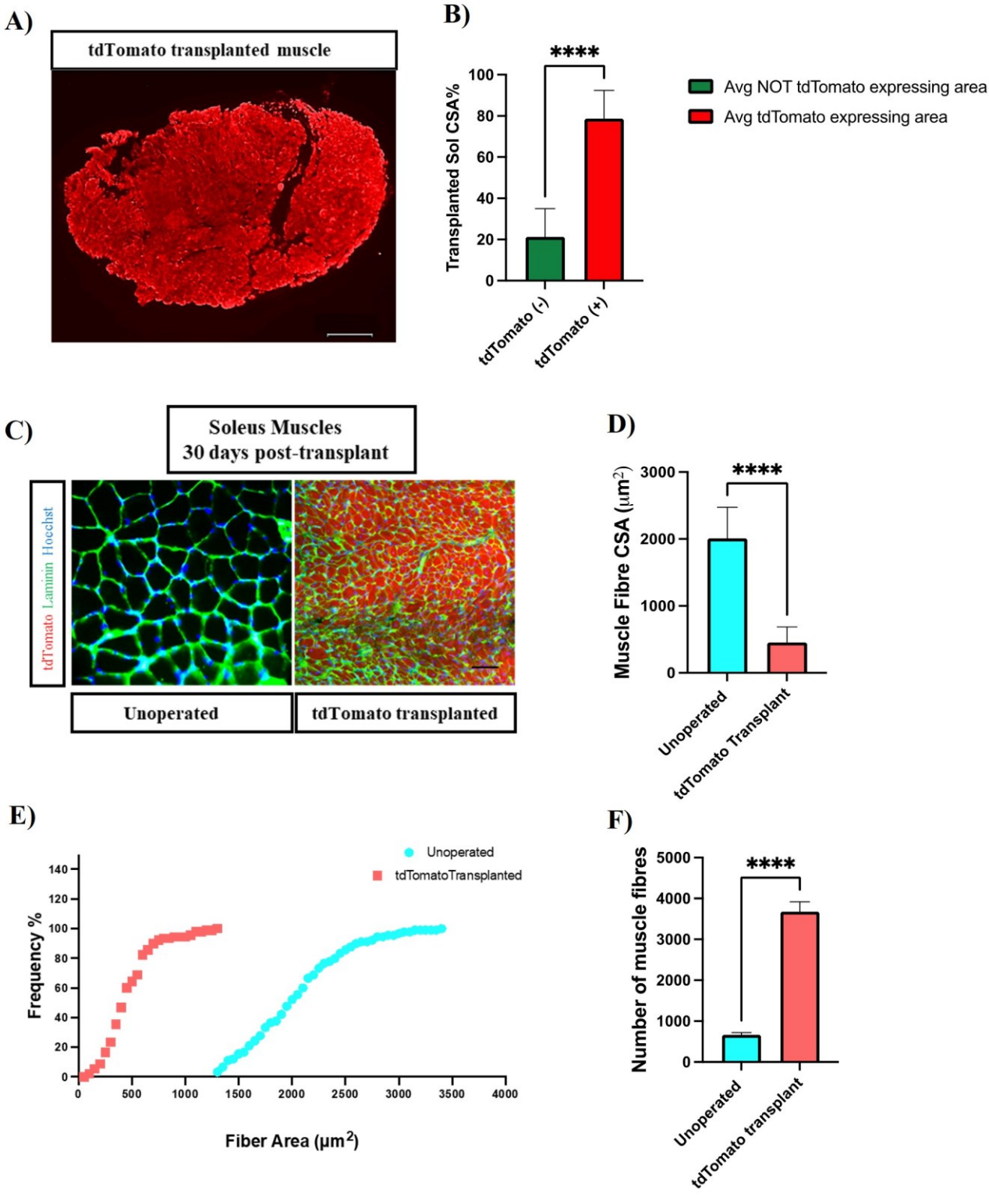
A)
tdTomato transplanted muscle
B)
****
Transplanted Sol CSA%
100
80
60
40
20
0
tdTomato (-)
tdTomato (+)
Avg NOT tdTomato expressing area
Avg tdTomato expressing area
C)
Soleus Muscles
30 days post-transplant
tdTomato Laminin Hoechst
Unoperated
tdTomato transplanted
D)
****
Muscle Fibre CSA (μm²)
3000
2000
1000
0
Unoperated
tdTomato Transplant
E)
Unoperated
tdTomatoTransplanted
Frequency %
140
120
100
80
60
40
20
0
0
500
1000
1500
2000
2500
3000
3500
4000
Fiber Area (μm²)
F)
****
Number of muscle fibres
5000
4000
3000
2000
1000
0
Unoperated
tdTomato transplant

Figure 3.5. ChR2 expressing myoblasts engraft into the irradiated/notexin-injected soleus muscles. A) Representative image of an unoperated soleus muscle alongside a soleus muscle that underwent transplantation with ChR2-expressing ES cell-derived myoblasts following irradiation and notexin injection, observed 60 days post-transplant. B) Representative bright-field and green fluorescence images comparing unoperated soleus muscles with transplanted soleus muscle with ChR2-expressing myoblasts following irradiation and notexin injection. Scale bar = 1000 μm. C) Mean (± SD) wet weight values and D) muscle weight/body weight ratio of both unoperated soleus muscles and those transplanted with ChR2-expressing myoblasts after irradiation and notexin injection, assessed 30-90 days post-transplantation. P=0.6406 and P= 0.5052 respectively (Welch's t-test).

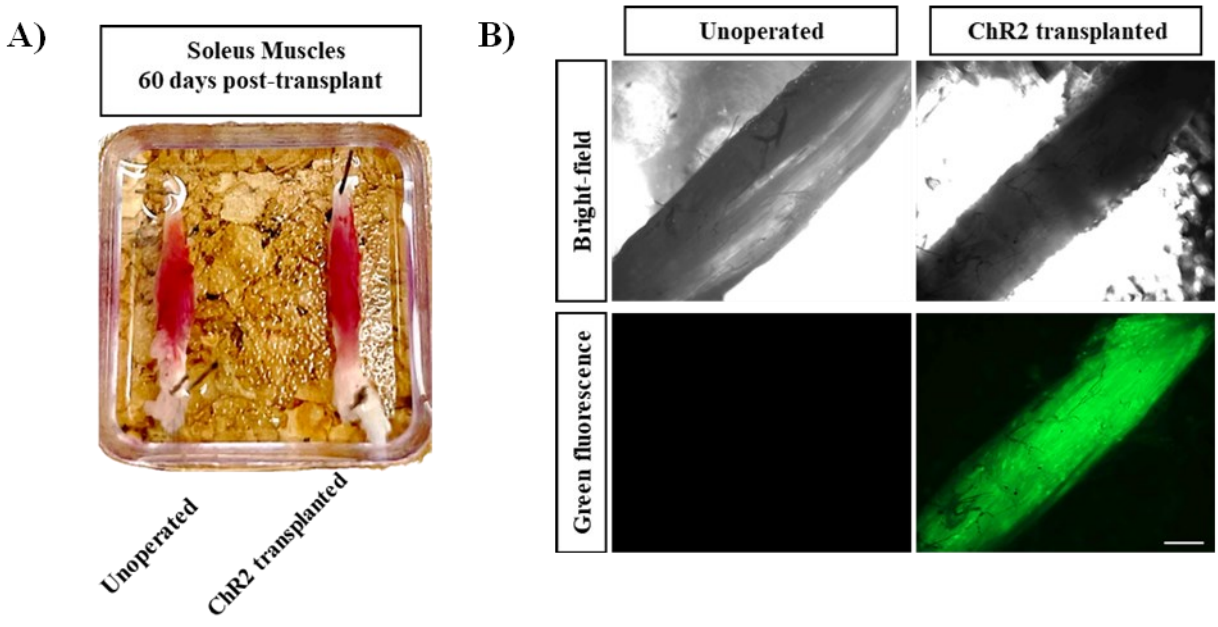
A)
Soleus Muscles
60 days post-transplant
Unoperated
ChR2 transplanted
B)
Unoperated
ChR2 transplanted
Bright-field
Green fluorescence

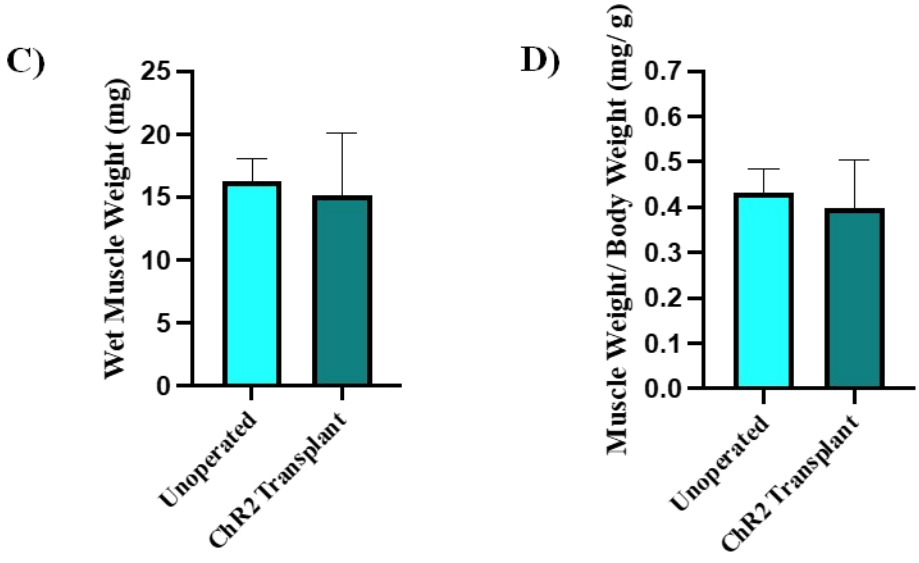
C)
Wet Muscle Weight (mg)
25
20
15
10
5
0
Unoperated
ChR2 Transplant
D)
Muscle Weight/ Body Weight (mg/ g)
0.7
0.6
0.5
0.4
0.3
0.2
0.1
0.0
Unoperated
ChR2 Transplant

Figure 3.6. ChR2 expressing muscles are activated with blue light stimulations. A) Representative image of blue LED light activation of a ChR2 transplanted soleus muscle 30-90 days post-transplant. B) Twitch contraction (pink trace) elicited by neural stimulation and blue LED light activation (blue traces) for 1, 10 and 100 ms. C) Quantification of the mean (± SD) twitch contraction amplitude evoked by neural stimulation and contractile force amplitudes elicited by blue light activation from 1-500 ms. Mean of each column is compared to the mean of neural activation column. * $p < 0.05$ (Brown-Forsythe and Welch ANOVA test). D) Mean (± SD) contractile force evoked by 50 ms optical stimulation across varying light intensities from 1 to 24 mV. E) Quantification of depolarization magnitudes across different myofibres, induced by escalating intensities of blue light stimulation. F) Mean (± SD) depolarization values of myofibres in response to increasing intensities of blue light stimulation. G) Quantification of the mean (± SD) depolarization amplitude, and H) depolarization magnitude in myofibres elicited by blue light activation over durations from 1 to 500 ms. Quantification of the mean depolarization amplitude (± SD) and H) depolarization magnitude in myofibres elicited by blue light activation over durations from 1 to 500 ms.

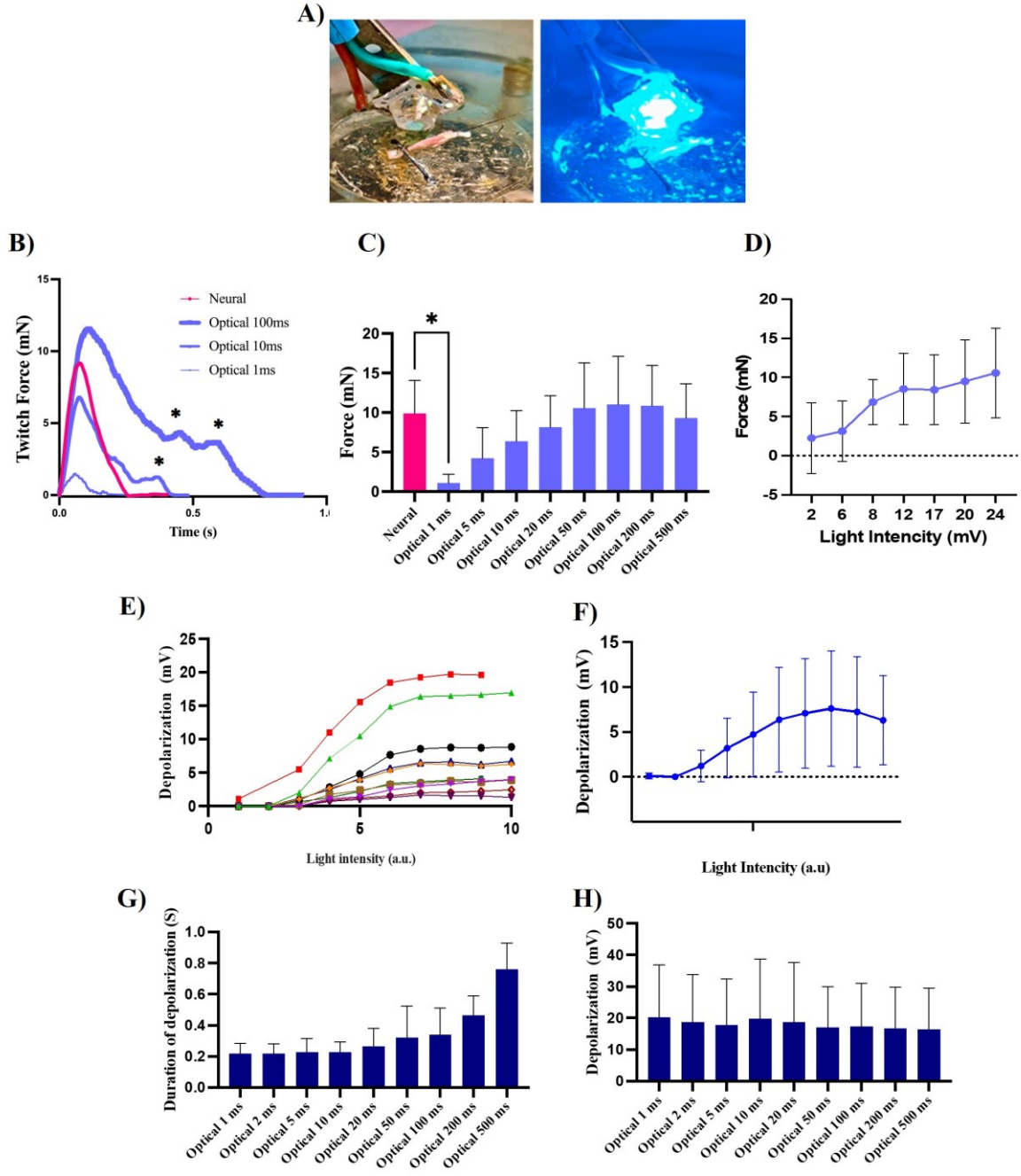
A)
B)
Twitch Force (mN)
Neural
Optical 100ms
Optical 10ms
Optical 1ms
Time (s)
C)
Force (mN)
Neural
Optical 1 ms
Optical 5 ms
Optical 10 ms
Optical 20 ms
Optical 50 ms
Optical 100 ms
Optical 200 ms
Optical 500 ms
D)
Force (mN)
Light Intencity (mV)
E)
Depolarization (mV)
Light intensity (a.u.)
F)
Depolarization (mV)
Light Intencity (a.u)
G)
Duration of depolarization (S)
Optical 1 ms
Optical 2 ms
Optical 5 ms
Optical 10 ms
Optical 20 ms
Optical 50 ms
Optical 100 ms
Optical 200 ms
Optical 500 ms
H)
Depolarization (mV)
Optical 1 ms
Optical 2 ms
Optical 5 ms
Optical 10 ms
Optical 20 ms
Optical 50 ms
Optical 100 ms
Optical 200 ms
Optical 500 ms

Figure 3.7. Force produced by optical stimulation in the transplanted muscles expressing ChR2 through AAV-PHP.eB-CAG-ChR2-EYFP transduction. A) Twitch contraction (pink trace) evoked by neural stimulation, alongside blue LED light activation (blue trace) for a duration of 50 ms. B) Quantification of the mean (± SD) twitch contraction amplitude induced by neural stimulation and the contractile force amplitudes elicited by blue light activation over durations from 1 to 500 ms, with each column's mean compared to the neural activation column. ** $p < 0.01$ and * $p < 0.05$ (One-way ANOVA test). C) Mean (± SD) contractile force evoked by 50 ms optical stimulation across varying light intensities from 1 to 24 mV.

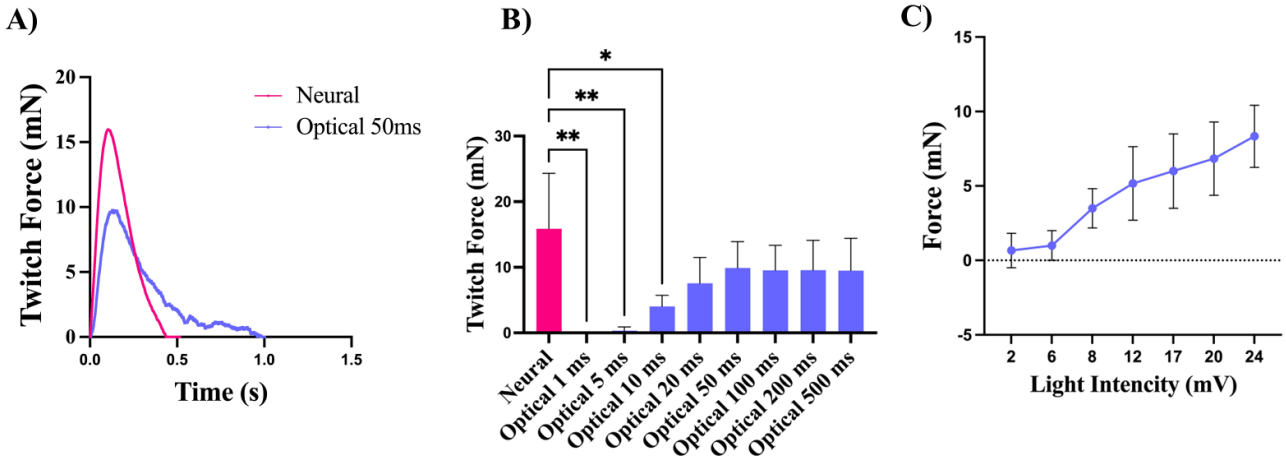
A)
Twitch Force (mN)
Time (s)
Neural
Optical 50ms
B)
Twitch Force (mN)
Neural
Optical 1 ms
Optical 5 ms
Optical 10 ms
Optical 20 ms
Optical 50 ms
Optical 100 ms
Optical 200 ms
Optical 500 ms
C)
Force (mN)
Light Intencity (mV)

Chapter 4: Anatomical and Physiological Characterization of tdTomato-Expressing Muscles Reinnervated by Endogenous Motoneurons

4.1 Abstract

Skeletal muscles are essential for movement and posture and have a strong regenerative capacity due to their resident stem cells, known as satellite cells. However, in cases of severe injuries like VML, muscle atrophy from denervation caused by PNI, or degenerative diseases like muscular dystrophy, the natural regenerative ability of skeletal muscles is often insufficient, leading to impaired function. Myoblast transplantation is a promising approach to replace injured or genetically disordered muscles with healthy, regenerated muscle fibres developed from exogenous cells, allowing for the introduction of specific genes into the muscle. Previously, using a new method of differentiation, we produced mouse ES cell-derived skeletal muscle fibres expressing ChR2 or tdTomato *in vitro* (described in chapter 2). Before transplanting these cells into the host soleus muscles, the muscles were irradiated, and notexin, a myotoxic agent, was injected to completely ablate the soleus muscles in mice, ensuring no natural regeneration could occur. The muscles were successfully regenerated and expressed the introduced genes. ChR2-expressing muscles contracted in response to blue light stimulation, while tdTomato-expressing muscles showed increased mass compared to control muscles, though with much smaller fibre sizes and a higher number of fibres (described in chapter 3). In this study, we examined the functional characteristics of these tdTomato expressing muscles, which had a different fibre number and size compared to control muscles. The results showed that the regenerated muscles were successfully innervated by endogenous motor axons, and the tdTomato-expressing muscles exhibited normal contractile responses when stimulated by these nerves. Intracellular electrophysiological recordings indicated that synaptic transmission in the transplanted muscles was largely normal. An examination of the number of fibres innervated by motor axons revealed over 80% innervation, with newly established NMJs localized in the same areas as those in control muscles. Interestingly, the regenerated muscles were composed entirely of fast-twitch fibres, differing from the typical composition of the soleus muscle, which usually contains a higher proportion of slow-twitch fibres. Despite this shift in fibre type, the regenerated muscles demonstrated contractile forces comparable to those of unoperated muscles.

4.2 Introduction

Skeletal muscles are among the body's most abundant tissues, comprising 40 - 45% of body mass. They are essential for movements such as walking, hand grasping, breathing, and swallowing (Dumont et al., 2015; J. Liu et al., 2018; Tedesco et al., 2010). These muscles possess a high capacity for regeneration after injuries by activating and proliferating their quiescent stem cells, known as satellite cells (Dumont et al., 2015; Laumonier & Menetrey, 2016; Morgan & Partridge, 2003). However, certain injuries, such as muscle atrophy due to PNI, VML, and diseases like muscular dystrophy, surpass the muscle's threshold for self-recovery, and the muscle cannot regain its functionality without external intervention (Aguilar et al., 2018; T. Gordon, 2020; Guiraud & Davies, 2019; Ribeiro et al., 2019).

In PNIs, such as BPIs, prolonged denervation due to proximal nerve damage results in muscle atrophy and fibrosis, significantly impairing muscle regeneration and reducing the chance of functional recovery to 10% (Fu & Gordon, 1995; T. Gordon, 2020). Additionally, drastic skeletal muscle injuries, such as VML, characterized by the traumatic or surgical loss of substantial skeletal muscle tissue beyond the body's regenerative capabilities, lead to significant functional impairment (Kim et al., 2020; Wu et al., 2012). In these situations, the self-repair process is impeded by extensive nerve and blood supply loss, alongside inflammation-induced fibrosis, resulting in permanent muscle loss, chronic scar tissue formation, and lasting disabilities (Das et al., 2020; Turner & Badylak, 2012). Furthermore, muscle diseases such as muscular dystrophy, a group of serious genetic disorders, cause progressive muscle deterioration (Biressi et al., 2020; Lovering et al., 2005). These conditions are caused by mutations in genes encoding cytoskeletal and

membrane proteins crucial for muscle structure and function, leading to the gradual degradation and loss of muscle fibres, thus impeding sustained muscle recovery (Tedesco et al., 2010).

Cell transplantation strategies could be pivotal in developing new approaches for muscle regeneration, particularly in conditions mentioned above. Researchers have explored various cell types for this purpose, including stem cells and myoblasts (Lev & Seliktar, 2018). The concept of skeletal muscle transplantation emerged in the late 1980s through the pioneering work of Partridge and colleagues, who demonstrated that injecting myoblasts into the hind limbs of mdx mice, a model for Duchenne muscular dystrophy (DMD), led to a substantial reconstitution of dystrophin-positive muscle fibres (Partridge et al., 1989). However, early attempts at muscle cell transplantation faced challenges such as low survival rates and limited migratory ability of the transplanted cells (Beauchamp et al., 1999). Since then, numerous myoblast and satellite cell engraftments have been performed, leading to significant improvements in techniques and outcomes, which have the potential to positively impact the lives of many patients (Hekmatnejad & Rudnicki, 2022).

Previously, we successfully regenerated soleus muscles by transplanting ES cell-derived myoblasts expressing tdTomato or ChR2 after irradiating the leg to inactivate muscle satellite cells and degrading the fibres with notexin injection. The muscles were successfully regenerated using both types of ES cell-derived myoblasts. Interestingly, the tdTomato-expressing myoblasts produced a larger mass of soleus muscle, containing a much higher number of red fibres, but with a smaller diameter than the control fibres. Additionally, ChR2-expressing myoblasts regenerated muscles that contracted in response

to blue light illumination without nerve stimulation, which could potentially restore some level of function in completely denervated muscles in patients with SCI and PNI (described in chapter 3).

Here, we conducted a detailed anatomical and physiological characterization of the transplanted tdTomato-expressing muscles. First, we found that the regenerated muscles were successfully innervated. By stimulating the nerve, we compared the contractile force of the regenerated tdTomato expressing muscles to unoperated control muscles and observed that normal contractile forces were achieved in the regenerated muscles. Furthermore, an examination of synaptic transmissions through intracellular recordings revealed that miniature end-plate potential (mEPP) amplitudes were significantly higher in the transplanted muscles, likely due to differences in muscle fibre size and input resistance (Katz & Thesleff, 1957). All other factors in the engrafted muscles—including the frequency of mEPPs, mEPP rise time, half-width, decay time, end-plate potential (EPP) amplitudes, and quantal contents—were normal and comparable to those of the unoperated muscles. We then investigated the innervation percentage of regenerated muscle fibres derived from the grafted exogenous cells. The majority (>80%) of the ES cell-derived muscle fibres were innervated by endogenous motor axons. Additionally, we examined the location of the newly established NMJs on the regenerated muscles. α-Bungarotoxin (α-BTX) labelling indicated that AChR on these muscles were located in approximately the same area as in the unoperated control soleus muscles, suggesting that motor axons and muscle fibres are guided to establish NMJs in designated regions. Finally, we sought to determine the type of fibres composing the regenerated soleus muscles through immunostaining for both slow and fast-type myosin. The results showed that these

muscles were composed solely of fast-type myosin, unlike the normal soleus muscles, which consist of a combination of slow and fast muscle fibres, with a majority being slow types. These findings underscore the potential of cell transplantation as a therapeutic strategy for severe muscle injuries and genetic muscle diseases. The ability to restore muscle function through cell-based therapies represents a significant step forward in the field of regenerative medicine and offers hope for individuals affected by muscle injuries and diseases.

4.3 Materials and Methods

4.3.1 *Ex vivo* Soleus Muscle Isometric Tension

The soleus muscle, along with a short segment of its innervating nerve, was dissected from mice anesthetized with a mixture of isoflurane and oxygen. The muscle was immediately transferred to a recording chamber coated with Sylgard (Dow Corning) and continuously perfused with oxigenated Tyrode's solution containing 125 mM NaCl, 24 mM $NaHCO_3$, 5.37 mM KCl, 1 mM $MgCl_2$, 1.8 mM $CaCl_2$, and 27.75 mM dextrose. After fixing the proximal tendon with an insect pin and tying it securely, the distal tendon was attached with a fine thread and connected to a force transducer (FT 03; Grass Technologies).

Electrical stimulations were delivered to the innervating nerve via a fine-tipped glass suction electrode connected to an S88 stimulator (Grass Technologies), which was isolated from the ground using a constant current stimulus isolator (PSIU6; Grass Technologies). Once the muscle length was adjusted to achieve the largest isometric contraction, neural forces were recorded via a Digidata 1320A analog-to-digital board, using AxoScope 10.2

software (Molecular Devices). Tetanus forces were recorded at 50 Hz for a 1 second duration.

4.3.2 Intracellular Recordings of Myofibres

After isometric tension measurement, muscles were pre-incubated for 60 minutes in oxygenated Tyrode solution containing 5μM μCTX GIIIB (Alomone Labs, Jerusalem, Israel) to inhibit muscle contractions triggered by nerve stimulation. Muscles were then transferred to a Sylgard-coated recording chamber, pinned and perfused with μCTX-free oxygenated Tyrode solution for the duration of the recording.

Sharp tip glass electrodes with a resistance between 15-30 MΩ filled with 3M KCl were used. Spontaneous mEPPs and nerve-evoked EPPs were captured using a MultiClamp 700B amplifier and subsequently digitized utilizing MultiClamp Digidata 1140A. The generation of nerve-evoked transmitter release was accomplished by stimulating the soleus nerve with a suction electrode, connected to a Grass S88 stimulator that was electrically isolated using an SIU5 stimulus isolation unit.

Data collection was performed using Clampex 10.3 software (Molecular Devices), with subsequent analysis conducted using MiniAnalysis software (Synaptosoft). The quantal content (m) was calculated using the direct method, where the mean amplitude of EPPs (elicited at a frequency of 1Hz) and mEPPs (recorded for a duration of 30 seconds) were used (m= mean EPP amplitude / mean mEPP amplitude). Instances where a stimulus failed to elicit a change in the resting membrane potential were categorized as failures. Resting membrane potentials were between -55 mV and -85 mV, and any recordings showing a

change greater than 10% from the initial resting membrane potential by the conclusion of the recording session were discarded.

4.3.3 Muscle Immunohistochemistry

Soleus muscles were positioned at their physiological length in cryomolds, secured with insect pins. Prior to sectioning, the muscles were examined under a microscope to detect any red fluorescence. The samples were then immersed in a solution consisting of 20% sucrose (Fisher Chemical) in PBS mixed with tissue freezing medium O.C.T. Compound (Tissue Tek) at a 1:2 ratio. Once prepared, the muscles were swiftly frozen in a 2-methylbutane (Sigma-Aldrich) bath that had been pre-cooled with liquid nitrogen. Afterward, the frozen muscles were stored at -80 °C for a minimum of 24 hours before sectioning.

Using a cryostat (Leica), the muscles were sectioned longitudinally at 40 μm or cross-sectioned at 20 μm and transferred to microscope slides. The sections were subsequently fixed in 4% PFA for 15 minutes, followed by three washes with PBS. After this preparation, the sections were ready for incubation with primary antibodies. A solution of 1% BSA (VWR) in PBS plus 0.5% PBS-Triton was used for antibody application.

For the analysis of endplate morphology, the longitudinal sections were incubated overnight at room temperature with mouse anti-SV2 IgG1 (1:50, Developmental Studies Hybridoma Bank). Following this incubation, the sections were washed three times with PBS to remove any unbound antibodies. The sections were subsequently treated with a secondary antibody, Alexa Fluor 488-conjugated goat anti-mouse IgG1 (1:500, Invitrogen), along with Alexa Fluor 647-conjugated α-BTX (1:500, Invitrogen). The slides

were placed in the dark on a gentle shaker for 2 hours. After an additional three washes with PBS to remove excess antibodies, the slides were mounted using a lab-made mounting medium composed of 50% glycerol/PBS and 0.03 mg/ml ρ-Phenylenediamine, and coverslips were carefully placed on top of the mounted sections to preserve them.

For the identification of muscle fibre types, cross-sections were incubated overnight at room temperature with mouse anti-BA-D5 IgG2b (specific to slow MHC) (1:10, Developmental Studies Hybridoma Bank) and rabbit anti-fast myosin skeletal heavy chain IgG (1:500, Abcam). After three PBS washes, secondary antibodies including Alexa Fluor 488-conjugated goat anti-mouse IgG2b (1:500, Invitrogen) and either Alexa Fluor 546-conjugated goat anti-rabbit IgG or Alexa Fluor 647-conjugated goat anti-rabbit IgG (1:500, Invitrogen) were applied. The sections were incubated with these secondary antibodies for 2 hours, again in the dark and on a gentle shaker. Following another three washes with PBS, the sections were mounted using the previously mentioned mounting medium, and coverslips were placed on top of the sections to protect and preserve the samples for further analysis.

The tissues were not specifically stained for tdTomato; the red fluorescence visible in the images is a result of the natural fluorescence of the tdTomato-expressing muscles.

4.3.4 Imaging

Z-stacks of the NMJs (synaptic vesicle protein 2 (SV2) and α-BTX colocalization) and muscle fibre type determination images were captured using a ZEISS LSM 880 laser scanning confocal microscope (Zeiss Microimaging) operated with Zeiss Zen (black

edition) software. The images were then processed using the Z-project function of Fiji (ImageJ) software.

NMJ localization images were captured using an upright fluorescence microscope (Leica Instruments) with Zen-Blue (Zeiss) software.

Brightness and contrast adjustments were made to the images using either Zen-Blue software or ImageJ. Additionally, the colours of the fast and slow myosin staining were inverted using ImageJ.

4.3.5 Innervation Quantification

Slides of longitudinal sections of soleus muscle after staining were checked for identifying co-labelling of α-BTX and SV2 using upright fluorescence microscope (Leica Instruments). Numerous pictures of α-BTX positive areas were taken on far-red channel and were checked if there is a colocalization of SV2, presynaptic vesicle structures pictured on green channel. Co-localizations were counted as successful innervations whereas α-BTX positive labelling without co-localization with SV2 were counted as not innervated. Approximately 350-400 endplates per test group were examined for presence of innervation and NMJ.

4.3.6 Statistical Analysis

All statistical analyses and graph creation were conducted using GraphPad Prism (Prism 10) software. T-tests were used to compare the two groups: unoperated and transplanted tdTomato-expressing muscles. All results are presented as mean ± standard deviation, with $P < 0.05$ considered statistically significant.

4.4 Results

4.4.1 Regenerated Muscles Expressing tdTomato Exhibit Contractile Forces Comparable to Control Muscles

After transplanting tdTomato-expressing myoblasts into the soleus muscles of mice that had been previously irradiated and treated with notexin to eliminate all endogenous muscle fibres and prevent any regeneration through the activation of the muscle's own satellite cells, we assessed if muscles were innervated and evaluated the functionality of the regenerated muscles containing these transplanted myoblasts. Upon confirming that the muscles were innervated, we measured *ex vivo* muscle twitch and tetanic contractile forces in response to nerve stimulation 30 to 60 days post-transplantation (n=3) (Fig. 4.1A, B). The average twitch force exhibited by the tdTomato-expressing muscles was 20.4 ± 2.9 mN, which did not differ significantly from the control muscles, which showed a twitch force of 18.23 ± 5.6 mN (P = 0.5986) (Fig. 4.1C). Additionally, an examination of tetanic contractile forces revealed no significant differences between unoperated muscles (102.9 ± 4.7 mN) and tdTomato-expressing muscles (118.43 ± 28 mN) (P = 0.4441) (Fig. 4.1D).

These results indicate that the regenerated muscles, formed through the engraftment of exogenous muscle cells, are fully functional. Although the differences were not statistically significant, the tdTomato-expressing muscles produced slightly higher forces in both twitch and tetanus tests, consistent with the larger CSA of these muscles. This suggests that the transplanted myoblasts successfully contributed to muscle regeneration and function.

4.4.2 Normal Synaptic Transmission at NMJs in Transplanted Muscles

To comprehensively assess synaptic transmission in the transplanted muscles, sharp electrode intracellular electrophysiological recordings were performed on both unoperated and transplanted soleus muscle fibres one month post-transplantation (Fig. 4.2A). Our observations revealed that the amplitude of mEPPs was significantly higher in the tdTomato-expressing muscle fibres (0.61 ± 0.18 mV) compared to the unoperated muscle fibres (0.57 ± 0.19 mV) ($P < 0.0001$), (Fig. 4.2B). According to the foundational work of Katz & Thesleff (1957), differences in mEPP amplitude between muscle fibres of varying sizes are attributable to the physical dimensions of the fibres, with smaller fibres displaying larger mEPPs due to their higher input resistance. Additionally, it has been noted that mEPP are higher in younger mice and rats, decreasing as they age. This pattern reflects the increase in muscle fiber diameter with maturation and a corresponding decrease in input resistance (Bewick et al., 2004; McIntosh et al., 2023). Given that the diameters of muscle fibres in the tdTomato-expressing muscles were approximately 4.6 times smaller than control fibres, as mentioned in the chapter 3, this substantial increase in mEPP amplitude aligns with their findings. However, the frequency of mEPPs did not show a statistically significant difference between the two groups (unoperated: 1.14 ± 0.8 vs. transplanted: 0.82 ± 0.6; $P= 0.0675$) (Fig. 4.2C), and other parameters, including the rise time (unoperated: 1.57 ± 0.6 ms vs. transplanted: 1.53 ± 0.6; $P= 0.1744$ ms) (Fig. 4.2D), half-width (unoperated: 2.61 ± 0.9 ms vs. transplanted: 2.69 ± 0.9 ms; $P= 0.0.602$) (Fig. 4.2E), and decay time (unoperated: 2.167 ± 0.98 ms vs. transplanted: 2.166 ± 0.6 ms; $P= 0.9817$) (Fig. 4.2F) of mEPPs, were comparable to the unoperated muscle fibres.

Furthermore, we measured evoked neurotransmitter release by stimulating the innervating nerve at a frequency of 1 Hz and recording from the myofibres (Fig. 4.2G). These measurements revealed no significant difference in EPP amplitude between unoperated (18.73 ± 5.9 mV) and transplanted muscles (19.70 ± 6.3 mV) ($P > 0.9999$) (Fig. 4.2H). Additionally, quantal content, which reflects the number of neurotransmitter quanta released per nerve impulse, was found to be equivalent in both the transplanted and unoperated muscles (unoperated: 35.4 ± 9.05 vs. transplanted: 33.5 ± 7.1; $P= 0.4548$) (Fig. 4.2I).

Overall, these findings suggest that synaptic transmission in the transplanted muscles is largely unaltered, except for a higher mEPP amplitude, which is likely due to the smaller size of the muscle fibres in the tdTomato-expressing muscles. This suggests that, despite the size difference, the transplanted muscles maintain functional synaptic connections comparable to those in unoperated muscles.

4.4.3 Reinnervation of NMJs in tdTomato-Expressing Muscles by Endogenous Motor Axons

To evaluate the anatomical features of the tdTomato-expressing muscles, we aimed to assess the extent of innervation in the regenerated muscles by the endogenous soleus muscle's nerve axons. 30-60 days post-transplantation, the extracted soleus muscles were longitudinally sectioned and subjected to labelling with α-BTX, which binds specifically to AChRs in skeletal muscles, as well as staining for SV2 (n=3) (Fig. 4.3A).

Quantification of the colocalization between presynaptic SV2 and postsynaptic α-BTX indicated that 80.3 % ± 7.5 of the NMJs in the regenerated muscles were successfully innervated. This was compared to a 95.33% ± 3.05 innervation rate observed in the unoperated muscles (Fig. 4.3B). Although the innervation rate was slightly lower in the regenerated muscles, statistical analysis revealed no significant differences between the innervation rates of the regenerated and unoperated

muscles (P = 0.0541). This finding suggests that the exogenous muscle fibres are indeed capable of establishing functional NMJs with endogenous motor axons, thereby restoring the necessary neural connections for muscle function.

Further investigation into the spatial distribution of NMJs within the muscles regenerated from the exogenous myoblasts revealed that the newly formed NMJs were predominantly located in the same regions as the unoperated control muscles (Fig. 4.1C). This consistent positioning of NMJs in the regenerated muscles appears to be heavily influenced by the guidance provided by the basal lamina. According to (Marshall et al., 1977), even as muscle fibres degenerate, the basal lamina sheets remain intact, serving as a structural scaffold. This scaffold not only supports the regenerating muscle cells but also directs the regenerating nerve axons and muscle fibres to re-establish NMJs at their original locations. The formation of synapses at the denervated NMJs is not dependent on the integrity of the original postsynaptic muscle cell. Rather, the essential cues for synapse formation are provided and maintained by components external to the muscle cell itself, such as the basal lamina. These findings underscore the critical role of the ECM in guiding the regeneration process and ensuring that the newly formed muscle fibres are properly innervated, ultimately leading to the successful restoration of muscle function.

4.4.4 Characterization of Engrafted tdTomato-Expressing Muscle Fibres as Fast-Twitch Type

The composition of the soleus muscle includes both slow and fast-twitch muscle fibres. Specifically, the mouse soleus muscle is predominantly composed of slow-twitch fibres, which make up approximately 75.5% of the total muscle composition, with the remaining 24.5% being fast-twitch fibres, as identified by Crow & Kushmerick (1982). To investigate the fibre types, present in the tdTomato-expressing regenerated soleus muscles, cross-sections of both unoperated and tdTomato-expressing muscles were subjected to immunostaining with antibodies against fast and slow myosin. As anticipated, the unoperated muscle displayed a typical combination of fast,

slow and hybrid muscle fibres, reflecting the natural composition of the soleus muscle (Fig. 4.4A). In contrast, the transplanted muscle showed a striking difference, with all the red fibres exclusively expressing fast myosin, indicating a complete absence of slow-twitch fibres (Fig. 4.4B).

This finding highlights a significant shift in the fibre composition of the regenerated soleus muscles, where fast-twitch fibres dominate, in stark contrast to the fibre composition observed in unoperated muscles. The predominance of fast-twitch fibres in the regenerated muscles was not entirely unexpected, given that all the ES cell-derived muscle fibres, which had been cultured *in vitro* and subsequently transplanted into the irradiated and notexin-treated soleus muscles, were characterized as fast-twitch muscle fibres.

4.5 Discussion

The objective of this study was to thoroughly assess the anatomical and physiological properties of regenerated soleus muscles achieved through the engraftment of ES cell-derived myoblasts into completely damaged muscles. To achieve this, as demonstrated in the previous chapter the target muscles were first subjected to irradiation to inactivate muscle satellite cells, thereby preventing their activation and proliferation following injury. Subsequently, these muscles were injected with notexin, a potent myotoxic and presynaptic neurotoxic phospholipase A2 known for its ability to destroy muscle fibres and disrupt NMJs (Dixon & Harris, 1996). Under these stringent conditions, the muscle is entirely abolished and shows no potential for natural regeneration. Furthermore, transplanting ES cell-derived myoblasts, expressing exogenous genes such as tdTomato or ChR2, resulted in muscle regeneration with the successful expression of these introduced genes. The aim of producing ChR2-expressing muscles was to activate permanently denervated muscles through stimulation with blue light. ChR2-expressing

muscles hold the potential for improving some degree of independence and quality of life for patients with paralysis due to SCI or PNI. Additionally, we generated tdTomato-expressing muscles to confirm that regenerated fibres were derived from transplanted exogenous myoblasts. Although these muscles cannot facilitate external activation without nerve stimulation, they could be beneficial in treating genetic muscle diseases like DMD, and muscle injuries such as VML. Also, in PNIs, the atrophied muscle can be replaced with regenerated tissue, providing healthy NMJs once motor axons regenerate.

Here, in this study, we specifically focused on evaluating the functionality and NMJ establishment capabilities of the regenerated muscles expressing tdTomato. These regenerated muscles exhibited a larger mass and CSA compared to unoperated control muscles. Additionally, they were characterized by a greater number of muscle fibres, albeit with smaller diameters. This raised critical questions regarding the functional integration and potential advantages of such regenerated muscles, particularly concerning their ability to establish effective NMJs and restore overall muscle functionality.

Our findings indicated that the regenerated tdTomato-expressing soleus muscles demonstrated 80% colocalization between α-BTX and SV2, signifying successful NMJ establishment between the endogenous nerve and exogenous muscle fibres. This high rate of innervation facilitated the generation of normal contractile forces upon nerve stimulation, underscoring the effective integration of the transplanted cells into the host muscle's neural circuitry. Furthermore, an analysis of the NMJ area in the regenerated soleus muscles revealed an area approximately equivalent to the NMJ area in control muscles. Moreover, intracellular electrophysiological assessments revealed largely normal synaptic transmission in the transplanted muscles, with the notable exception of increased

amplitudes of mEPPs attributed to differences in muscle fibre size and input resistance. Other key parameters, such as the frequency of mEPPs, rise time, decay time, EPP amplitudes, and quantal contents, were found to be similar to unoperated muscles, further supporting the functional integration of the transplanted cells. Interestingly, the regenerated muscles were composed solely of fast-twitch fibres in contrast with normal soleus muscles, which predominantly consist of slow twitch fibres. Despite this difference, the regenerated muscles achieved normal contractile forces, demonstrating functional equivalence to unoperated muscles.

For over a century, cell and stem cell therapies have been employed in clinical settings, starting with procedures such as blood transfusions, bone marrow transplants, and epidermal grafts for severe burns. These treatments have saved countless lives and have become well-established medical practices, long before the modern concept of stem cells was fully understood (Cossu et al., 2018). Skeletal muscles are ideal candidates for cell therapy because of their abundant stem cell population, giving them exceptional regenerative capabilities, unlike other adult muscle tissues such as the heart (Judson & Rossi, 2020). The pioneering research by Partridge et al., (1989) using the mdx mouse model for DMD was the first to demonstrate that injected myoblasts could successfully integrate into skeletal muscle and increased the level of dystrophin in the extensor digitorum longus (EDL) muscles. This pivotal discovery prompted the use of allogeneic myoblasts in clinical trials aimed at restoring muscle function in DMD patients (Huard et al., 1992; Karpati et al., 1993; Mendell et al., 1995; Tremblay, Bouchard, et al., 1993; Tremblay, Malouin, et al., 1993). Subsequent pilot studies were conducted on both DMD and Becker Muscular Dystrophy (BMD) patients (Gussoni et al., 1997; Miller et al., 1997;

Neumeyer et al., 1998). Unfortunately, these early trials yielded limited or no clinical benefits, primarily due to issues with immunological rejection and extensive cell death following transplantation, leading to widespread skepticism about the future viability of this approach. Despite these setbacks, these pioneering studies confirmed the potential of cell therapy in human skeletal muscle and highlighted numerous unforeseen challenges that needed to be addressed. Over the past three decades, extensive research has explored various myogenic cell populations to identify those most effective for promoting skeletal muscle repair in clinical applications (Boyer et al., 2021). Despite significant advancements in muscle cell therapy, one of the major challenges that persists is the insufficient innervation following muscle myogenic cell transplantation *in vivo* (Judson & Rossi, 2020; Quarta et al., 2017). Thus, in addition to achieving successful cell engraftment, acquiring functional properties remains a critical goal of muscle cell therapy. Our regenerated muscles not only overcame this barrier by establishing hybrid NMJs but also exhibited functional contraction in response to stimulation from the endogenous nerve that innervates them.

In skeletal muscle, the ECM, known as the basal lamina, surrounds each muscle fibre and its associated satellite cells (Schüler et al., 2022). The basal lamina links networks of laminin and collagen polymers through the bridging functions of glycoproteins and heparan sulfate proteoglycans, such as nidogen and perlecan (Patton, 2003; Rayagiri et al., 2018; Rogers & Nishimune, 2017). Beyond providing structural support, the basal lamina actively participates in key biological processes and plays a role in regulating various muscle functions (Rogers & Nishimune, 2017). The components of the basal lamina play a crucial role in myogenesis and synaptogenesis, guiding cell growth, migration, and motor

axon adhesion (Foster et al., 1987; Hunter et al., 1989; Sanes, 2003). Specific collagen and laminin chains within the endplate basal lamina are localized to organize the pre- and post-synaptic structures of the NMJ, contributing to their assembly and function in mammals (Rogers & Nishimune, 2017). Indeed, during muscle regeneration after injury, AChRs and sodium channels reaccumulate at the NMJ, directed by the remaining components in the basal lamina even in denervated muscles. This reassembly ensures the proper restoration of neuromuscular function even after severe muscle damage (Lupa & Caldwell, 1994). Myotoxins such as cardiotoxin and notexin are highly toxic to skeletal muscle fibres and cause their deterioration, but they do not harm the basal lamina, blood vessels, or satellite cells (Gutiérrez & Ownby, 2003; Harris, 2003; Harris et al., 2003; Plant et al., 2006). Although the plasma membrane is damaged (Harris et al., 2003), the muscle retains the potential to regenerate, with new muscle fibres developing within the remaining basal lamina tubes (Harris, 2003). In our study, the chimeric innervation observed between the endogenous motor axons and the transplanted soleus muscle fibres was located almost at the original NMJ area. This suggests that the transplanted myoblasts grew within the existing basal lamina sheaths, guided by their molecular composition to maintain NMJ localization. This finding aligns with a study done by Nguyen et al. (2000), where sternomastoid muscles were removed from host mice's necks and replaced with immediately dissected sternomastoid muscles from newborn (P0) mouse pups. The NMJs between the host axons and the grafted muscle fibres preserved their original synaptic sites even before reinnervation occurred, and after reinnervation, host axons reoccupied these original synaptic sites.

Mammalian skeletal muscle is highly heterogeneous, consisting of various muscle fibre types with distinct enzymatic profiles, which correspond to their energy metabolism and contraction speed, each adapted to meet different functional demands. Fibres within the same MUs typically exhibit similar or identical metabolic characteristics, suggesting that muscle fibre type expression is largely regulated by neural input (Pette, 1985; Romanul & Van Der Meulen, 1967). The soleus muscle, although composed of both slow and fast-twitch fibres, is predominantly classified as a slow muscle due to its high content of slow-twitch fibres (Crow & Kushmerick, 1982; Schiaffino & Reggiani, 2011), but in our study, muscle regenerated from ES-derived myoblast transplantations consisted only of fast-twitch fibres, which contrasts with the typical nature of the soleus muscle. However, this outcome was anticipated since the myotube cultures *in vitro* were identified as fast-twitch fibres. Romanul & Van Der Meulen (1967) previously demonstrated that cross innervating the slow soleus muscle and fast flexor digitorum longus in cats or flexor hallucis longus in rats reversed their enzymatic properties and contraction times., indicating that nerve supply determines the energy metabolism of muscle fibres. Given that, our analysis occurred only one-month post-transplantation and considering that the electrical properties of adult motoneurons are closely aligned with the contractile properties of the muscle fibres they innervate (Rafuse et al., 1996), it is possible that these muscle characteristics may shift toward slow-twitch fibres over time, as they are innervated by motoneurons naturally controlling the soleus muscle. Additionally, Rafuse et al. (1997) showed that chronic low-frequency stimulation of the cat medial gastrocnemius muscle leads to the conversion of fast-twitch fibres to slow-twitch fibres. Therefore, even if the engrafted fast-twitch fibres do not naturally convert to slow-twitch fibres, chronic low-frequency

stimulation might be helpful to alter their characteristics and induce a shift toward slow-twitch fibres, which should be investigated in future experiments.

Taken together, this study demonstrates the functional integration and normal contractile forces in successfully regenerated skeletal muscle using tdTomato-expressing ES cell-derived myoblasts. These findings underscore the potential of ES cells differentiated into skeletal muscle fibres using a new method to restore muscle function after transplantation as a therapeutic strategy for severe muscle injuries and genetic muscle diseases. Continued advancements in this field hold promise for improving the standard of living for patients suffering from these debilitating conditions.

4.6 Figures

Figure 4.1. Transplanted, tdTomato expressing muscles generate the same contractile forces as unoperated muscles. A) Representative traces of twitch and B) tetanic contractile forces recorded from unoperated (blue trace) and tdTomato (red trace) expressing muscles 60-90 days after transplant. C) Quantification of the mean (± SD) twitch (P= 0.5986) and D) tetanic (P= 0.4441) forces recorded from unoperated and tdTomato expressing soleus muscles 60-90 days post-transplantation. (Welch's t-test).

A)

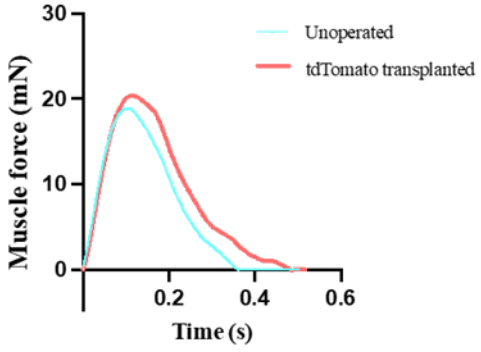
Unoperated
tdTomato transplanted
Muscle force (mN)
30
20
10
0
0.2
0.4
0.6
Time (s)

B)

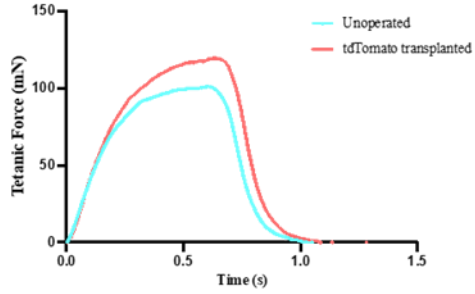
Unoperated
tdTomato transplanted
Tetanic Force (mN)
150
100
50
0
0.0
0.5
1.0
1.5
Time (s)

C)

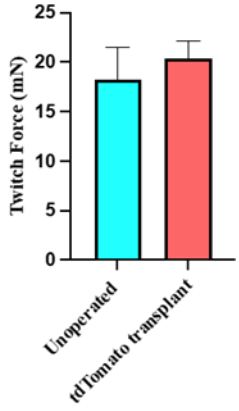
Twitch Force (mN)
25
20
15
10
5
0
Unoperated
tdTomato transplant

D)

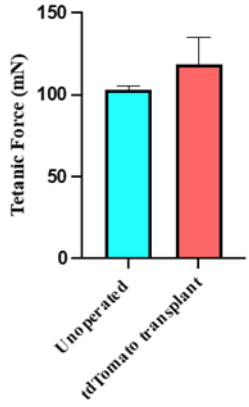
Tetanic Force (mN)
150
100
50
0
Unoperated
tdTomato transplant

Figure 4.2. Synaptic transmission at NMJs in transplanted muscles is normal. A) Representative traces of mEPPs recorded from unoperated and tdTomato expressing myofibres. B) Mean (± SD) mEPP amplitude (**** $P < 0.0001$), C) mEPP frequency ($P= 0.0675$), D) mEPP rise time ($p= 0.1744$), E) mEPP half width ($p= 0.0602$) and F) mEPP decay time ($p= 0.9817$) (Welch's t-test) recorded from unoperated and tdTomato expressing myofibres. G) Representative traces of evoked EPPs recorded from unoperated and tdTomato expressing myofibres. H) Mean (± SD) EPP amplitude recorded from unoperated and tdTomato expressing myofibres. $P>0.9999$ (Welch's t-test). I) Mean (± SD) quantal content in unoperated and tdTomato expressing soleus muscles. $P= 0.4548$ (Welch's t-test).

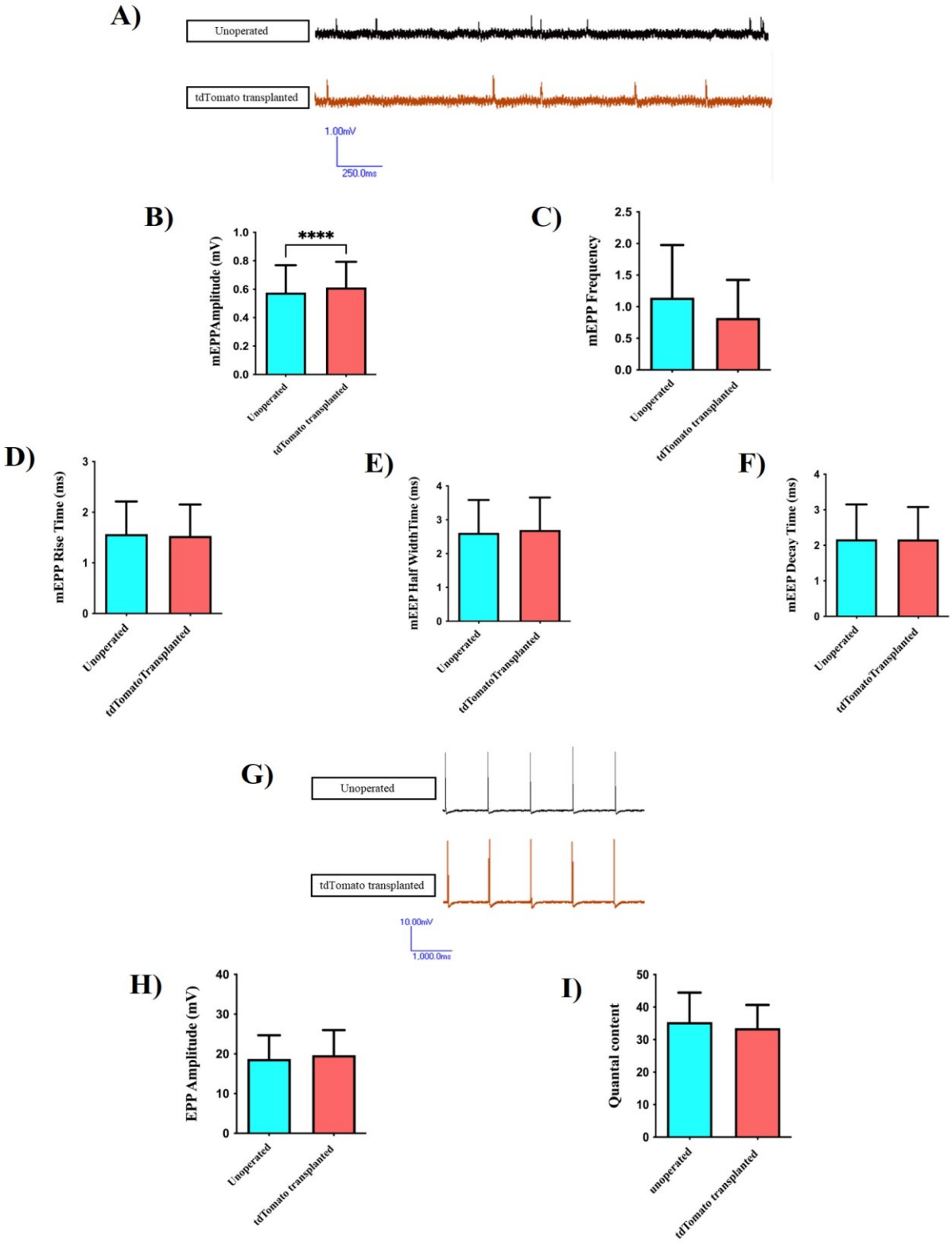
A)
Unoperated
tdTomato transplanted
1.00mV
250.0ms
B)
mEPPAmplitude (mV)
****
Unoperated
tdTomato transplanted
C)
mEPP Frequency
Unoperated
tdTomato transplanted
D)
mEPP Rise Time (ms)
Unoperated
tdTomatoTransplanted
E)
mEEP Half WidthTime (ms)
Unoperated
tdTomatoTransplanted
F)
mEEP Decay Time (ms)
Unoperated
tdTomatoTransplanted
G)
Unoperated
tdTomato transplanted
10.00mV
1,000.0ms
H)
EPP Amplitude (mV)
Unoperated
tdTomato transplanted
I)
Quantal content
unoperated
tdTomato transplanted

Figure 4.3. NMJs in tdTomato-expressing muscles are reinnervated by endogenous motor axons. A) Representative image of tdTomato expressing soleus muscle fibres shows colocalization of SV2 immunostaining and α-BTX labelling indicating that the NMJs were functionally innervated, 60 days after cell transplant. Scale bar=50 μm. B) Mean (± SD) endplates innervation percentage in unoperated and tdTomato expressing soleus muscles 60 days post-transplant. P= 0.0541 (Welch's t-test). C) The image represents localization of AChRs, marked with α-BTX, on longitudinal sections in unoperated and tdTomato expressing soleus muscles. Scale bar= 500 μm.

A)

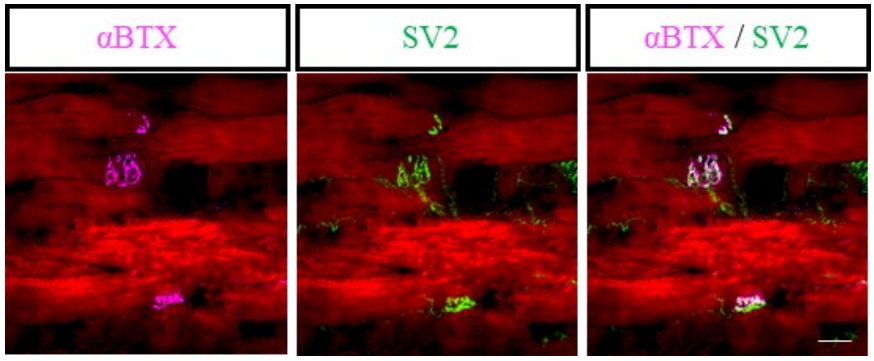
αBTX
SV2
αBTX / SV2

B)

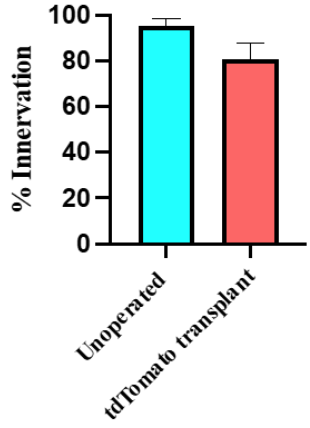
% Innervation
100
80
60
40
20
0
Unoperated
tdTomato transplant

C)

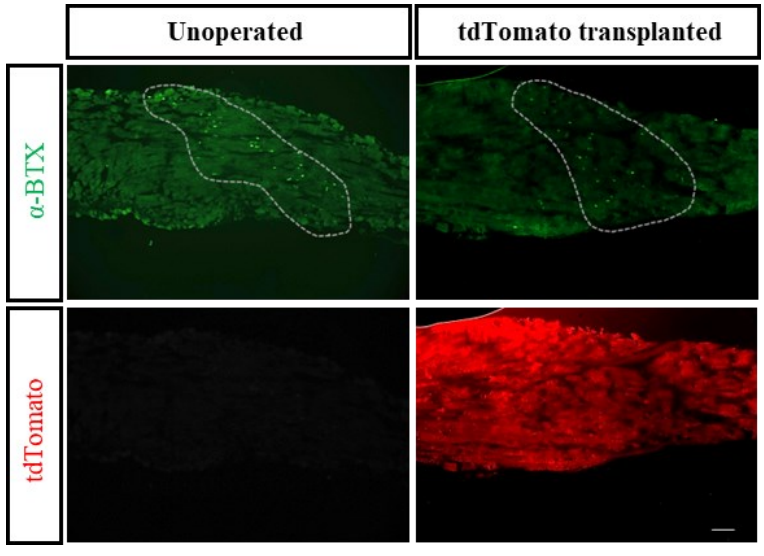
Unoperated
tdTomato transplanted
α-BTX
tdTomato

Figure 4.4. Engrafted muscle fibres are fast-twitch fibres. A) Representative cross section of an unoperated soleus muscle, immunostained for fast and slow myosin and Hoechest. Image indicates combination of fast, slow and hybrid fibres. Scale bar 500 and 50 μm. B) Representative cross section of a tdTomato- expressing soleus muscle, immunostained for fast and slow myosin. Transplanted muscle fibres are all fast-twitch fibres.

A)

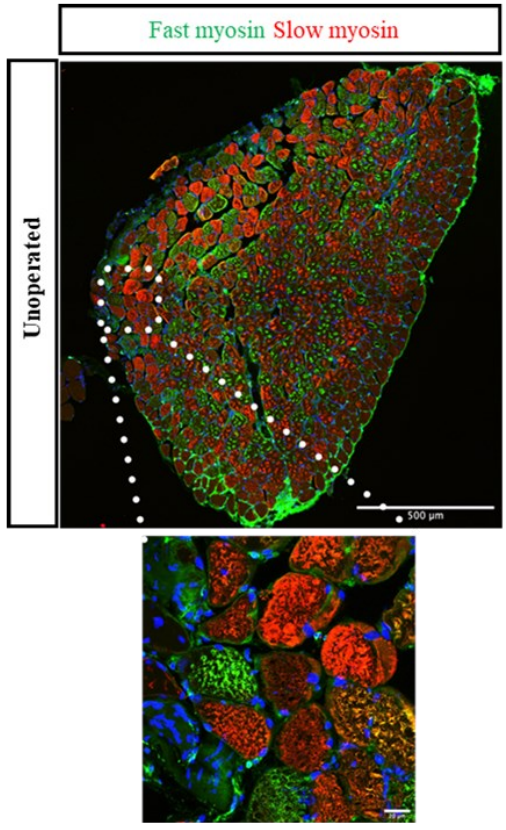
Fast myosin Slow myosin
Unoperated
500 µm

B)

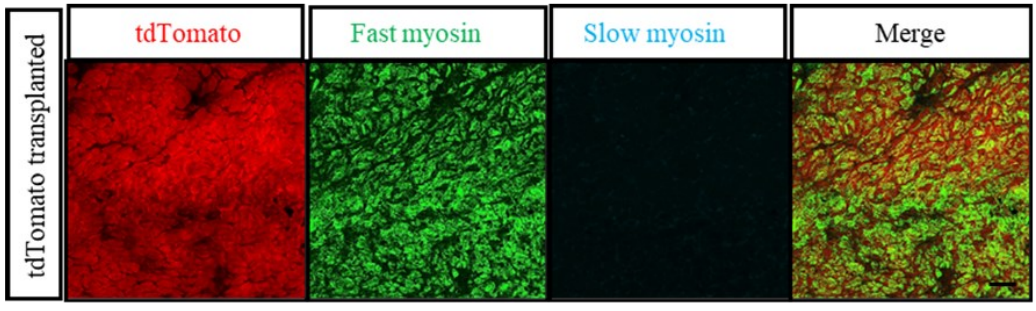
tdTomato transplanted
tdTomato
Fast myosin
Slow myosin
Merge

Chapter 5: Gene Delivery to Embryonic Stem Cell-Derived Skeletal Muscle Cells Using Ionizable Lipid Nanoparticles

5.1 Abstract

Lipid nanoparticles (LNPs) are advanced non-viral vectors developed for efficient gene delivery, offering advantages over viral systems in terms of safety, biocompatibility, and design adaptability. Initially designed based on liposomal structures, LNPs have been extensively employed in delivering nucleic acids, such as messenger RNA (mRNA) and pDNA, across various tissues. This study investigates the use of ionizable LNPs for the delivery of pDNA into mouse ES cell-derived skeletal muscle cells. The objective was to assess the transfection efficiency, cytotoxicity, and apolipoprotein E (ApoE)-dependence of LNP-mediated gene delivery using the tdTomato reporter gene. Twenty-six different concentrations of LNPs, with and without human ApoE isoforms (ApoE2 and ApoE4), were tested *in vitro*. Results demonstrated that LNPs efficiently transfected the muscle cells, and while LNP uptake did not rely solely on ApoE, its presence enhanced transfection efficiency. LNPs selectively transfected myotubes, with minimal transfection in non-muscle cells present in culture, indicating a high degree of cell-type specificity. Importantly, no significant cytotoxicity or inhibition of myofibre formation was observed over the time. These findings underscore the potential of LNPs as a safe and efficient tool for skeletal muscle gene delivery, laying the groundwork for future *in vivo* gene therapy experiments, such as the intramuscular injection of LNPs or the transplantation of LNP-transfected cells into damaged, non-regenerating muscles.

5.2 Introduction

One of the major challenges in gene therapy and the delivery of external DNA or RNA polymers to target cells or organs is efficient delivery (Cullis & Hope, 2017; Whitehead et al., 2009). The challenges in delivering naked RNA or DNA molecules are substantial. These molecules are rapidly degraded by biological fluids and do not accumulate in target tissues when administered systemically. Even if they manage to reach the target tissue, they cannot easily enter the target cells. Additionally, the immune system is highly efficient at detecting and eliminating vectors carrying genetic material, making it difficult for these molecules to evade immune surveillance and achieve successful delivery (Bowie & Unterholzner, 2008). To address these obstacles, LNPs have been developed as non-viral carriers over recent decades (Felgner et al., 1987). LNPs are easy to formulate and produce, have a lower likelihood of triggering immune responses, are biocompatible, enable efficient absorption in the body, can carry larger genetic materials, are capable of multiple doses, and are highly adaptable in design (Cullis & Hope, 2017; Sercombe et al., 2015; Swetha et al., 2023; Swingle et al., 2021). Additionally, LNPs can be optimized for specific cell targeting and therapeutic applications by adjusting the lipid-to-mRNA ratio (Swetha et al., 2023). However, some challenges with LNP delivery still stands, such as unintended interactions with serum proteins, rapid clearance, off-target effects, and endosomal degradation (Swingle et al., 2021).

The development of LNP systems, which feature a hydrophobic core of neutral ionizable lipids and polar regions carrying nucleic acids, was influenced by earlier research on bilayer liposome structures (Cullis & Felgner, 2024; Cullis & Hope, 2017; Tenchov et al., 2021). This was further supported by foundational research on lipid behavior, including

studies on lipid polymorphism and asymmetry. Additionally, experience gained from creating liposomal drug formulations, particularly for anticancer treatments, played a significant role in shaping the design of modern LNP systems (Cullis & Felgner, 2024). LNPs are now widely used to encapsulate and deliver various types of nucleic acids, including pDNA (Ambegia et al., 2005; Wheeler et al., 1999), mRNA (Chen et al., 2023; Du et al., 2023; Melamed et al., 2023; Polack et al., 2020; Thorogood et al., 2023; A. B. Vogel et al., 2021), small interfering RNA (siRNA) (Rungta et al., 2013; Zimmermann et al., 2006), immunostimulatory oligonucleotides (Raney et al., 2008; K. D. Wilson et al., 2009), and antisense oligonucleotides (Maurer et al., 2001; Semple et al., 2001). The use of LNPs has become increasingly popular in therapeutic applications, particularly since the COVID-19 pandemic, during which SARS-CoV-2 mRNA vaccines (Moderna and Pfizer/BioNTech) utilized LNP carriers (Corbett et al., 2020; A. B. Vogel et al., 2021).

LNP entry into cells occurs through endocytosis (Chatterjee et al., 2024; Patel et al., 2023; Rungta et al., 2013). In organs with high concentrations of ApoE, such as the brain and liver, ApoE serves as a crucial endogenous ligand, binding to ionizable LNPs and facilitating receptor-mediated endocytosis through low-density lipoprotein receptors (LDLR) (Patel et al., 2023; Yan et al., 2005). ApoE also plays a significant role in muscle regeneration and is highly expressed in muscle satellite cells (B. I. Burke et al., 2023). Additionally, very low-density lipoprotein receptors (VLDLR) are abundant in skeletal muscle cells, facilitating ApoE binding and aiding endocytosis (Go & Mani, 2012; Iwasaki et al., 2005).

LNPs have been shown to successfully transfect a variety of tissues, including the liver (Jayaraman et al., 2012; Khan et al., 2014), lungs (Q. Li et al., 2020; Lokugamage et al.,

2021; Parhiz et al., 2018), skin (Bolsoni et al., 2023), and brain (Palanki et al., 2023; Rungta et al., 2013, 2015), however our knowledge on muscle transfection is limited.

In this study, we examined the transfection efficiency and cytotoxicity of various LNP concentrations on ES cell-derived skeletal muscle cells *in vitro*. We employed ionizable LNPs to deliver the tdTomato gene to these cells. A total of 26 different concentrations of LNP-tdTomato, both with and without two human ApoE isoforms (ApoE2 and ApoE4), were tested to determine the optimal concentration for transfecting muscle cells and to investigate whether LNP uptake in muscle cells is ApoE-dependent After transfection, we observed the cells for at least 16 days, monitoring signs of proliferation, myofibre formation, and tdTomato gene expression. LNP uptake in muscle cells was efficient, with a concentration of 4 μg/ml showing the best transfection results. While LNP transfection was not entirely dependent on the presence of ApoE in the medium, both ApoE isoforms enhanced LNP uptake. Throughout the observation period, no significant toxicity or cellular damage was observed at any of the tested concentrations. The cells continued to grow and consistently expressed the tdTomato gene. Additionally, LNPs demonstrated effective selectivity, specifically targeting skeletal muscle cells without significantly transfecting other cell types, such as fibroblasts, present in the culture. These results indicate that the LNPs were well-tolerated by skeletal muscle cells at the tested concentrations, providing efficient and highly selective gene delivery.

5.3 Materials and Methods

5.3.1 Embryonic Body Formation

For this experiment, we used wild-type mouse ES cells (a gift from Gregory L. Cox, The Jackson Laboratory). ES cells were quickly thawed and immediately transferred into a tube containing Hanks' Balanced Salt Solution (HBSS) (Thermo Fisher Scientific). Following centrifugation, the cell pellet was resuspended in ES cell medium. This medium was prepared with 82.5 ml Knockout DMEM (Invitrogen), supplemented with 15 ml ES Grade Fetal Bovine Serum (VWR), penicillin-streptomycin (Thermo Fisher Scientific), 1 ml 2-mercaptoethanol, 1 ml Nonessential Amino Acids (NEAA), 500 µl Hepes (Invitrogen), 10 µl Mouse Recombinant LIF (Stemcell Technologies), 10 µl Mirdametinib, and 10 µl GSK3β inhibitor (Stem Cell Technologies). The cells were then plated onto cell culture dishes pre-coated with MTOC-treated PMEF in 5 ml of ES medium. Over the next few days, the cells began forming colonies. Subsequent passages were performed every two days, and once the ES cells reached sufficient growth, the medium was replaced to initiate embryoid body formation. The cells were gently rinsed with HBSS, detached using TripLE Express enzyme (Thermo Fisher Scientific). After centrifuge, the cells were resuspended in differentiation medium, which was composed of 125 ml Neurobasal medium (Invitrogen), 125 ml Advanced DMEM/F12 (Invitrogen), 2.85 ml 2-mercaptoethanol (Embryomax), 2.85 ml Glutamax (Invitrogen), and 28.5 ml Knockout Serum Replacement (Invitrogen). To purify the ES cell population, the cell suspension was plated onto gelatin-coated dishes and incubated for 30 minutes, allowing PMEFs to adhere to the gelatin layer. Non-adherent cells were collected, centrifuged, and

resuspended. These cells were then cultured in suspension in differentiation medium at 37°C for two days to promote the formation of embryoid bodies.

5.3.2 ES Cell Differentiation to Skeletal Muscle

Embryoid bodies were generated and, after two days, transferred to suspension culture dishes containing STEMDiff APEL medium (Stem Cell Technologies), supplemented with 0.5 μM GSK3β inhibitor, 20 μM Forskolin, and 10 ng/mL bFGF (all from Stem Cell Technologies) for a period of five days. Subsequently, three embryoid bodies were chosen and plated into individual wells, each containing circular Thermanox coverslips that had been pre-coated with Matrigel. The same STEMDiff medium, containing GSK3β inhibitor, Forskolin, and bFGF were added. After three days, once the embryoid bodies adhered to the coverslips, the medium was replaced with DMEM muscle medium (Thermo Fisher Scientific) supplemented with 2% horse serum and 1% penicillin-streptomycin (Thermo Fisher Scientific). The day of DMEM application was considered as day 0. The cells were maintained in this medium until the end date which was refreshed every 3 days.

5.3.3 Culture Dissociation and Replating

The DMEM medium was discarded. The cells were then rinsed with EDTA (Thermo Fisher Scientific) for 10 minutes. Afterward, 2X Trypsin EDTA and 10X DNase were added to the cells, followed by gentle trituration to dissociate the cells. The resulting cell suspensions were centrifuged, and the cell pellets were resuspended in muscle medium. After counting the number of cells, 100,000 cells were replated in each cell culture wells, each containing circular coverslips that had been pre-coated with Matrigel.

5.3.4 LNP and ApoE transduction

On the second day after cell replating, LNPs at concentrations of 4, 2, 0.4, and 0.2 µg/µl (produced by Dr. Pieter Cullis's laboratory, UBC Nanomedicines Research Group) were prepared based on the pDNA concentration provided for each vial and diluted in 500 µl of DMEM medium per well. Different concentrations of Recombinant Human ApoE2 (Abcam) or Recombinant Human ApoE4 (Peprotech) were added to the DMEM medium containing LNPs and applied to each well. After 24 hours, the medium was discarded, and fresh medium was added to each well.

5.3.5 Immunohistochemistry

Cultures were fixed in 4% PFA for 15 minutes. After fixation, cells were gently rinsed three times with 1x PBS. The samples were then incubated overnight at 4°C with primary antibody, mouse rabbit anti-desmin IgG (1:1000, Abcam), which was diluted in a solution of 1% BSA (VWR) in PBS with 0.5% PBS-Triton. Following three additional washes with PBS, secondary antibody, Alexa Fluor 488-conjugated goat anti-rabbit IgG (1:500, Invitrogen) was applied for 1-2 hours at room temperature in the dark. After another series of PBS rinses, nuclei were stained with Hoechst 33342 (Sigma-Aldrich) at 0.1 µg/ml in PBS for 10 minutes. Following the final wash, circular coverslips were mounted onto microscope slides using a lab-prepared mounting medium composed of 1:2 glycerol in 1x PBS, with 0.03 mg/ml ρ-phenylenediamine.

5.3.6 Western blot

After washing with HBSS, cells were lysed using cold RIPA buffer (Thermo Fisher Scientific) containing protease inhibitor cocktail tablets (Complete Mini, Roche Diagnostics, Mannheim, Germany). The lysed cells were kept at 4°C for 30 minutes and

then centrifuged at 14,000 RPM for 20 minutes at 4°C. The pellets were discarded, and the protein concentration of the supernatants was determined using a BCA assay (Pierce BCA assay kit, Thermo Fisher Scientific). A 4X SDS sample buffer was prepared by mixing 4 ml of 10% SDS, 2 ml of glycerol, 0.309 g of dithiothreitol, and 0.2 g of bromophenol blue in 50 ml of distilled water. The samples were boiled for 10 minutes and separated on a 10% acrylamide gel. Following electrophoresis, the proteins were transferred onto an Immuno-blot PVDF membrane (BIO-RAD), which was blocked for 1 hour at room temperature with 4% milk in TBS-T. The membranes were then incubated overnight with primary antibodies—rabbit anti-desmin IgG (1:1000, Abcam) or rabbit anti-RFP IgG (1:1000, Rockland), both diluted in 1% milk in TBS-T. After washing, the membranes were incubated with an HRP-conjugated goat anti-rabbit IgG secondary antibody (1:10000, Cell Signaling Technology) for 1 hour at room temperature. Protein bands were detected using chemiluminescence (Thermo Fisher Scientific) and visualized on high-performance chemiluminescence film (GE Healthcare). The blots were then stripped using stripping buffer (Thermo Fisher Scientific), re-blocked, and re-probed with rabbit anti-Glyceraldehyde 3-phosphate dehydrogenase (GAPDH) IgG (1:5000, Rockland) as the primary antibody, followed by incubation with the same HRP-conjugated secondary antibody mentioned above. The films were developed, and protein band sizes were analyzed using ImageJ software.

5.3.7 Imaging

Images were captured using an upright fluorescent microscope (Leica Instruments), and the subsequent image analysis was conducted using Zen-Blue software (Zeiss).

5.3.8 Statistical Analysis

Statistical analysis and graph generation were performed using GraphPad Prism (version 10) software. Multiple comparisons were done using Brown- Forsythe and Welch ANOVA tests. Data were presented as mean ± SD, and statistical significance was set at $P < 0.05$.

5.4 Results

5.4.1 LNPs Transfect ES Cell-Derived Skeletal Muscle Cells

LNPs are among the most advanced drug delivery systems used in clinical applications. To date in addition to the mRNA vaccines, six other LNP-based medications have received FDA approval for clinical treatments (T. M. Allen & Cullis, 2004; P. J. C. Lin et al., 2013). These nanoparticles can deliver various nucleic acid forms into the cells (Jung et al., 2022; Samaridou et al., 2020) Although LNPs have been shown to transfect a range of tissues, such as neural cells in the brain (Rungta et al., 2013) and hepatocytes in the liver (Jayaraman et al., 2012; Khan et al., 2014), we aimed to determine whether LNPs could also be taken up by skeletal muscle cells and deliver tdTomato pDNA into these cells. Previous studies have demonstrated that neurons and hepatoma cells rely on ApoE for efficient LNP uptake, as ApoE plays a crucial role in cholesterol and lipid transport in both liver and brain tissue (Han, 2004; Mahley & Rall, 2000; Nuriel et al., 2017). ApoE, by adsorbing onto the LNPs, bind these nanoparticles to its receptors and facilitate LNP endocytosis (Patel et al., 2023; Yan et al., 2005). Thus, we investigated whether ApoE is similarly required for LNP transfection of the muscle cells.

For this experiment, wild-type mouse ES cell-derived skeletal muscle cultures were used. After the cells had matured, they were dissociated, replated, and allowed to settle for two days. We then exposed the cells to 26 different concentrations of LNPs carrying the tdTomato gene, in the presence or absence of recombinant human ApoE isoforms (ApoE2 and ApoE4). Specifically, we tested four concentrations of LNP- tdTomato (4 μg/ml, 2 μg/ml, 0.4 μg/ml, and 0.2 μg/ml), each with varying ApoE2 or ApoE4 concentrations (0, 0.1 μg/ml, 0.2 μg/ml, 1 μg/ml and 2 μg/ml). After 24 hours, the medium was washed, and the cells were allowed to grow at least 15 days post-transfection. The process is illustrated in Figure. 5.1A.

Figure 5.1B depicts myofibre cultures treated with 4 μg/ml LNP- tdTomato in the presence and absence of 1 or 2 μg/ml ApoE2 or ApoE4, 15 days post-transfection. Western blot analyses were performed after lysing the cells, and desmin and tdTomato expression levels were normalized to GAPDH level a house keeping protein. Ultimately, the tdTomato/desmin ratio was calculated for each sample. Western blot results indicated that cells treated with 4 μg/ml LNP-tdTomato (Fig. 5.1C) exhibited the highest tdTomato/desmin ratio, compared to those treated with 2 μg/ml (Fig. 5.1D), 0.4 μg/ml (Fig. 5-1E), and 0.2 μg/ml (Fig. 5-1F). No significant differences were observed between the samples within each LNP group, nor between the 2 μg/ml (Fig. 5.1D) and 4 μg/ml LNP groups (Fig. 5.1C). Similarly, no differences were detected between the 0.4 μg/ml (Fig. 5.1E) and 0.2 μg/ml (Fig. 5.1F) LNP groups. The comparison of tdTomato levels to desmin level indicated that 0.4 μg/ml (Fig. 5.1E) and 0.2 μg/ml (Fig. 5.1F) LNPs were insufficient to transfect the cells in each culture well. When comparing higher LNP concentrations, although there was no substantial difference in transfection efficiency

between the 2 µg/ml (Fig. 5.1D) and 4 µg/ml (Fig. 5.1C) concentrations, the 4 µg/ml group showed overall better results. Furthermore, unlike in neural and hepatoma cells, LNP uptake by skeletal muscle cells was not entirely dependent on ApoEs. However, the presence of ApoEs, particularly ApoE4, enhanced transfection efficiency and resulted in higher tdTomato expression in the muscle cells.

5.4.2 LNP Transfection of Skeletal Myofibres is Long-Lasting

Skeletal muscle cultures were monitored at various time points after transfection to assess the longevity of tdTomato expression during myoblast growth and maturation into myofibres, as well as to determine whether LNP-tdTomato exhibit any toxicity that could damage the myofibres. Figure 5.2 illustrates the myofibre cultures on days 4, 8, and 16 post-transfections, where the myofibres continue to strongly express tdTomato and maintain a healthy appearance. Notably, these cultures exhibited no signs of cell stress or damage, which is indicative of the biocompatibility of the LNPs used in this study.

Furthermore, while the figure captures the results up to day 16, it is important to note that these cell cultures have been observed to survive for up to two months while still expressing tdTomato (data not shown). This suggests that the pDNA introduced via LNPs remains stable and effective for an extended period. Additionally, the lack of any adverse effects on the muscle cells' development further demonstrates that the LNP-based delivery system is not toxic to the cells, nor does it inhibit the maturation of myofibres.

This long-term stability and non-toxicity of LNP-mediated transfection make it a promising tool for gene delivery in skeletal muscle cells, particularly for research and therapeutic applications that require sustained gene expression.

5.4.3 LNPs Transfect the Myotubes Selectively

Interestingly, while studying the transfection of myotubes using LNP- tdTomato, we discovered that these vectors selectively transfect skeletal myotubes. This is noteworthy because the muscle cultures used were not 100% pure and contained other cell types, such as fibroblasts. As shown in Figure 5.3, the cells were fixed and immunostained for muscle-specific marker, desmin and Hoechst. The fibres expressing tdTomato largely co-expressed desmin, confirming their identity as myotubes. The Hoechst -stained nuclei which did not co-label with either tdTomato or desmin indicate the presence of non-muscle cell types, such as fibroblasts, within the culture.

This selective transfection suggests that LNPs have a strong preference for skeletal muscle cells, even in mixed cell populations, making them particularly effective for gene delivery to muscle cells. This specificity has significant implications for muscle gene therapy, as LNPs could be utilized to target muscle cells without affecting surrounding non-muscle cells, minimizing off-target effects.

5.5 Discussion

The efficient delivery of genetic material to target cells within living organisms has been a persistent obstacle in gene therapy. However, recent innovations, particularly in lipid-based technologies, have provided a means to overcome these limitations. LNPs have emerged as a breakthrough solution, facilitating the effective delivery of nucleic acid-based vaccines and therapies, thus transforming the landscape of gene therapy and unlocking new treatment possibilities for a broad range of diseases (Cullis & Felgner, 2024). Compared to viral vectors, LNPs offer numerous advantages, including enhanced safety profiles, improved tolerability, the capacity to encapsulate large nucleic acids, and

the potential for repeated dosing. Additionally, LNPs are more economical and easier to produce. These features, coupled with their ability to enable personalized, targeted treatments within weeks, have contributed to their rising popularity in fields such as gene therapy and mRNA vaccine development (Cullis & Felgner, 2024). One limitation of current LNP systems is their inability to deliver DNA to the nucleus of non-dividing cells, which limits gene expression in these cells. However, gene writing technologies that use mRNA to insert DNA sequences selectively may overcome this challenge (Pallarès-Masmitjà et al., 2021).

LNP systems have evolved from liposomal platforms, which are versatile nanocarriers designed to transport a range of compounds, from small molecules to proteins and genetic materials. As the first nanomedicine delivery system to move from theoretical development to clinical application, several liposomal formulations have gained regulatory approval and are currently in use (Cullis & Felgner, 2024; Cullis & Hope, 2017; Tenchov et al., 2021). LNPs facilitate cellular uptake through endosomal pathways, where the ionizable cationic lipids become protonated in the acidic endosomal environment. This protonation triggers interactions with naturally occurring anionic lipids, leading to the formation of non-bilayer structures that disrupt the endosomal membrane. This process enables the release of the nucleic acid cargo into the cytoplasm, where it is subsequently transported to the nucleus for transcription (Buck et al., 2019; Cullis & Felgner, 2024).

To date, LNPs have successfully delivered various nucleic acids, such as pDNA (Ambegia et al., 2005; Wheeler et al., 1999), mRNA (Polack et al., 2020), siRNA (P. J. C. Lin et al., 2013; Zimmermann et al., 2006), and anti-sense oligonucleotides (Maurer et al., 2001; Semple et al., 2001), targeting a wide range of tissues. These include the liver (Jayaraman

et al., 2012; Khan et al., 2014), lungs (Q. Li et al., 2020; Lokugamage et al., 2021; Parhiz et al., 2018), T cells (Rurik et al., 2022), endothelial cells (Parhiz et al., 2018; Sago et al., 2018), pancreas (Melamed et al., 2023), kidney (Lai et al., 2018), skin (Bolsoni et al., 2023), and heart (Evers et al., 2022). Direct LNP injections into the brain (Palanki et al., 2023; Rungta et al., 2013, 2015) and eyes (Herrera-Barrera et al., 2023) have also been documented. The success of COVID-19 mRNA vaccines has increased interest in LNP-based mRNA delivery. Chen et al. (2023) developed and optimized iso-A11B5C1, an ionizable lipid that targets muscle tissue with intramuscular delivery while limiting off-target effects on the liver and spleen. This method also triggered strong cellular immune responses. Additionally, a comparison of LNP-mRNA vaccines delivered through intramuscular and hydrodynamic limb vein (HLV) injections in mice showed that HLV injection provided broader and more even mRNA distribution across muscle groups, reduced muscle damage, and caused a milder inflammatory response, making it a better option for applications needing less tissue injury (Du et al., 2023). However, these studies focused on the immune system response and did not examine the extent of LNP uptake by muscle cells. In this study, we investigated the ability of an LNP-pDNA system to enter skeletal muscle cells *in vitro* and analyzed the subsequent expression of the gene of interest in muscle fibres. This research lays the groundwork for future *in vivo* intramuscular injections of these vectors, or the transplantation of skeletal muscle cells transfected by these LNPs.

A study by Bisgaier et al. (1989) found that liposome uptake into hepatoma cells *in vitro* was doubled in the presence of ApoE, while other types of apolipoproteins, specifically ApoE A-IV and ApoE A-I, reduced LNP insertion into the cells. Additionally, Akinc et

al. (2010) observed that LNPs encapsulating siRNAs for gene silencing were more effectively taken up by HeLa cell cultures in the presence of ApoE isoforms (ApoE2, ApoE3, or ApoE4). They also found that *in vivo*, LNP uptake was facilitated in the liver when endogenous ApoEs were present, while this uptake was completely abolished in ApoE knockout mice. This is because ApoE adsorption to LNPs allows recognition by scavenger and LDLRs located on hepatocyte surfaces. In addition to the liver, Rungta et al. (2013) studied LNP-siRNA uptake in both primary neuronal cultures *in vitro* and brain neurons through intracranial injections *in vivo*. Since ApoE is a major brain lipoprotein synthesized in astrocytes, they explored its role in LNP uptake by primary neuronal cells in the presence or absence of ApoE4, finding that LNPs were taken up by the cells in an ApoE-dependent manner. However, Parhiz et al. (2018) demonstrated that LNPs encapsulating mRNA conjugated with antibodies specific to the vascular cell adhesion molecule PECAM-1, designed to prevent liver uptake after systemic administration, were taken up to the lung cells in an ApoE-independent manner. It is known that ApoEs play a significant role in skeletal muscle regeneration and are highly expressed in quiescent satellite cells, with expression decreasing upon satellite cell activation (B. I. Burke et al., 2023). Interestingly, satellite cells derived from ApoE knockdown mice exhibit delayed activation and differentiation when cultured *ex vivo*, as well as reduced proliferation and differentiation *in vitro* (Barlow et al., 2021). In an *in vivo* skeletal muscle regeneration study, involving mice homozygous for either the human ApoE2, ApoE3, or ApoE4 allele, after TA muscle damage through barium chloride ($BaCl_2$) injections, no differences were observed among ApoE isoforms in their ability to activate muscle regeneration (B. I. Burke et al., 2023). Given ApoE's role in LNP uptake, our study aimed to investigate whether ApoEs influence LNP-pDNA uptake by ES-cell derived skeletal muscle cells *in vitro*. Our

findings revealed that muscle cells do not necessarily rely on ApoEs for LNP uptake, though both ApoE2 and ApoE4 improved the transfection efficiency.

LNPs overall are recognized as a safe drug delivery system. In a study assessing the cytotoxicity of three different LNP formulations—anionic, neutral, and cationic—encapsulating siRNAs in both adherent and non-adherent cell lines, results indicated that LNPs were largely non-toxic at conventional gene delivery concentrations. No significant reduction in cell viability was observed with anionic and neutral LNPs. However, cationic LNPs demonstrated some toxicity and reduced cell viability in adherent cells at higher concentrations (Syama et al., 2022). Ionizable LNPs, which change charge based on pH levels, exhibit lower toxicity compared to permanent cationic LNPs. This reduced toxicity is due to their protonation in acidic environments, making them less harmful in physiological conditions (Tang et al., 2023). Despite the safety profile, LNPs have a tendency to accumulate in the liver and spleen due to high ApoE concentrations, presenting a minor risk of hepatotoxicity (Bitounis et al., 2024; Tang et al., 2023). In our experiment, although we did not conduct a formal cell viability test (which could be included in future studies), we observed the cells for at least 16 days post-transfection. During this period, no toxicity or cell damage was noted at any of the concentrations we tested. The cells continued to proliferate, form long myofibres, and express the tdTomato gene. In future studies, higher LNP concentrations could be explored to further assess potential toxicity.

Furthermore, our study revealed the selective transfection of skeletal myotubes by LNPs, with little to no transfection observed in non-muscle cells such as fibroblasts. This specificity is significant, as it suggests that LNPs can target muscle cells effectively in mixed cell populations, minimizing off-target effects. Such selective targeting could have

important implications for muscle gene therapies, where precise delivery to muscle cells is critical for therapeutic efficacy and safety.

In conclusion, our study supports the use of LNPs as a safe and effective tool for gene delivery in skeletal muscle cells. The long-lasting expression, low toxicity, and selective transfection of myotubes make LNPs a promising candidate for further development in muscle gene therapy. Future research should continue to explore *in vivo* applications, including direct injection of LNPs into healthy skeletal muscle, as well as the transplantation of cells transfected by these vectors into injured, non-regenerating skeletal muscles.

5.6 Figures

Figure 5.1. LNP- tdTomato efficiently transfect the myoblast/ myotube cultures *in vitro*. A) Schematic illustration of myoblast/myotube culture transduction with LNPs encapsulated pDNAs *in vitro.* B) Myoblast/myotube cultures 15 days post-transfection with 4 µg/ml LNP- tdTomato, in the absence or presence of 1 µg/ml or 2 µg/ml ApoE2 or ApoE4, immunostained for desmin (green) and tdTomato (red). Scale bar = 100 µm. C) Western blot analysis and mean (± SD) of tdTomato/Desmin ratio in cell groups of myotube culture homogenates 15 days post-treatment with 4 µg/ml LNP- tdTomato and 0, 1, or 2 µg/ml ApoE2 or ApoE4 (Brown-Forsythe and Welch ANOVA). D) Western blot analysis and mean (± SD) of tdTomato/Desmin ratio of cell groups transfected with 2 µg/ml LNP- tdTomato and 0.1, 0.2, 1, or 2 µg/ml ApoE2 or ApoE4 (Brown-Forsythe and Welch ANOVA). E) Western blot analysis and mean (± SD) of tdTomato/Desmin ratio of cell groups transfected with 0.4 µg/ml LNP- tdTomato and 0, 1, or 2 µg/ml ApoE2 or ApoE4 (Brown-Forsythe and Welch ANOVA). F) Western blot analysis and mean (± SD) of tdTomato/Desmin ratio of cell groups transfected with 0.2 µg/ml LNP- tdTomato and 0.1, 0.2, 1, or 2 µg/ml ApoE2 or ApoE4 (Brown-Forsythe and Welch ANOVA).

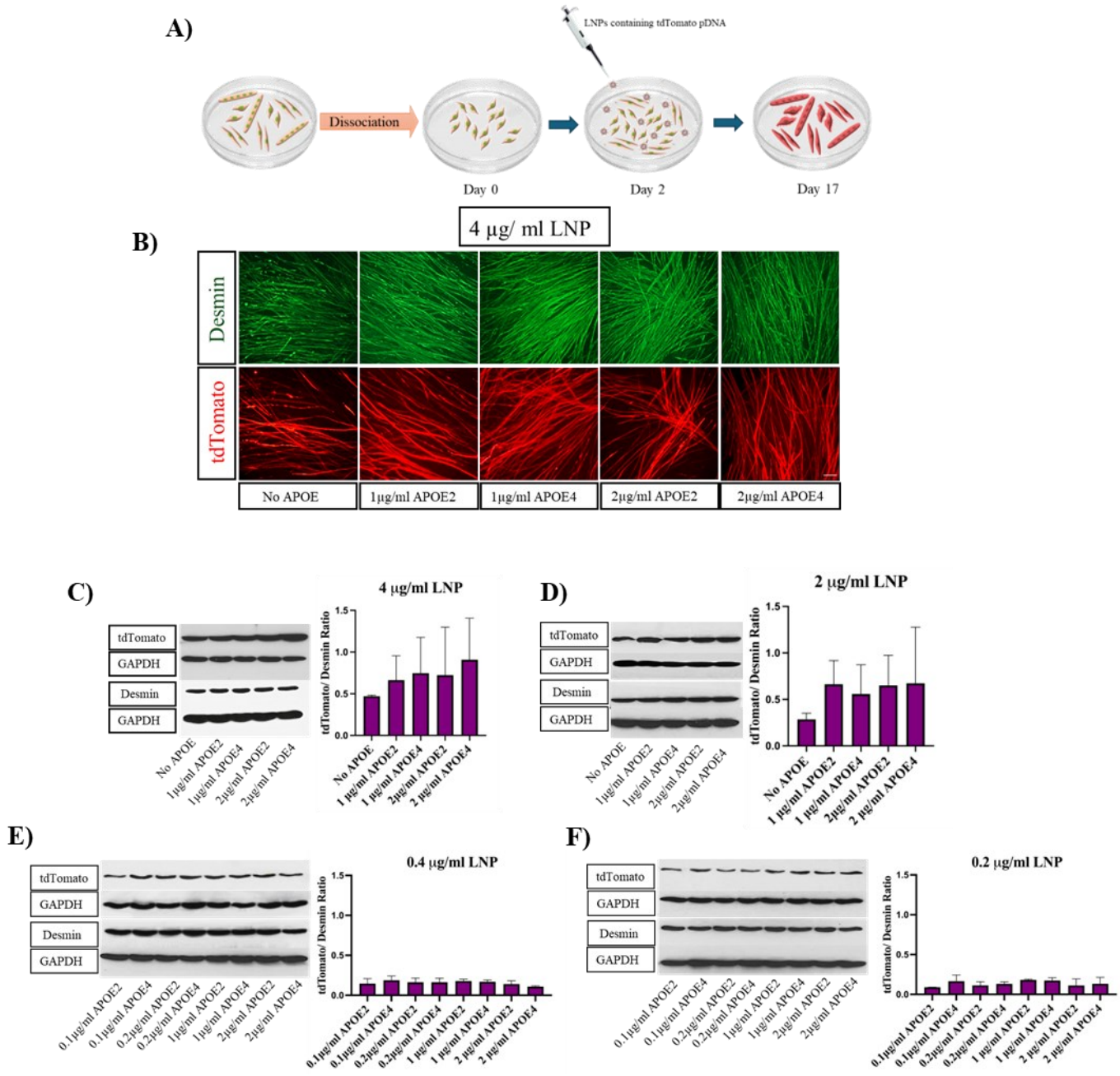
A)
LNPs containing tdTomato pDNA
Dissociation
Day 0
Day 2
Day 17
B)
4 µg/ ml LNP
Desmin
tdTomato
No APOE
1µg/ml APOE2
1µg/ml APOE4
2µg/ml APOE2
2µg/ml APOE4
C)
tdTomato
GAPDH
Desmin
GAPDH
4 µg/ml LNP
tdTomato/ Desmin Ratio
D)
2 µg/ml LNP
E)
0.4 µg/ml LNP
F)
0.2 µg/ml LNP

Figure 5.2. tdTomato expression via LNP transfection remains stable over an extended period. A) Myoblast/myotube cultures transfected with 4 µg/ml LNP- tdTomato and 2 µg/ml ApoE4, immunostained for tdTomato (red) on days 4, 8, and 16 *in vitro*. Scale bar =100 µm

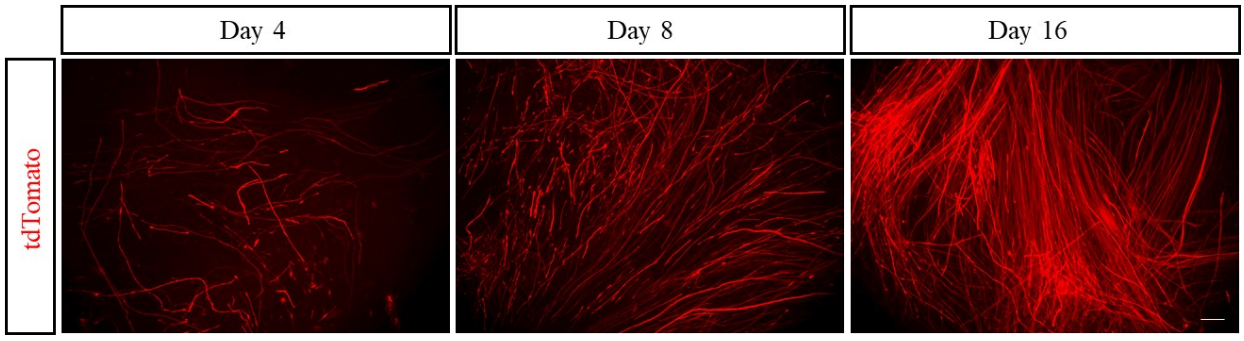
Day 4
Day 8
Day 16
tdTomato

Figure 5.3. Selective transfection of myotubes via LNPs. A) Myoblast/myotube cultures transfected with 4 μg/ml LNP-tdTomato and 2 μg/ml ApoE4, immunostained for tdTomato (red), desmin (green), and Hoechst (purple). Scale bar = 100 μm.

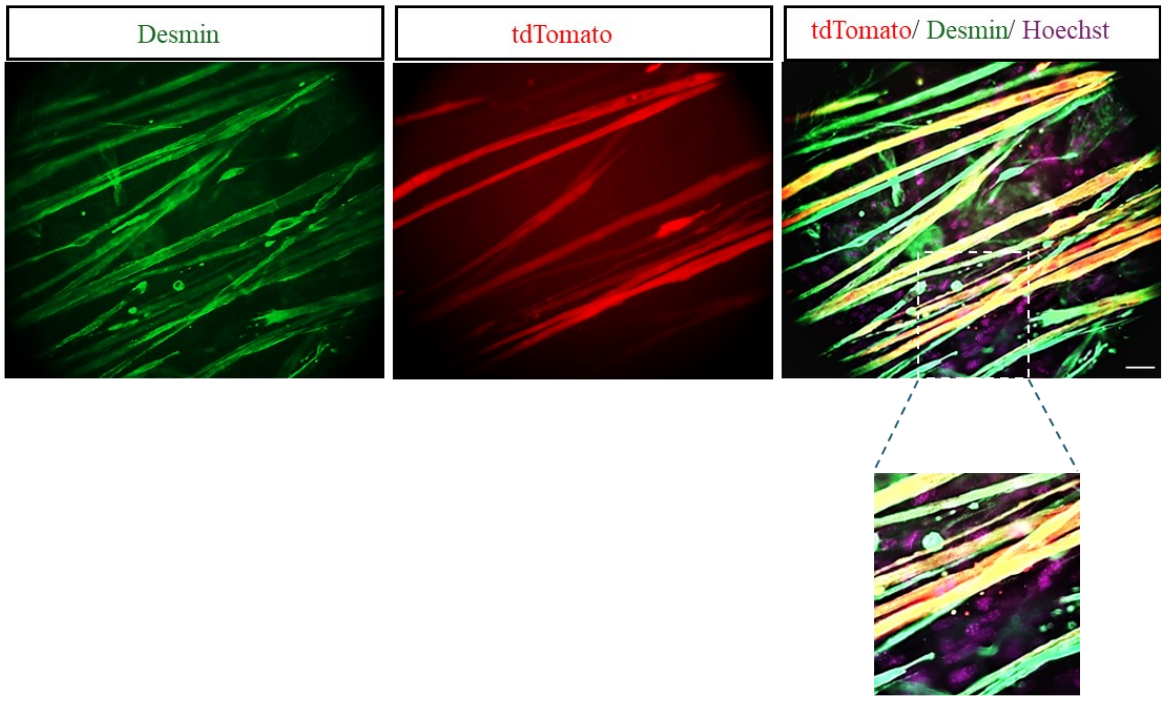
Desmin
tdTomato
tdTomato/ Desmin/ Hoechst

Chapter 6: General Discussion

All studies included in this thesis collectively aimed to advance the field of skeletal muscle regeneration and function restoration, with a particular emphasis on the development and validation of innovative techniques utilizing ES cell-derived myoblasts and optogenetics. These investigations have thoroughly explored methods to produce functional ES cell-derived myoblasts that express external genes of interest, which could be transplanted into injured or denervated muscles to regenerate skeletal muscle and restore muscle function in cases of severe injury and paralysis, highlighting the potential therapeutic applications, particularly using optogenetics.

Additionally, the study has investigated the ability of the regenerated muscles, achieved through the transplantation of ES cell-differentiated myoblasts into notexin-injured muscles with regeneration impeded by irradiation, to establish functional NMJs. Also, we compared the force produced by these regenerated muscles and their intracellular characteristics with the non-operated normal muscles.

Finally, to explore the novel and alternative ways to introduce exogenous genes into ES cell-derived myoblasts, we investigated the efficiency of ionizable LNPs for gene transfer into these cells. Our findings demonstrate that LNPs achieve high transduction specificity with no observed cytotoxicity, indicating their suitability as a promising tool for gene delivery into skeletal muscles.

This general discussion synthesizes the key findings from these studies, situates them within the broader landscape of muscle regeneration research, and underscores the significant implications for future therapeutic strategies.

6.1 Stem Cell-Based Muscle Regeneration

This thesis primarily concentrated on differentiating mouse ES cells into functional skeletal muscle cells, capable of expressing external genes such as ChR2 for use in optogenetic applications. The successful differentiation of ES cells into myoblasts, as demonstrated in the chapter 2, represents a pivotal advancement, particularly in generating myoblasts that express crucial skeletal muscle-specific markers, including myosin and desmin. These differentiated cells were shown to maintain their viability *in vitro* for extended periods, highlighting their potential for therapeutic applications in the realm of muscle transplantation and regeneration. Our differentiation method employed three substances, specifically forskolin, bFGF, and BIO, which were reported by C. Xu et al. (2013) to be beneficial for the myogenesis of hiPSCs. However, our findings indicated a much faster differentiation and maturation process for mouse skeletal muscle cells cultured *in vitro* compared to their study. Furthermore, a detailed examination of the developmental characteristics of these differentiated cells revealed proper differentiation from quiescent satellite cells toward mature myofibres, alongside a concurrent repopulation of the satellite cell pool.

Our differentiation protocols employed were not only effective in generating myoblasts but also successful in producing functional muscle fibres capable of responding to optical stimuli. These studies underscore the capacity of these cells to express external genes, such as tdTomato and ChR2. The production of ChR2-expressing myoblasts facilitates the development of muscle fibres that can be controlled via light stimulation, a capability that is suitable for potential clinical applications, especially in treating conditions involving denervated muscles that have become permanently paralyzed.

Moreover, the use of AAV vectors for gene transduction further demonstrated the versatility of this approach. The AAV-mediated transduction of ChR2 into ES cell-derived myoblasts provided an alternative to creating transgenic lines, offering a more straightforward and potentially clinically applicable method for generating optically responsive muscle tissue. This is particularly significant as it opens up new avenues for non-transgenic therapeutic strategies, which could be more readily translated into human clinical applications.

However, one concern remains: the wild-type ES cell-differentiated myofibres were all the fast-twitch type, and none of the fibres expressed slow MHCs. It is possible that these fast-twitch fibres might switch to expressing slow MHC after more sustained activation. We have not yet examined the ChR2-expressing myofibres to determine if there is any difference in fibre types since these cells can be more frequently activated through light stimulation, and this aspect should be thoroughly investigated in future studies.

Overall, we successfully produced functional skeletal muscle cells *in vitro*, exhibiting all the characteristic features of skeletal muscles, making them suitable for transplantation and cell replacement therapy *in vivo*.

6.2 Myoblast Transplantation

The American Society of Gene and Cell Therapy defines “cell therapy” as the process of administering live, intact cells or promoting the expansion of a specific cell population within a patient to treat various diseases (Negroni et al., 2016). Interestingly, the first successful instance of cell therapy occurred as early as 1665 in the United Kingdom, with the inaugural blood transfusion performed on dogs (Lower, 1665). Over time, blood

transfusions have evolved into a routine medical procedure. Subsequent advancements in transplantation have included bone marrow transplants, and epidermal grafting for severe injuries (Cossu et al., 2018).

The field of myogenic cell transplantation began in 1989, leading by the pioneering work of Partridge et al. (1989), who initiated the engraftment of normal muscle myoblasts into the EDL muscles of mice with DMD. Their work demonstrated an increase in dystrophin levels within these treated muscles. Following this, the first human clinical trials commenced in the early 1990s, targeting individuals with DMD. Between 1990 and 1993, six independent clinical trials were conducted, involving the injection of healthy myoblasts into the muscles of young DMD patients aged 5 to 20 years (Gussoni et al., 1992; Huard et al., 1991, 1992; Karpati et al., 1993; Law et al., 1990). However, the range of dystrophin expression observed in these studies varied widely, from as little as 1% in one study to as much as 10-40% in another. Moreover, the improvements in muscle strength were modest at best, with some cases showing no improvement or even a decline in muscle function. These early clinical attempts were limited in their success, and by 1994, Cho (1994) had argued in a publication that the continuation of myoblast transfer trials, as they were being conducted, was unethical. Although early trials had limited success, these groundbreaking studies demonstrated the potential of cell therapy for skeletal muscle regeneration. since then, numerous myogenic cell transplantation efforts have continued, including the use of satellite cells, myoblasts, pluripotent stem cell-derived myogenic progenitors, and other types of progenitor cells from various sources, all in pursuit of optimal outcomes (Boyer et al., 2021). More recently, significant progress has been made in bioengineering, with

many studies focusing on engineering muscle tissues to improve the effectiveness of grafts (Bursac et al., 2015).

After conducting successful muscle replacement, one of the main challenges that remains is insufficient innervation by endogenous motor axons (Judson & Rossi, 2020; Quarta et al., 2017). Therefore, not only are cell engraftment and proliferation crucial, but proper innervation of the regenerated fibres is also essential to restore muscle functionality.

In this thesis, we demonstrate one of the most successful muscle recovery models to date. By generating functional ES cell-derived myoblasts and transplanting them into completely destroyed muscle tissue with no potential for regeneration, we not only restored muscle mass but also achieved full functional recovery. This includes the successful transplantation of myoblasts expressing tdTomato and ChR2, leading to the complete restoration of muscle force.

Additionally, it was intriguing to discover that chimeric innervation between the regenerated muscle with the transplanted cells, along with endogenous motor axons, occurred in approximately the same location where natural NMJs are found in unoperated muscles. This phenomenon is attributed to the cues provided by the ECM scaffolds, which guide the formation of AChRs (Anglister et al., 1985). Notexin, a type of myotoxin, deteriorates muscle fibres and the plasma membrane without damaging satellite cells, blood vessels, or the ECM (Gutiérrez & Ownby, 2003; Harris, 2003; Harris et al., 2003; Plant et al., 2006). As a result, transplanted cells grow into the remaining basal lamina tubes, allowing NMJs to establish themselves in nearly the same location as they were previously (Harris, 2003).

6.3 Muscle Activation via Optogenetics

Despite decades of research into muscle progenitor cell transplantation, the field of muscle optogenetics is still in its infancy, representing a highly novel area of study. Optogenetics involves the integration of genetic and optical techniques to control and modulate specific cellular functions within living tissues, either by enhancing or inhibiting particular activities (Deisseroth, 2011). The optogenetic toolbox includes light-sensitive proteins capable of altering membrane potential in response to light (Natasha et al., 2013).

The first opsin, bacteriorhodopsin, was discovered in 1971, and shortly thereafter, other opsins were identified: halorhodopsin (Matsuno-Yagi & Mukohata, 1977), ChR1 (Nagel et al., 2002), and ChR2 (Nagel et al., 2003). It was not until 2005 that Boyden and his team successfully expressed ChR2 in mammalian neurons for the first time (Boyden et al., 2005). Since then, extensive research has been conducted to express ChR2 in neurons to activate neural circuits, and more recently, optogenetic applications have been explored in cardiac and skeletal muscle tissues, both *in vitro* and *in vivo* (Bruegmann et al., 2010; Crocini et al., 2016; Magown et al., 2015; Rousseau et al., 2023; Zaglia et al., 2015).

In our study, introducing the ChR2 gene into ES cell-derived myofibres, either through AAV or via transgenic method, led to successful contraction of the fibres when blue light from a fluorescent microscope was applied. On occasion, the light-evoked depolarizations were so strong that the fibres were torn from the Matrigel substrate, necessitating careful examination of these cells for their light response.

Additionally, transplanting these cells into soleus muscles to inhibit regenerative capacity, followed by notexin-induced injury, resulted in light-evoked muscle contractions. The

muscle force generated was comparable to that produced by neural stimulation in the case of myoblasts expressing ChR2 transgenically. However, when myoblasts transduced with AAV-PHP.eB-CAG-ChR2-EYFP were engrafted, although the muscles were responsive to light stimulation and generated force, it was slightly lower than the force produced by neural stimulation. This discrepancy in force magnitude between neural and optical stimulation warrants further investigation in future studies, and possible reasons are discussed below.

6.4 Future Directions

6.4.1 ChR2 Gene Delivery into Myofibres via AAV Transfection

AAVs are extensively utilized as vectors in gene therapy and are one of the viral vectors approved for delivering genes to humans, primarily due to their highly favorable safety profile, which is attributed to the complete removal of viral coding sequences (Cohen et al., 2023; Mingozzi & High, 2013; D. Wang et al., 2019). In AAVs, the transgene, which is controlled by a promoter, is encapsulated within a viral capsid for targeted delivery to specific cells. In optogenetics, the transgene often encodes an opsin—commonly ChR2—and the capsid serotype is chosen based on its preferential affinity for the desired cell type (Cohen et al., 2023). AAVs predominantly persist in host cells as episomal DNA, meaning they exist as separate DNA molecules within the nucleus, without integrating into the host's chromosomal DNA, although they can rarely integrate into the genome. This episomal state allows for prolonged transgene expression, particularly in non-dividing cells such as neurons and mature myofibres (Penaud-Budloo et al., 2008).

In 1996, two studies reported on the intramuscular injection of AAV vectors into the hindlimb muscles of mice, both demonstrating the long-term survival of the transferred genes in skeletal myofibres. Xiao et al. (1996) observed that AAVs carrying lacZ persisted for 19 months in the TA muscle, while Kessler et al. (1996) found gene expression lasting for at least 8 months. While AAVs are effective at durably transfecting mature myofibres, Arnett et al. (2014) found that rAAV6 preferentially transduces differentiated myofibres but does not efficiently transfect muscle precursor cells, either *in vitro* or *in vivo*. In their experiment, C2C12 myoblasts were transduced with rAAV6-CMV-βGal at a MOI of 100, with cells passaged every two days and diluted 1:10, resulting in the loss of 90% of the population with each passage. Additionally, they demonstrated that intramuscular injection of rAAV6-CMV-AP into the EDL muscle at different time points after notexin-induced injury, which stimulates muscle regeneration via satellite cell activation, was more successful when the injection occurred at a later stage. Specifically, AAV transduction efficiency increased five-fold when the vector was injected four days after injury compared to two days post injury, correlating with their *in vitro* findings that AAVs are more likely to transduce developed myofibres rather than satellite cells. Thus, one of the significant limitations of AAVs is their inability to effectively transfect proliferating muscle precursor cells, with transfection being largely restricted to non-dividing myofibres (Lu et al., 2003). However, a contrasting study reported that AAV9-treated TA muscles, when grafted into immune-deficient mice, underwent necrosis and subsequent regeneration from the satellite cells of the grafted muscle. The regenerated muscles expressed the gene delivered by AAV, suggesting that satellite cells had been transfected by the vector (Nance et al., 2019).

Due to these conflicting observations regarding AAV transfection of satellite cells, it is necessary to examine the ability and efficiency of AAV-PHP.eB-CAG-ChR2-EYFP in transfecting satellite cells compared to mature myofibres in future studies. This is because, for transplantation, muscle fibres must be dissociated into single myoblasts, which then proliferate and re-form new muscle fibres *in vivo*. Thus, it is essential that the satellite cells responsible for muscle regeneration express ChR2. Otherwise, due to AAVs' inability to integrate into the host genome, the ChR2 gene may become diluted over successive cell divisions.

Additionally, a potential explanation for the lower optical force observed could be that not all fibres were infected by the virus, leading to incomplete ChR2 expression in the muscle, which requires further investigation in future studies.

Another potential future experiment could involve the intramuscular injection of AAV-PHP.eB-CAG-ChR2-EYFP after regenerating muscle by transplanting wild-type ES cell-derived myoblasts. The results could then be compared to ones obtained from myoblast transfection prior to transplantation.

6.4.2 ChR2 Gene Delivery into Myofibres via LNPs

LNPs have garnered significant attention for their ability to deliver a range of therapeutic agents, particularly nucleic acids, and gene therapy treatments (Cullis & Hope, 2017; Hou et al., 2021; Mukai et al., 2022). A prime example of the impact of these delivery systems on public health is the successful use of LNP carriers in mRNA-based COVID-19 vaccines (Moderna and Pfizer/BioNTech) (Corbett et al., 2020; A. B. Vogel et al., 2021). Beyond

mRNA vaccines, several other FDA-approved medications utilizing LNP carriers are currently being used in clinical trials (T. M. Allen & Cullis, 2004; P. J. C. Lin et al., 2013).

LNPs are relatively simple to formulate and manufacture, exhibit low immunogenicity, are biocompatible, and promote efficient absorption within the body. They can encapsulate larger genetic materials, support multiple dosing regimens, and offer considerable flexibility in design (Cullis & Hope, 2017; Sercombe et al., 2015; Swetha et al., 2023; Swingle et al., 2021)

LNPs enter cells via endocytosis (Chatterjee et al., 2024; Patel et al., 2023; Rungta et al., 2013). Ionizable lipids, a key component of LNPs, not only aid in the encapsulation of nucleic acids and mRNA but also facilitate efficient endosomal escape and the release of these molecules once the LNPs are internalized by cells (Mukai et al., 2022; Rietwyk & Peer, 2017). The liver, particularly hepatocytes, is the primary site of LNP uptake following intravenous administration due to the strong interaction between LNPs and ApoE in the bloodstream and the high concentration of LDLR on these cells (Akinc et al., 2010). This mechanism has also been observed in neurons in the brain (Rungta et al., 2013). Additionally, skeletal muscle cells express VLDLR, which mediate ApoE endocytosis (Go & Mani, 2012; Iwasaki et al., 2005). Importantly, our *in vitro* studies revealed that while LNP uptake by skeletal muscle cells is not entirely dependent on ApoE, but the presence of ApoE enhances this process.

Given these advantages, our research demonstrated that LNPs efficiently delivered pDNA to skeletal muscle cells and showed a strong tendency to transfect muscle cells over non-muscle cells that were present in the culture. This finding suggests the potential for

expanding the study to *in vivo* models by transplanting LNP-transfected myoblasts into irradiated and notexin-injected muscles to assess whether regenerated muscles can express the exogenous gene delivered by LNPs.

Additionally, as Cullis & Felgner (2024) pointed out, current LNP systems effectively deliver encapsulated pDNA into the cytoplasm, resulting in significant transfection in rapidly dividing cells, both *in vitro* and *in vivo*, due to nuclear membrane breakdown during cell division. Therefore, it is likely that transplanting LNP-ChR2 transfected myoblasts may yield better results compared to AAV-ChR2 transduced myoblasts. So, comparing the results between these two transplantation approaches could provide valuable insights.

6.4.3 Channelrhodopsin-2 Types

The variant of ChR2 used in all our experiments was ChR2-H134R, one of the most widely utilized versions of ChR2. This variant features a mutation at position 134, where histidine is replaced by arginine, resulting in larger stationary photocurrents and greater ion flows compared to the wild-type ChR2. However, this alteration also slows the channel's kinetics (Bruegmann et al., 2010; J. Y. Lin, 2011; Nagel et al., 2005; Tanaka & Okusa, 2018). The delayed channel closing time, approximately 20 ms, can affect the consistency of repetitive stimulation at frequencies above 30 Hz in skeletal muscles (Bruegmann et al., 2015). In neurons, this delay may lead to action potential doublets being triggered by a single pulse of light (Nagel et al., 2005).

Our experiments involving optical tetanic stimulation of regenerated soleus muscles, using ChR2-expressing myoblasts, demonstrated impaired tetanic force, a non-sustained force

with an initial peak declining to the basal level, at both 50 Hz and 100 Hz of stimulation (results not shown). This impairment most likely occurs because the delayed channel closure prevents repolarization between pulses. This phenomenon is similar to constant illumination without pulsing, where the refractoriness of L-type Ca^{2+} channels, combined with reduced Ca^{2+} accumulation and diminished force, contributes to the decreased performance (Robin & Allard, 2013). This indicates that short phases of repolarization are essential for maintaining continuous tetanic contractions in skeletal muscles (Bruegmann et al., 2015).

To mitigate this effect, future studies could explore the use of ChR variants with faster kinetics. Several alternatives with reduced desensitization are available, particularly chimeric variants derived from ChR1 and ChR2, such as ChD, ChEF, and ChIEF, which show promise in improving temporal precision. These variants offer an enhanced steady-state phase response with minimal peak photocurrent, delivering consistent performance during extended light exposure and repetitive high-frequency light pulses (J. Y. Lin et al., 2009). Additionally, these chimeric channels feature faster kinetics, with a closing time of 10 ms or less, demonstrate better expression in mammalian cells, and are more efficiently trafficked to the cell membrane (Kleinlogel et al., 2011; J. Y. Lin et al., 2009; H. Wang et al., 2009).

6.4.4 Muscle Fibre Types

Skeletal muscles in mammals exhibit considerable heterogeneity, consisting of various types of muscle fibres that differ in their enzymatic profiles (Pette, 1985; Romanul & Van Der Meulen, 1967). These fibres are generally classified into two main groups: type I and type II, based on the MHC isoforms they express. Type I fibres are slow-twitch, while type

II fibres are fast-twitch (Scott et al., 2001; Talbot & Mavez, 2016). The phenotypic differentiation of primary muscle fibres occurs in the absence of nerves or neural activity, and their spatial distribution remains organized. This suggests that during development, the phenotypes of muscle fibres are not influenced by the firing patterns of the innervating motoneurons (Rafuse et al., 1996). However, different classes of motoneurons tend to selectively innervate the appropriate types of developed muscle fibres (M. Vogel & Landmesser, 1987). Motoneurons are guided by environmental signals within the limb to select their target muscles, and once the axons reach the muscle, they rely on more localized cues to establish connections with the correct muscle fibre types. Nevertheless, in the absence of matching fibre types, motoneurons can innervate unsuitable fibres and alter their characteristics to align with the motoneuron's fast or slow properties (Rafuse et al., 1996).

In our *in vitro* cultures of ES cell-derived myoblasts, we observed the development of only fast-twitch fibre types. Given that the electrical properties of motoneurons influence the contractile properties of the muscle fibres they innervate, it would be valuable to investigate whether these fibres undergo type changes after being co-cultured with motoneurons and forming NMJ. Furthermore, it would be interesting to explore whether constant optical stimulation of the ChR2 expressing muscle cultures could induce changes in fibre types.

Additionally, the soleus muscle typically consists of both fast and slow fibre types, though it is predominantly composed of slow fibres (Crow & Kushmerick, 1982; Edgerton et al., 1975; Schiaffino & Reggiani, 2011; Thompson, 2002). However, our regenerated soleus muscles, which were transplanted with tdTomato-expressing myoblasts, were composed

entirely of fast fibres when assessed at one- and two-months post-transplantation. Since these fibres are innervated by the natural endogenous motor axons of the soleus muscle, there is potential for them to adapt their fibre types to match the motoneurons that innervate them. Future studies could extend the observation period to examine whether a fibre type switch occurs over a longer timeframe.

6.4.5 Myoblast Number for Transplantation

A range of muscle precursor cell numbers for transplantation into mouse hindlimb skeletal muscles has been reported in the literature. For instance, Morgan et al. (1993) transplanted 5 x 10^5 muscle precursor cells into the TA muscle, while Vilquin et al. (1995) injected 4 x 10^6 myoblasts, and Huard et al., (1994) transplanted 5 x 10^6 human myoblasts. More recently, Metzler et al. (2022) injected only 1 x 10^5 hiPSC-derived muscle progenitor cells. Similarly, Wernig et al. (1995, 2000) and Law et al. (1988) reported transplanting 1 x 10^6 myoblasts into the soleus muscle, and Petersen & Huard (2000) injected 5 x 10^5 myoblasts into the same muscle.

In our case, the number of cells used for each transplantation (5 x 10^5) was the maximum we could inject into the injured soleus muscles. The soleus muscles are extremely fragile and necrotic following irradiation and notexin injection, as notexin destroys all muscle fibres, while irradiation deactivates the satellite cells, preventing any natural regeneration. In such conditions, cell injection must be performed carefully, as using more than 4-5 µl of cell suspension causes damage to the muscle surface, leading to cell leakage.

Initially, we chose this relatively high number of cells because we aimed to achieve optimal regeneration. However, the results from tdTomato-expressing muscles revealed

an exceptionally high number of regenerated myofibres—5.5 times more than in unoperated control muscles. Interestingly, the CSA of these fibres was 4.6 times smaller. It would be valuable for future studies to transplant different numbers of cells into the soleus muscle and compare the resulting number of regenerated muscle fibres and their CSAs. This could help determine whether varying the cell dose influences the overall muscle regeneration process and fibre morphology.

6.5 Conclusion

In conclusion, the collective findings from this thesis represent a significant advancement in the field of muscle regeneration and function restoration. First, a protocol was developed to differentiate mouse ES cells into functional skeletal muscle cells for use in cell replacement therapies. These myoblast cultures were successfully engineered to express exogenous markers such as tdTomato and ChR2. The ChR2-expressing myoblasts contracted in response to light, produced to facilitate optical control of muscle function post-transplantation. Developmental analysis of the differentiated muscle cells revealed the progression of ES cell-derived myoblasts from a quiescent state to fully differentiated myofibres, all of which were fast-twitch fibre types.

Furthermore, transplanting these *in vitro* cultured myogenic cells into the mouse soleus muscle, which had been completely damaged by notexin injection and was unable to regenerate due to hindlimb irradiation, resulted in successful muscle regeneration and functional recovery. The regenerated muscles expressing ChR2 were fully responsive to light and produced the same contractile forces as direct neural stimulation. Muscles regenerated by transplanting tdTomato-expressing myoblasts not only increased muscle mass but also established functional innervation with endogenous motor axons. These

muscles produced slightly higher, though not significantly different, muscle forces compared to unoperated contralateral soleus muscles.

Additionally, in our search for alternative methods to introduce external genes, we transfected myoblasts with LNPs, resulting in specific and high expression of tdTomato in the myofibres. This appears to be a promising approach for future clinical applications of the ChR2 gene in muscle tissues.

As the field continues to advance, the integration of stem cell therapy with optogenetic technologies holds promise for developing novel treatments for a wide range of muscle-related conditions. However, realizing the full therapeutic potential of these methods will necessitate ongoing research, innovation, and thoughtful attention to the ethical and practical challenges they present. With further refinements and reaching to clinical validation, these technologies could significantly improve the quality of life for individuals suffering from muscle injuries, degenerative diseases, and paralysis, bringing us closer to the goal of restoring full muscle function in affected patients.

REFERENCES

Abilez, O. J., Wong, J., Prakash, R., Deisseroth, K., Zarins, C. K., & Kuhl, E. (2011). Multiscale computational models for optogenetic control of cardiac function. *Biophysical Journal*, *101*(6), 1326–1334. https://doi.org/10.1016/j.bpj.2011.08.004

Aguilar, C. A., Greising, S. M., Watts, A., Goldman, S. M., Peragallo, C., Zook, C., Larouche, J., & Corona, B. T. (2018). Multiscale analysis of a regenerative therapy for treatment of volumetric muscle loss injury. *Cell Death Discovery*, *4*(1). https://doi.org/10.1038/s41420-018-0027-8

Ahuja, C. S., Wilson, J. R., Nori, S., Kotter, M. R. N., Druschel, C., Curt, A., & Fehlings, M. G. (2017). Traumatic spinal cord injury. *Nature Reviews Disease Primers*, *3*. https://doi.org/10.1038/nrdp.2017.18

Akinc, A., Querbes, W., De, S., Qin, J., Frank-Kamenetsky, M., Jayaprakash, K. N., Jayaraman, M., Rajeev, K. G., Cantley, W. L., Dorkin, J. R., Butler, J. S., Qin, L., Racie, T., Sprague, A., Fava, E., Zeigerer, A., Hope, M. J., Zerial, M., Sah, D. W., … Maier, M. A. (2010). Targeted delivery of RNAi therapeutics with endogenous and exogenous ligand-based mechanisms. *Molecular Therapy*, *18*(7), 1357–1364. https://doi.org/10.1038/mt.2010.85

Alilain, W. J., Li, X., Horn, K. P., Dhingra, R., Dick, T. E., Herlitze, S., & Silver, J. (2008). Light-induced rescue of breathing after spinal cord injury. *Journal of Neuroscience*, *28*(46), 11862–11870. https://doi.org/10.1523/JNEUROSCI.3378-08.2008

Allen, R. E., Sheehan, S. M., Taylor, R. G., Kendall, T. L., & Rice, G. M. (1995). Hepatocyte growth factor activates quiescent skeletal muscle satellite cells in vitro. *Journal of Cellular Physiology*, *165*(2), 307–312. https://doi.org/10.1002/jcp.1041650211

Allen, T. M., & Cullis, P. R. (2004). Drug Delivery Systems: Entering the Mainstream. *Science*, *303*(5665), 1818–1822. https://doi.org/10.1126/science.1095833

Alvites, R., Rita Caseiro, A., Santos Pedrosa, S., Vieira Branquinho, M., Ronchi, G., Geuna, S., Varejão, A. S. P., & Colette Maurício, A. (2018). Peripheral nerve injury and axonotmesis: State of the art and recent advances. *Cogent Medicine*, *5*(1), 1466404. https://doi.org/10.1080/2331205x.2018.1466404

Ambegia, E., Ansell, S., Cullis, P., Heyes, J., Palmer, L., & MacLachlan, I. (2005). Stabilized plasmid-lipid particles containing PEG-diacylglycerols exhibit extended circulation lifetimes and tumor selective gene expression. *Biochimica et Biophysica Acta - Biomembranes*, *1669*(2), 155–163. https://doi.org/10.1016/j.bbamem.2005.02.001

Anderson, K. D. (2004). Targeting recovery: Priorities of the spinal cord-injured population. *Journal of Neurotrauma*, *21*(10), 1371–1383. https://doi.org/10.1089/neu.2004.21.1371

Anglister, L., McMahan, U. J., & Marshall, R. M. (1985). Basal lamina directs acetylcholinesterase accumulation at synaptic sites in regenerating muscle. *Journal of Cell Biology*, *101*(3), 735–743. https://doi.org/10.1083/jcb.101.3.735

Aravanis, A. M., Wang, L. P., Zhang, F., Meltzer, L. A., Mogri, M. Z., Schneider, M. B., & Deisseroth, K. (2007). An optical neural interface: in vivo control of rodent motor cortex with integrated fiberoptic and optogenetic technology. *Journal of Neural Engineering*, *4*(3). https://doi.org/10.1088/1741-2560/4/3/S02

Arnett, A. L., Konieczny, P., Ramos, J. N., Hall, J., Odom, G., Yablonka-Reuveni, Z., Chamberlain, J. R., & Chamberlain, J. S. (2014). Adeno-associated viral vectors do not efficiently target muscle satellite cells. *Molecular Therapy Methods and Clinical Development*, *1*(April), 14038. https://doi.org/10.1038/mtm.2014.38

Asano, T., Ishizua, T., & Yawo, H. (2012). Optically controlled contraction of photosensitive skeletal muscle cells. *Biotechnology and Bioengineering*, *109*(1), 199–204. https://doi.org/10.1002/bit.23285

Augusto, V., Padovani, C. R., & Campos, G. E. R. (2004). Skeletal Muscle Fiber Types in C57BL6J Mice. *Brazilian Journal of Morphological Science*, *21*(2), 89–94.

Barlow, J., Sfyri, P. P., Mitchell, R., Verpoorten, S., Scully, D., Andreou, C., Papadopoulos, P., Patel, K., & Matsakas, A. (2021). Platelet releasate normalises the compromised muscle regeneration in a mouse model of hyperlipidaemia. *Experimental Physiology*, *106*(3), 700–713. https://doi.org/10.1113/EP088937

Bawa, P. N. S., Jones, K. E., & Stein, R. B. (2014). Assessment of size ordered recruitment. *Frontiers in Human Neuroscience*, *8*. https://doi.org/10.3389/fnhum.2014.00532

Bayot, M., Nassereddin, A., & Varacallo, M. (2023). *No Title*. StatPearls Publishing. https://www.ncbi.nlm.nih.gov/books/NBK500016/

Beauchamp, J. R., Morgan, J. E., Pagel, C. N., & Partridge, T. A. (1999). Dynamics of myoblast transplantation reveal a discrete minority of precursors with stem cell-like properties as the myogenic source. *Journal of Cell Biology*, *144*(6), 1113–1121. https://doi.org/10.1083/jcb.144.6.1113

Benevides, E. S., Sunshine, M. D., Rana, S., & Fuller, D. D. (2022). Optogenetic activation of the diaphragm. *Scientific Reports*, *12*(1). https://doi.org/10.1038/s41598-022-10240-w

Bentzinger, C. F., Wang, Y. X., & Rudnicki, M. A. (2012). Building muscle: molecular regulation of myogenesis. *Cold Spring Harbor Perspectives in Biology*, *4*(2). https://doi.org/10.1101/cshperspect.a008342

Bertelli, J. A., & Ghizoni, M. F. (2010). The possible role of regenerating axons in pain persistence after brachial plexus grafting. *Microsurgery*, *30*(7), 532–536. https://doi.org/10.1002/micr.20788

Bewick, G. S., Reid, B., Jawaid, S., Hatcher, T., & Shanley, L. (2004). Postnatal emergence of mature release properties in terminals of rat fast- and slow-twitch muscles. *European Journal of Neuroscience*, *19*(11), 2967–2976. https://doi.org/10.1111/j.0953-816X.2004.03418.x

Bhagavati, S., & Xu, W. (2005). Generation of skeletal muscle from transplanted embryonic stem cells in dystrophic mice. *Biochemical and Biophysical Research Communications*, *333*(2), 644–649. https://doi.org/10.1016/j.bbrc.2005.05.135

Biressi, S., Filareto, A., & Rando, T. A. (2020). Stem cell therapy for muscular dystrophies. *Journal of Clinical Investigation*, *130*(11), 5652–5664. https://doi.org/10.1172/JCI142031

Bischoff, R. (1986). Proliferation of muscle satellite cells on intact myofibers in culture. *Developmental Biology*, *115*(1), 129–139. https://doi.org/10.1016/0012-1606(86)90234-4

Bischoff, R. (1990). Interaction between satellite cells and skeletal muscle fibers. *Development*, *109*(4), 943–952. https://doi.org/10.1242/dev.109.4.943

Bisgaier, C. L., Siebenkas, M. V., & Williams, K. J. (1989). Effects of apolipoproteins A-IV and A-I on the uptake of phospholipid liposomes by hepatocytes. *Journal of Biological Chemistry*, *264*(2), 862–866. https://doi.org/10.1016/s0021-9258(19)85022-6

Bitounis, D., Jacquinet, E., Rogers, M. A., & Amiji, M. M. (2024). Strategies to reduce the risks of mRNA drug and vaccine toxicity. *Nature Reviews Drug Discovery*, *23*(4), 281–300. https://doi.org/10.1038/s41573-023-00859-3

Bolsoni, J., Liu, D., Mohabatpour, F., Ebner, R., Sadhnani, G., Tafech, B., Leung, J., Shanta, S., An, K., Morin, T., Chen, Y., Arguello, A., Choate, K., Jan, E., Ross, C. J. D., Brambilla, D., Witzigmann, D., Kulkarni, J., Cullis, P. R., & Hedtrich, S. (2023). Lipid Nanoparticle-Mediated Hit-and-Run Approaches Yield Efficient and Safe In Situ Gene Editing in Human Skin. *ACS Nano*, *17*(21), 22046–22059. https://doi.org/10.1021/acsnano.3c08644

Boonen, K. J. M., & Post, M. J. (2008). The muscle stem cell niche: Regulation of satellite cells during regeneration. *Tissue Engineering - Part B: Reviews*, *14*(4), 419–431. https://doi.org/10.1089/ten.teb.2008.0045

Borisov, A. B., Dedkov, E. I., & Carlson, B. M. (2005). Abortive myogenesis in denervated skeletal muscle: Differentiative properties of satellite cells, their migration, and block of terminal differentiation. *Anatomy and Embryology*, *209*(4), 269–279. https://doi.org/10.1007/s00429-004-0429-7

Bottinelli, R., & Reggiani, C. (2000). Human skeletal muscle fibres: Molecular and functional diversity. *Progress in Biophysics and Molecular Biology*, *73*(2–4), 195–262. https://doi.org/10.1016/S0079-6107(00)00006-7

Bowie, A. G., & Unterholzner, L. (2008). Viral evasion and subversion of pattern-recognition receptor signalling. *Nature Reviews Immunology*, *8*(12), 911–922. https://doi.org/10.1038/nri2436

Boyden, E. S., Zhang, F., Bamberg, E., Nagel, G., & Deisseroth, K. (2005). Millisecond-timescale, genetically targeted optical control of neural activity. *Nature Neuroscience*, *8*(9), 1263–1268. https://doi.org/10.1038/nn1525

Boyer, O., Butler-Browne, G., Chinoy, H., Cossu, G., Galli, F., Lilleker, J. B., Magli, A., Mouly, V., Perlingeiro, R. C. R., Previtali, S. C., Sampaolesi, M., Smeets, H., Schoewel-Wolf, V., Spuler, S., Torrente, Y., & Van Tienen, F. (2021). Myogenic Cell Transplantation in Genetic and Acquired Diseases of Skeletal Muscle. *Frontiers in Genetics*, *12*. https://doi.org/10.3389/fgene.2021.702547

Breyer, J. M., Vergara, P., & Perez, A. (2021). Epidemiology of Adult Traumatic Brachial Plexus Injuries. *Operative Brachial Plexus Surgery: Clinical Evaluation and Management Strategies*, 63–68. https://doi.org/10.1007/978-3-030-69517-0_5

Bruegmann, T., Malan, D., Hesse, M., Beiert, T., Fuegemann, C. J., Fleischmann, B. K., & Sasse, P. (2010). Optogenetic control of heart muscle in vitro and in vivo. *Nature Methods*, *7*(11), 897–900. https://doi.org/10.1038/nmeth.1512

Bruegmann, T., Van Bremen, T., Vogt, C. C., Send, T., Fleischmann, B. K., & Sasse, P. (2015). Optogenetic control of contractile function in skeletal muscle. *Nature Communications*, *6*, 1–8. https://doi.org/10.1038/ncomms8153

Bryson, J. B., Machado, C. B., Crossley, M., Stevenson, D., Bros-Facer, V., Burrone, J., Greensmith, L., & Lieberam, I. (2014). Optical control of muscle function by transplantation of stem cell-derived motor neurons in mice. *Science*, *344*(6179), 94–97. https://doi.org/10.1126/science.1248523

Buck, J., Grossen, P., Cullis, P. R., Huwyler, J., & Witzigmann, D. (2019). Lipid-based DNA therapeutics: Hallmarks of non-viral gene delivery. *ACS Nano*, *13*(4), 3754–3782. https://doi.org/10.1021/acsnano.8b07858

Burden, S. J., Sargent, P. B., & McMahan, U. J. (1979). Acetylcholine receptors in regenerating muscle accumulate at original synaptic sites in the absence of the nerve. *Journal of Cell Biology*, *82*(2), 412–425. https://doi.org/10.1083/jcb.82.2.412

Burke, B. I., Goh, J., Albathi, F. A., Valentino, T. R., Nolt, G. L., Joshi, J. K., Dungan, C. M., Johnson, L. A., Wen, Y., Ismaeel, A., & McCarthy, J. J. (2023). ApoE isoform does not influence skeletal muscle regeneration in adult mice. *Frontiers in Physiology*, *14*(November), 1–10. https://doi.org/10.3389/fphys.2023.1302695

Burke, R. E. (1981). Motor Units: Anatomy, Physiology, and Functional Organization. In *Comprehensive Physiology* (pp. 345–422). Wiley. https://doi.org/10.1002/cphy.cp010210

Bursac, N., Juhas, M., & Rando, T. A. (2015). Synergizing Engineering and Biology to Treat and Model Skeletal Muscle Injury and Disease. *Annual Review of Biomedical Engineering*, *17*(1), 217–242. https://doi.org/10.1146/annurev-bioeng-071114-040640

Caillaud, M., Richard, L., Vallat, J. M., Desmoulière, A., & Billet, F. (2019). Peripheral nerve regeneration and intraneural revascularization. *Neural Regeneration Research*, *14*(1), 24–33. https://doi.org/10.4103/1673-5374.243699

Calancie, B., Molano, M. R., & Broton, J. G. (2004). EMG for assessing the recovery of voluntary movement after acute spinal cord injury in man. *Clinical Neurophysiology*, *115*(8), 1748–1759. https://doi.org/10.1016/j.clinph.2004.03.002

Capetanaki, Y., Milner, D. J., & Weitzer, G. (1997). Desmin in muscle formation and maintenance: Knockouts and consequences. *Cell Structure and Function*, *22*(1), 103–116. https://doi.org/10.1247/csf.22.103

Carpaneto, J., & Micera, S. (2015). Application of orthoses and neurostimulation in neurorehabilitation. In *Oxford Textbook of Neurorehabilitation* (pp. 363–373). Oxford University Press. https://doi.org/10.1093/med/9780199673711.003.0030

Chal, J., & Pourquié, O. (2017). Making muscle: Skeletal myogenesis in vivo and in vitro. *Development (Cambridge)*, *144*(12), 2104–2122. https://doi.org/10.1242/dev.151035

Chan, K. Y., Jang, M. J., Yoo, B. B., Greenbaum, A., Ravi, N., Wu, W.-L., Sánchez-Guardado, L., Lois, C., Mazmanian, S. K., Deverman, B. E., & Gradinaru, V. (2017). Engineered AAVs for efficient noninvasive gene delivery to the central and peripheral nervous systems. *Nature Neuroscience*, *20*(8), 1172–1179. https://doi.org/10.1038/nn.4593

Chatterjee, S., Kon, E., Sharma, P., & Peer, D. (2024). Endosomal escape: A bottleneck for LNP-mediated therapeutics. *Proceedings of the National Academy of Sciences*, *121*(11). https://doi.org/10.1073/pnas.2307800120

Chen, J., Xu, Y., Zhou, M., Xu, S., Varley, A. J., Golubovic, A., Lu, R. X. Z., Wang, K. C., Yeganeh, M., Vosoughi, D., & Li, B. (2023). Combinatorial design of ionizable lipid nanoparticles for muscle-selective mRNA delivery with minimized off-target effects. *Proceedings of the National Academy of Sciences*, *120*(50). https://doi.org/10.1073/pnas.2309472120

Cho, M. K. (1994). Are clinical trials of cell transplantation for Duchenne muscular dystrophy ethical? *IRB; a Review of Human Subjects Research*, *16*(1–2), 12–15. https://doi.org/10.2307/3563575

Chromiak, J. A., & Antonio, J. (2008). Skeletal Muscle Plasticity. In *Essentials of Sports Nutrition Study Guide* (pp. 16–36). Humana Press. https://doi.org/10.1007/978-1-59745-302-8_2

Cohen, E. M., Knapman, F. L., & Bilston, L. E. (2023). Optogenetic Control of Muscles: Potential Uses and Limitations. *Human Gene Therapy*, *34*(9–10), 416–429. https://doi.org/10.1089/hum.2022.236

Collinger, J. L., Boninger, M. L., Bruns, T. M., Curley, K., Wang, W., & Weber, D. J. (2013). Functional priorities, assistive technology, and brain-computer interfaces after spinal cord injury. *The Journal of Rehabilitation Research and Development*, *50*(2), 145. https://doi.org/10.1682/JRRD.2011.11.0213

Collins, C. A., Olsen, I., Zammit, P. S., Heslop, L., Petrie, A., Partridge, T. A., & Morgan, J. E. (2005). Stem cell function, self-renewal, and behavioral heterogeneity of cells from the adult muscle satellite cell niche. *Cell*, *122*(2), 289–301. https://doi.org/10.1016/j.cell.2005.05.010

Comai, G., & Tajbakhsh, S. (2014). Molecular and cellular regulation of skeletal myogenesis. In *Current Topics in Developmental Biology* (1st ed., Vol. 110). Elsevier Inc. https://doi.org/10.1016/B978-0-12-405943-6.00001-4

Cope, T. C., & Sokoloff, A. J. (1999). Orderly recruitment among motoneurons supplying different muscles. *Journal of Physiology Paris*, *93*(1–2), 81–85. https://doi.org/10.1016/S0928-4257(99)80138-7

Corbett, K. S., Edwards, D. K., Leist, S. R., Abiona, O. M., Boyoglu-Barnum, S., Gillespie, R. A., Himansu, S., Schäfer, A., Ziwawo, C. T., DiPiazza, A. T., Dinnon, K. H., Elbashir, S. M., Shaw, C. A., Woods, A., Fritch, E. J., Martinez, D. R., Bock, K. W., Minai, M., Nagata, B. M., … Graham, B. S. (2020). SARS-CoV-2 mRNA vaccine design enabled by prototype pathogen preparedness. *Nature*, *586*(7830), 567–571. https://doi.org/10.1038/s41586-020-2622-0

Cosgrove, B. D., & Blau, H. M. (2010). Skeletal Muscle Stem Cells. In *Principles of Regenerative Medicine, Second Edition* (Second Edi, Issue Dmd). Elsevier Inc. https://doi.org/10.1016/B978-0-12-381422-7.10020-3

Cosgrove, B. D., Sacco, A., Gilbert, P. M., & Blau, H. M. (2009). A home away from home: Challenges and opportunities in engineering in vitro muscle satellite cell niches. *Differentiation*, *78*(2–3), 185–194. https://doi.org/10.1016/j.diff.2009.08.004

Cossu, G., Birchall, M., Brown, T., De Coppi, P., Culme-Seymour, E., Gibbon, S., Hitchcock, J., Mason, C., Montgomery, J., Morris, S., Muntoni, F., Napier, D., Owji, N., Prasad, A., Round, J., Saprai, P., Stilgoe, J., Thrasher, A., & Wilson, J. (2018). Lancet Commission: Stem cells and regenerative medicine. *Lancet (London, England)*, *391*(10123), 883–910. https://doi.org/10.1016/S0140-6736(17)31366-1

Criss Hartzell, H., & Fambrough, D. M. (1972). Acetylcholine receptors: Distribution and extrajunctional density in rat diaphragm after denervation correlated with acetylcholine sensitivity. *Journal of General Physiology*, *60*(3), 248–262. https://doi.org/10.1085/jgp.60.3.248

Crocini, C., Ferrantini, C., Coppini, R., Scardigli, M., Yan, P., Loew, L. M., Smith, G., Cerbai, E., Poggesi, C., Pavone, F. S., & Sacconi, L. (2016). Optogenetics design of mechanistically-based stimulation patterns for cardiac defibrillation. *Scientific Reports*, *6*(1), 35628. https://doi.org/10.1038/srep35628

Crow, M. T., & Kushmerick, M. J. (1982). Chemical energetics of slow- and fast-twitch muscles of the mouse. *Journal of General Physiology*, *79*(1), 147–166. https://doi.org/10.1085/jgp.79.1.147

Cullis, P. R., & Felgner, P. L. (2024). The 60-year evolution of lipid nanoparticles for nucleic acid delivery. *Nature Reviews Drug Discovery*, *23*(9), 709–722. https://doi.org/10.1038/s41573-024-00977-6

Cullis, P. R., & Hope, M. J. (2017). Lipid Nanoparticle Systems for Enabling Gene Therapies. *Molecular Therapy*, *25*(7), 1467–1475. https://doi.org/10.1016/j.ymthe.2017.03.013

Das, S., Browne, K. D., Laimo, F. A., Maggiore, J. C., Hilman, M. C., Kaisaier, H., Aguilar, C. A., Ali, Z. S., Mourkioti, F., & Cullen, D. K. (2020). Pre-innervated tissue-engineered muscle promotes a pro-regenerative microenvironment following volumetric muscle loss. *Communications Biology*, *3*(1), 1–14. https://doi.org/10.1038/s42003-020-1056-4

David, S., & Aguayo, A. J. (1981). Axonal Elongation into Peripheral Nervous System "Bridges" After Central Nervous System Injury in Adult Rats. *Science*, *214*(4523), 931–933. https://doi.org/10.1126/science.6171034

Day, K., Paterson, B., & Yablonka-Reuveni, Z. (2009). A distinct profile of myogenic regulatory factor detection within Pax7 + Cells at S phase supports a unique role of Myf5 during posthatch chicken myogenesis. *Developmental Dynamics*, *238*(4), 1001–1009. https://doi.org/10.1002/dvdy.21903

Deisseroth, K. (2011). *Optogenetics*. *8*(1), 26–29.

Deschenes, M. R. (2019). Adaptations of the neuromuscular junction to exercise training. *Current Opinion in Physiology*, *10*, 10–16. https://doi.org/10.1016/j.cophys.2019.02.004

Dhawan, J., & Rando, T. A. (2005). Stem cells in postnatal myogenesis: Molecular mechanisms of satellite cell quiescence, activation and replenishment. *Trends in Cell Biology*, *15*(12), 666–673. https://doi.org/10.1016/j.tcb.2005.10.007

Dixon, R. W., & Harris, J. B. (1996). Myotoxic Activity of the Toxic Phospholipase, Notexin, from the Venom of the Australian Tiger Snake. *Journal of Neuropathology & Experimental Neurology*, *55*(12), 1230–1237. https://doi.org/10.1097/00005072-199612000-00006

Du, X., Yada, E., Terai, Y., Takahashi, T., Nakanishi, H., Tanaka, H., Akita, H., & Itaka, K. (2023). Comprehensive Evaluation of Lipid Nanoparticles and Polyplex Nanomicelles for Muscle-Targeted mRNA Delivery. *Pharmaceutics*, *15*(9), 1–14. https://doi.org/10.3390/pharmaceutics15092291

Duchateau, J., & Enoka, R. M. (2011). Human motor unit recordings: Origins and insight into the integrated motor system. *Brain Research*, *1409*, 42–61. https://doi.org/10.1016/j.brainres.2011.06.011

Dumont, N. A., Bentzinger, C. F., Sincennes, M. C., & Rudnicki, M. A. (2015). Satellite cells and skeletal muscle regeneration. *Comprehensive Physiology*, *5*(3), 1027–1059. https://doi.org/10.1002/cphy.c140068

Dux, L., Cooper, B. J., Sewry, C. A., & Dubowitz, V. (1993). Notechis scutatus venom increases the yield of proliferating muscle cells from biopsies of normal and dystrophic canine muscle-A possible source for myoblast transfer studies. *Neuromuscular Disorders*, *3*(1), 23–29. https://doi.org/10.1016/0960-8966(93)90038-L

Edgerton, V. R., Smith, J. L., & Simpson, D. R. (1975). Muscle fibre type populations of human leg muscles. *The Histochemical Journal*, *7*(3), 259–266. https://doi.org/10.1007/BF01003594

Eftimie, R., Brenner, H. R., & Buonanno, A. (1991). Myogenin and MyoD join a family of skeletal muscle genes regulated by electrical activity. *Proceedings of the National Academy of Sciences of the United States of America*, *88*(4), 1349–1353. https://doi.org/10.1073/pnas.88.4.1349

Enoka, R. M., & Duchateau, J. (2008). Muscle fatigue: What, why and how it influences muscle function. *Journal of Physiology*, *586*(1), 11–23. https://doi.org/10.1113/jphysiol.2007.139477

Evers, M. J. W., Du, W., Yang, Q., Kooijmans, S. A. A., Vink, A., van Steenbergen, M., Vader, P., de Jager, S. C. A., Fuchs, S. A., Mastrobattista, E., Sluijter, J. P. G., Lei, Z., & Schiffelers, R. (2022). Delivery of modified mRNA to damaged myocardium by systemic administration of lipid nanoparticles. *Journal of Controlled Release*, *343*(September 2021), 207–216. https://doi.org/10.1016/j.jconrel.2022.01.027

Fambrough, D. M. (1974). Acetylcholine receptors: Revised estimates of extrajunctional receptor density in denervated rat diaphragm. *Journal of General Physiology*, *64*(4), 468–472. https://doi.org/10.1085/jgp.64.4.468

Fambrough, D. M. (1979). Control of acetylcholine receptors in skeletal muscle. *Physiological Reviews*, *59*(1), 165–227. https://doi.org/10.1152/physrev.1979.59.1.165

Feldman, J. L., & Stockdale, F. E. (1991). Skeletal muscle satellite cell diversity: Satellite cells form fibers of different types in cell culture. *Developmental Biology*, *143*(2), 320–334. https://doi.org/10.1016/0012-1606(91)90083-F

Felgner, P. L., Gadek, T. R., Holm, M., Roman, R., Chan, H. W., Wenz, M., Northrop, J. P., Ringold, G. M., & Danielsen, M. (1987). Lipofection: a highly efficient, lipid-mediated DNA-transfection procedure. *Proceedings of the National Academy of Sciences*, *84*(21), 7413–7417. https://doi.org/10.1073/pnas.84.21.7413

Feng, Z., & Ko, C. P. (2007). Neuronal glia interactions at the vertebrate neuromuscular junction. *Current Opinion in Pharmacology*, *7*(3), 316–324. https://doi.org/10.1016/j.coph.2006.12.003

Ferenczi, E. A., Tan, X., & Huang, C. L. H. (2019). Principles of Optogenetic Methods and Their Application to Cardiac Experimental Systems. *Frontiers in Physiology*, *10*(September). https://doi.org/10.3389/fphys.2019.01096

Fitts, R. H. (2008). The cross-bridge cycle and skeletal muscle fatigue. *Journal of Applied Physiology*, *104*(2), 551–558. https://doi.org/10.1152/japplphysiol.01200.2007

Foster, R. F., Thompson, J. M., & Kaufman, S. J. (1987). A laminin substrate promotes myogenesis in rat skeletal muscle cultures: Analysis of replication and development using antidesmin and anti-BrdUrd monoclonal antibodies. *Developmental Biology*, *122*(1), 11–20. https://doi.org/10.1016/0012-1606(87)90327-7

Frontera, W. R., & Ochala, J. (2015). Skeletal Muscle: A Brief Review of Structure and Function. *Behavior Genetics*, *45*(2), 183–195. https://doi.org/10.1007/s00223-014-9915-y

Fu, S. Y., & Gordon, T. (1995). Contributing factors to poor functional recovery after delayed nerve repair: Prolonged denervation. *Journal of Neuroscience*, *15*(5 II), 3886–3895. https://doi.org/10.1523/jneurosci.15-05-03886.1995

Fu, S. Y., & Gordon, T. (1997). The cellular and molecular basis of peripheral nerve regeneration. *Molecular Neurobiology*, *14*(1–2), 67–116. https://doi.org/10.1007/BF02740621

Fuglevand, A. J., Winter, D. A., & Patla, A. E. (1993). Models of recruitment and rate coding organization in motor-unit pools. *Journal of Neurophysiology*, *70*(6), 2470–2488. https://doi.org/10.1152/jn.1993.70.6.2470

Gattazzo, F., Urciuolo, A., & Bonaldo, P. (2014). Extracellular matrix: A dynamic microenvironment for stem cell niche. *Biochimica et Biophysica Acta (BBA) - General Subjects*, *1840*(8), 2506–2519. https://doi.org/10.1016/j.bbagen.2014.01.010

Gaudet, A. D., Popovich, P. G., & Ramer, M. S. (2011). Wallerian degeneration: Gaining perspective on inflammatory events after peripheral nerve injury. *Journal of Neuroinflammation*, *8*(1), 110. https://doi.org/10.1186/1742-2094-8-110

Ge, L., Arul, K., Ikpeze, T., Baldwin, A., Nickels, J. L., & Mesfin, A. (2018). Traumatic and Nontraumatic Spinal Cord Injuries. *World Neurosurgery*, *111*, e142–e148. https://doi.org/10.1016/j.wneu.2017.12.008

Gerrard, J. C., Hay, J. P., Adams, R. N., Williams, J. C., Huot, J. R., Weathers, K. M., Marino, J. S., & Arthur, S. T. (2021). Current thoughts of notch's role in myoblast regulation and muscle-associated disease. *International Journal of Environmental Research and Public Health*, *18*(23). https://doi.org/10.3390/ijerph182312558

Gillies, A. R., & Lieber, R. L. (2011). Structure and function of the skeletal muscle extracellular matrix. *Muscle and Nerve*, *44*(3), 318–331. https://doi.org/10.1002/mus.22094

Gilman, S., & Arbor, A. (1983). Handbook of physiology. Section 1: The nervous system, vol II. Motor control, parts 1 and 2. Section editors: John M. Brookhart and Vernon B. Mountcastle volume editor: Vernon B. Brooks Bethesda, MD, American Physiological Society, 1981 1480 pp, illustrat. *Annals of Neurology*, *13*(1), 111–111. https://doi.org/10.1002/ana.410130130

Girardi, F., & Le Grand, F. (2018). Wnt Signaling in Skeletal Muscle Development and Regeneration. In *Progress in Molecular Biology and Translational Science* (Vol. 153). Elsevier Inc. https://doi.org/10.1016/bs.pmbts.2017.11.026

Go, G. W., & Mani, A. (2012). Low-density lipoprotein receptor (LDLR) family orchestrates cholesterol homeostasis. *Yale Journal of Biology and Medicine*, *85*(1), 19–28.

Gordon, A., Huxley;, & Julian. (1966). The variation in isometric tension with sarcomere. *The Journal of Physiology*, *184*, 170–192. http://e.guigon.free.fr/rsc/article/GordonAMEtAl66a.pdf

Gordon, T. (2020). Peripheral nerve regeneration and muscle reinnervation. *International Journal of Molecular Sciences*, *21*(22), 1–24. https://doi.org/10.3390/ijms21228652

Gordon, T., & Borschel, G. H. (2017). The use of the rat as a model for studying peripheral nerve regeneration and sprouting after complete and partial nerve injuries. *Experimental Neurology*, *287*, 331–347. https://doi.org/10.1016/j.expneurol.2016.01.014

Gorgey, A. S., & Dudley, G. A. (2007). Skeletal muscle atrophy and increased intramuscular fat after incomplete spinal cord injury. *Spinal Cord*, *45*(4), 304–309. https://doi.org/10.1038/sj.sc.3101968

Gradinaru, V., Mogri, M., Thompson, K. R., Henderson, J. M., & Deisseroth, K. (2009). Optical deconstruction of parkinsonian neural circuitry. *Science*, *324*(5925), 354–359. https://doi.org/10.1126/science.1167093

Grinsell, D., & Keating, C. P. (2014). Peripheral Nerve Reconstruction after Injury: A Review of Clinical and Experimental Therapies. *BioMed Research International*, *2014*. https://doi.org/10.1155/2014/698256

Gros, J., Manceau, M., Thomé, V., & Marcelle, C. (2005). A common somitic origin for embryonic muscle progenitors and satellite cells. *Nature*, *435*(7044), 954–958. https://doi.org/10.1038/nature03572

Grumbles, R. M., & Thomas, C. K. (2017). Motoneuron death after human spinal cord injury. *Journal of Neurotrauma*, *34*(3), 581–590. https://doi.org/10.1089/neu.2015.4374

Guiraud, S., & Davies, K. E. (2019). Regenerative biomarkers for Duchenne muscular dystrophy. *Neural Regeneration Research*, *14*(8), 1317–1320. https://doi.org/10.4103/1673-5374.253534

Gulino, R. (2023). Synaptic Dysfunction and Plasticity in Amyotrophic Lateral Sclerosis. *International Journal of Molecular Sciences*, *24*(5). https://doi.org/10.3390/ijms24054613

Gundelach, L. A., Hüser, M. A., Beutner, D., Ruther, P., & Bruegmann, T. (2020). Towards the clinical translation of optogenetic skeletal muscle stimulation. In *Pflugers Archiv European Journal of Physiology* (Vol. 472, Issue 5, pp. 527–545). Springer. https://doi.org/10.1007/s00424-020-02387-0

Gupta, R., Chan, J. P., Uong, J., Palispis, W. A., Wright, D. J., Shah, S. B., Ward, S. R., Lee, T. Q., & Steward, O. (2021). *injury*. *135*(July), 220–227. https://doi.org/10.3171/2020.8.JNS201461.J

Gussoni, E., Blau, H. M., & Kunkel, L. M. (1997). The fate of individual myoblasts after transplantation into muscles of DMD patients. *Nature Medicine*, *3*(9), 970–977. https://doi.org/10.1038/nm0997-970

Gussoni, E., Pavlath, G. K., Lanctot, A. M., Sharma, K. R., Miller, R. G., Steinman, L., & Blau, H. M. (1992). Normal dystrophin transcripts detected in Duchenne muscular dystrophy patients after myoblast transplantation. *Nature*, *356*(6368), 435–438. https://doi.org/10.1038/356435a0

Gutiérrez, J. M., & Ownby, C. L. (2003). Skeletal muscle degeneration induced by venom phospholipases A 2: Insights into the mechanisms of local and systemic myotoxicity. *Toxicon*, *42*(8), 915–931. https://doi.org/10.1016/j.toxicon.2003.11.005

Gutmann, E. (1948). Effect of delay of innervation on recovery of muscle after nerve lesions. *Journal of Neurophysiology*, *11*(4), 279–294. https://doi.org/10.1152/jn.1948.11.4.279

Han, X. (2004). The role of apolipoprotein E in lipid metabolism in the central nervous system. *Cellular and Molecular Life Sciences*, *61*(15), 1896–1906. https://doi.org/10.1007/s00018-004-4009-z

Harris, J. B. (2003). Myotoxic phospholipases A2 and the regeneration of skeletal muscles. *Toxicon*, *42*(8), 933–945. https://doi.org/10.1016/j.toxicon.2003.11.011

Harris, J. B., Vater, R., Wilson, M., & Cullen, M. J. (2003). Muscle fibre breakdown in venom-induced muscle degeneration. *Journal of Anatomy*, *202*(4), 363–372. https://doi.org/10.1046/j.1469-7580.2003.00171.x

Harvey, P. J., Grochmal, J., Tetzlaff, W., Gordon, T., & Bennett, D. J. (2005). An investigation into the potential for activity-dependent regeneration of the rubrospinal tract after spinal cord injury. *European Journal of Neuroscience*, *22*(12), 3025–3035. https://doi.org/10.1111/j.1460-9568.2005.04514.x

Hasty, P., Bradley, A., Morris, J. H., Edmondson, D. G., Venutit, J. M., Olson, E. N., & Kleln, W. H. (1993). Mice With a Targeted Mutation in the. *Nature*, *364*, 501–506.

Hekmatnejad, B., & Rudnicki, M. A. (2022). Transplantation to study satellite cell heterogeneity in skeletal muscle. *Frontiers in Cell and Developmental Biology*, *10*(August), 1–11. https://doi.org/10.3389/fcell.2022.902225

Henneman, E., & Mendell, L. (1981). Functional organization of motoneuron pool and its inputs. In *Handbook of physiology, The nervous system, motor control* (pp. 423–507). American Physiological Society. https://scholar.google.com/scholar_lookup?&title=Functional organization of motoneuron pool and its inputs&pages=423-507&publication_year=1981&author=Henneman%2CE&author=Mendell%2CLM

Henneman, E., Somjen, G., & Carpenter, D. O. (1965a). EXCITABILITY AND INHIBITIBILITY OF MOTONEURONS OF DIFFERENT SIZES. *Journal of Neurophysiology*, *28*(3), 599–620. https://doi.org/10.1152/jn.1965.28.3.599

Henneman, E., Somjen, G., & Carpenter, D. O. (1965b). FUNCTIONAL SIGNIFICANCE OF CELL SIZE IN SPINAL MOTONEURONS. *Journal of Neurophysiology*, *28*(3), 560–580. https://doi.org/10.1152/jn.1965.28.3.560

Herbison, G. J., Jaweed, M. M., & Ditunno, J. F. (1982). Muscle fiber types. *Archives of Physical Medicine and Rehabilitation*, *63*(5), 227–230. http://www.ncbi.nlm.nih.gov/pubmed/6462127

Herman, A. M., Huang, L., Murphey, D. K., Garcia, I., & Arenkiel, B. R. (2014). Cell type-specific and time-dependent light exposure contribute to silencing in neurons expressing Channelrhodopsin-2. *ELife*, *3*. https://doi.org/10.7554/eLife.01481

Hernández-Hernández, J. M., García-González, E. G., Brun, C. E., & Rudnicki, M. A. (2017). The myogenic regulatory factors, determinants of muscle development, cell identity and regeneration. *Seminars in Cell & Developmental Biology*, *72*, 10–18. https://doi.org/10.1016/j.semcdb.2017.11.010

Herrera-Barrera, M., Ryals, R. C., Gautam, M., Jozic, A., Landry, M., Korzun, T., Gupta, M., Acosta, C., Stoddard, J., Reynaga, R., Tschetter, W., Jacomino, N., Taratula, O., Sun, C., Lauer, A. K., Neuringer, M., & Sahay, G. (2023). Peptide-guided lipid nanoparticles deliver mRNA to the neural retina of rodents and nonhuman primates. *Science Advances*, *9*(2), 1–16. https://doi.org/10.1126/sciadv.add4623

Hill, A. . (1938). The heat of shortening and the dynamic constants of muscle. *Proceedings of the Royal Society of London. Series B - Biological Sciences*, *126*(843), 136–195. https://doi.org/10.1098/rspb.1938.0050

Hitachi, K., Kiyofuji, Y., Yamaguchi, H., Nakatani, M., Inui, M., & Tsuchida, K. (2023). Simultaneous loss of skeletal muscle myosin heavy chain IIx and IIb causes severe skeletal muscle hypoplasia in postnatal mice. *FASEB Journal*, *37*(1), 1–19. https://doi.org/10.1096/fj.202200581R

Hong, I. H., & Etherington, S. J. (2011). Neuromuscular Junction. In *Encyclopedia of Life Sciences*. Wiley. https://doi.org/10.1002/9780470015902.a0023202

Hou, X., Zaks, T., Langer, R., & Dong, Y. (2021). Lipid nanoparticles for mRNA delivery. *Nature Reviews Materials*, *6*(12), 1078–1094. https://doi.org/10.1038/s41578-021-00358-0

Huang, X., Jiang, J., & Xu, J. (2022). Denervation-Related Neuromuscular Junction Changes: From Degeneration to Regeneration. *Frontiers in Molecular Neuroscience*, *14*(February), 1–8. https://doi.org/10.3389/fnmol.2021.810919

Huard, J., Bouchard, J.-P., Roy, R., Labrecque, C., Dansereau, G., Lemieux, B., & Tremblay, J. P. (1991). Correspondence Section: Myoblast transplantation produced dystrophin-positive muscle fibres in a 16-year-old patient with Duchenne muscular dystrophy. *Clinical Science*, *81*(2), 287–288. https://doi.org/10.1042/cs0810287

Huard, J., Bouchard, J. P., Roy, R., Malouin, F., Dansereau, G., Labrecque, C., Albert, N., Richards, C. L., Lemieux, B., & Tremblay, J. P. (1992). Human myoblast transplantation: Preliminary results of 4 cases. *Muscle & Nerve*, *15*(5), 550–560. https://doi.org/10.1002/mus.880150504

Huard, J., Verreault, S., Roy, R., Tremblay, M., & Tremblay, J. P. (1994). High efficiency of muscle regeneration after human myoblast clone transplantation in SCID mice. *Journal of Clinical Investigation*, *93*(2), 586–599. https://doi.org/10.1172/JCI117011

Huebner, E. A., & Strittmatter, S. M. (2009). *Axon Regeneration in the Peripheral and Central Nervous Systems* (pp. 305–360). https://doi.org/10.1007/400_2009_19

Hui, T., Jing, H., & Lai, X. (2021). Neuromuscular junction-specific genes screening by deep RNA-seq analysis. *Cell and Bioscience*, *11*(1), 1–15. https://doi.org/10.1186/s13578-021-00590-9

Hunter, D. D., Porter, B. E., Bulock, J. W., Adams, S. P., Merlie, J. P., & Sanes, J. R. (1989). Primary sequence of a motor neuron-selective adhesive site in the synaptic basal lamina protein s-laminin. *Cell*, *59*(5), 905–913. https://doi.org/10.1016/0092-8674(89)90613-2

Ishizuka, T., Kakuda, M., Araki, R., & Yawo, H. (2006). Kinetic evaluation of photosensitivity in genetically engineered neurons expressing green algae light-gated channels. *Neuroscience Research*, *54*(2), 85–94. https://doi.org/10.1016/j.neures.2005.10.009

Iwasaki, T., Takahashi, S., Takahashi, M., Zenimaru, Y., Kujiraoka, T., Ishihara, M., Nagano, M., Suzuki, J., Miyamori, I., Naiki, H., Sakai, J., Fujino, T., Miller, N. E., Yamamoto, T. T., & Hattori, H. (2005). Deficiency of the very low-density lipoprotein (VLDL) receptors in streptozotocin-induced diabetic rats: Insulin dependency of the VLDL receptor. *Endocrinology*, *146*(8), 3286–3294. https://doi.org/10.1210/en.2005-0043

Iyer, S. M., Montgomery, K. L., Towne, C., Lee, S. Y., Ramakrishnan, C., Deisseroth, K., & Delp, S. L. (2014). Virally mediated optogenetic excitation and inhibition of pain in freely moving nontransgenic mice. *Nature Biotechnology*, *32*(3), 274–278. https://doi.org/10.1038/nbt.2834

Iyer, S. R., Shah, S. B., & Lovering, R. M. (2021). The neuromuscular junction: Roles in aging and neuromuscular disease. *International Journal of Molecular Sciences*, *22*(15). https://doi.org/10.3390/ijms22158058

Jain, N. B., Ayers, G. D., Peterson, E. N., Harris, M. B., Morse, L., O'Connor, K. C., & Garshick, E. (2015). Traumatic spinal cord injury in the United States, 1993-2012. *JAMA - Journal of the American Medical Association*, *313*(22), 2236–2243. https://doi.org/10.1001/jama.2015.6250

Jayaraman, M., Ansell, S. M., Mui, B. L., Tam, Y. K., Chen, J., Du, X., Butler, D., Eltepu, L., Matsuda, S., Narayanannair, J. K., Rajeev, K. G., Hafez, I. M., Akinc, A., Maier, M. A., Tracy, M. A., Cullis, P. R., Madden, T. D., Manoharan, M., & Hope, M. J. (2012). Maximizing the potency of siRNA lipid nanoparticles for hepatic gene silencing in vivo. *Angewandte Chemie - International Edition*, *51*(34), 8529–8533. https://doi.org/10.1002/anie.201203263

Jeschke, M., & Moser, T. (2015). Considering optogenetic stimulation for cochlear implants. *Hearing Research*, *322*, 224–234. https://doi.org/10.1016/j.heares.2015.01.005

Jiang, Z., Le, Y., Chen, M., Yang, Y., Xu, X., Li, C., Zhang, K., Zhao, S., & Zhou, R. (2021). A modified protocol for the high yield production of a recombinant adeno-associated virus vector. *Gene Reports*, *24*, 101227. https://doi.org/10.1016/j.genrep.2021.101227

Johnson, A. L., Kamal, M., & Parise, G. (2023). The Role of Supporting Cell Populations in Satellite Cell Mediated Muscle Repair. *Cells*, *12*(15). https://doi.org/10.3390/cells12151968

Judson, R. N., & Rossi, F. M. V. (2020). Towards stem cell therapies for skeletal muscle repair. In *npj Regenerative Medicine* (Vol. 5, Issue 1). Nature Research. https://doi.org/10.1038/s41536-020-0094-3

Juhas, M., & Bursac, N. (2013). Engineering skeletal muscle repair. *Current Opinion in Biotechnology*, *24*(5), 880–886. https://doi.org/10.1016/j.copbio.2013.04.013

Jung, H. N., Lee, S. Y., Lee, S., Youn, H., & Im, H. J. (2022). Lipid nanoparticles for delivery of RNA therapeutics: Current status and the role of in vivo imaging. *Theranostics*, *12*(17), 7509–7531. https://doi.org/10.7150/thno.77259

Karlin, A. (2002). Ion channel structure: Emerging structure of the Nicotinic Acetylcholine receptors. *Nature Reviews Neuroscience*, *3*(2), 102–114. https://doi.org/10.1038/nrn731

Karpati, G., Ajdukovic, D., Arnold, D., Gledhill, R. B., Guttmann, R., Holland, P., Koch, P. A., Shoubridge, E., Spence, D., Vanasse, M., Watters, G. V., Abrahamowicz, M., Duff, C., & Worton, R. G. (1993). Myoblast transfer in duchenne muscular dystrophy. *Annals of Neurology*, *34*(1), 8–17. https://doi.org/10.1002/ana.410340105

Katz, B., & Thesleff, S. (1957). On the factors which determine the amplitude of the miniature end-plate potential. *The Journal of Physiology*, *137*(2), 267–278. https://doi.org/10.1113/jphysiol.1957.sp005811

Kawabe, Y. I., Wang, Y. X., McKinnell, I. W., Bedford, M. T., & Rudnicki, M. A. (2012). Carm1 regulates Pax7 transcriptional activity through MLL1/2 recruitment during asymmetric satellite stem cell divisions. *Cell Stem Cell*, *11*(3), 333–345. https://doi.org/10.1016/j.stem.2012.07.001

Kawaguchi, K., & Fujita, N. (2024). Shaping transverse-tubules: central mechanisms that play a role in the cytosol zoning for muscle contraction. *Journal of Biochemistry*, *175*(2), 125–131. https://doi.org/10.1093/jb/mvad083

Kehoe, S., Zhang, X. F., & Boyd, D. (2012). FDA approved guidance conduits and wraps for peripheral nerve injury: A review of materials and efficacy. *Injury*, *43*(5), 553–572. https://doi.org/10.1016/j.injury.2010.12.030

Kessler, P. D., Podsakoff, G. M., Chen, X., McQuiston, S. A., Colosi, P. C., Matelis, L. A., Kurtzman, G. J., & Byrne, B. J. (1996). Gene delivery to skeletal muscle results in sustained expression and systemic delivery of a therapeutic protein. *Proceedings of the National Academy of Sciences of the United States of America*, *93*(24), 14082–14087. https://doi.org/10.1073/pnas.93.24.14082

Khan, O. F., Zaia, E. W., Yin, H., Bogorad, R. L., Pelet, J. M., Webber, M. J., Zhuang, I., Dahlman, J. E., Langer, R., & Anderson, D. G. (2014). Ionizable amphiphilic dendrimer-based nanomaterials with alkyl-chain-substituted amines for tunable sirna delivery to the liver endothelium in vivo. *Angewandte Chemie - International Edition*, *53*(52), 14397–14401. https://doi.org/10.1002/anie.201408221

Khodabukus, A., Prabhu, N., Wang, J., & Bursac, N. (2018). In Vitro Tissue-Engineered Skeletal Muscle Models for Studying Muscle Physiology and Disease. *Advanced Healthcare Materials*, *7*(15). https://doi.org/10.1002/adhm.201701498

Kim, J. T., Kasukonis, B., Dunlap, G., Perry, R., Washington, T., & Wolchok, J. C. (2020). *Regenerative Repair of Volumetric Muscle Loss Injury is Sensitive to Age*. *26*, 3–14. https://doi.org/10.1089/ten.tea.2019.0034

Kleinlogel, S., Feldbauer, K., Dempski, R. E., Fotis, H., Wood, P. G., Bamann, C., & Bamberg, E. (2011). Ultra light-sensitive and fast neuronal activation with the Ca 2+-permeable channelrhodopsin CatCh. *Nature Neuroscience*, *14*(4), 513–518. https://doi.org/10.1038/nn.2776

Ko, C. P., & Robitaille, R. (2015). Perisynaptic schwann cells at the neuromuscular synapse: Adaptable, multitasking glial cells. *Cold Spring Harbor Perspectives in Biology*, *7*(10), 1–19. https://doi.org/10.1101/cshperspect.a020503

Kuang, S., & Rudnicki, M. A. (2008). The emerging biology of satellite cells and their therapeutic potential. *Trends in Molecular Medicine*, *14*(2), 82–91. https://doi.org/10.1016/j.molmed.2007.12.004

Kuo, I. Y., & Ehrlich, B. E. (2015). Signaling in muscle contraction. *Cold Spring Harbor Perspectives in Biology*, *7*(2), 1–14. https://doi.org/10.1101/cshperspect.a006023

Lai, C., Pursell, N., Gierut, J., Saxena, U., Zhou, W., Dills, M., Diwanji, R., Dutta, C., Koser, M., Nazef, N., Storr, R., Kim, B., Martin-Higueras, C., Salido, E., Wang, W., Abrams, M., Dudek, H., & Brown, B. D. (2018). Specific Inhibition of Hepatic Lactate Dehydrogenase Reduces Oxalate Production in Mouse Models of Primary Hyperoxaluria. *Molecular Therapy*, *26*(8), 1983–1995. https://doi.org/10.1016/j.ymthe.2018.05.016

Laumonier, T., & Menetrey, J. (2016). Muscle injuries and strategies for improving their repair. *Journal of Experimental Orthopaedics*, *3*(1). https://doi.org/10.1186/s40634-016-0051-7

Law, P. K., Bertorini, T. E., Goodwin, T. G., Chen, M., Fang, Q., Li, H. J., Kirby, D. S., Florendo, J. A., Herrod, H. G., & Golden, G. S. (1990). Dystrophin production induced by myoblast transfer therapy in Duchenne muscular dystrophy. *The Lancet*, *336*(8707), 114–115. https://doi.org/10.1016/0140-6736(90)91628-N

Law, P. K., Goodwin, T. G., & Wang, M. G. (1988). Normal myoblast injections provide genetic treatment for murine dystrophy. *Muscle & Nerve*, *11*(6), 525–533. https://doi.org/10.1002/mus.880110602

Le Grand, F., & Rudnicki, M. A. (2007). Skeletal muscle satellite cells and adult myogenesis. *Current Opinion in Cell Biology*, *19*(6), 628–633. https://doi.org/10.1016/j.ceb.2007.09.012

Lepper, C., Conway, S. J., & Fan, C. M. (2009). Adult satellite cells and embryonic muscle progenitors have distinct genetic requirements. *Nature*, *460*(7255), 627–631. https://doi.org/10.1038/nature08209

Lev, R., & Seliktar, D. (2018). Hydrogel biomaterials and their therapeutic potential for muscle injuries and muscular dystrophies. *Journal of the Royal Society Interface*, *15*(138). https://doi.org/10.1098/rsif.2017.0380

Li, L., Vasan, L., Kartono, B., Clifford, K., Attarpour, A., Sharma, R., Mandrozos, M., Kim, A., Zhao, W., Belotserkovsky, A., Verkuyl, C., & Schmitt-Ulms, G. (2023). Advances in Recombinant Adeno-Associated Virus Vectors for Neurodegenerative Diseases. *Biomedicines*, *11*(10), 1–38. https://doi.org/10.3390/biomedicines11102725

Li, L., Xiong, W. C., & Mei, L. (2018). Neuromuscular Junction Formation, Aging, and Disorders. *Annual Review of Physiology*, *80*, 159–188. https://doi.org/10.1146/annurev-physiol-022516-034255

Li, Q., Chan, C., Peterson, N., Hanna, R. N., Alfaro, A., Allen, K. L., Wu, H., Dall'Acqua, W. F., Borrok, M. J., & Santos, J. L. (2020). Engineering Caveolae-Targeted Lipid Nanoparticles to Deliver mRNA to the Lungs. *ACS Chemical Biology*, *15*(4), 830–836. https://doi.org/10.1021/acschembio.0c00003

Lieberman, A. R. (1971). *The Axon Reaction: A Review of the Principal Features of Perikaryal Responses to Axon Injury* (pp. 49–124). https://doi.org/10.1016/S0074-7742(08)60183-X

Lin, J. Y. (2011). A user's guide to channelrhodopsin variants: Features, limitations and future developments. *Experimental Physiology*, *96*(1), 19–25. https://doi.org/10.1113/expphysiol.2009.051961

Lin, J. Y., Lin, M. Z., Steinbach, P., & Tsien, R. Y. (2009). Characterization of engineered channelrhodopsin variants with improved properties and kinetics. *Biophysical Journal*, *96*(5), 1803–1814. https://doi.org/10.1016/j.bpj.2008.11.034

Lin, P. J. C., Tam, Y. Y. C., Hafez, I., Sandhu, A., Chen, S., Ciufolini, M. A., Nabi, I. R., & Cullis, P. R. (2013). Influence of cationic lipid composition on uptake and intracellular processing of lipid nanoparticle formulations of siRNA. *Nanomedicine: Nanotechnology, Biology, and Medicine*, *9*(2), 233–246. https://doi.org/10.1016/j.nano.2012.05.019

Liu, J., Saul, D., Böker, K. O., Ernst, J., Lehman, W., & Schilling, A. F. (2018). Current Methods for Skeletal Muscle Tissue Repair and Regeneration. *BioMed Research International*, *2018*. https://doi.org/10.1155/2018/1984879

Liu, Y., Yang, X., He, Z., Li, J., Li, Y., Wu, Y., Manyande, A., Feng, M., & Xiang, H. (2023). Spinal cord injury: global burden from 1990 to 2019 and projections up to 2030 using Bayesian age-period-cohort analysis. *Frontiers in Neurology*, *14*(December). https://doi.org/10.3389/fneur.2023.1304153

Llewellyn, M. E., Thompson, K. R., Deisseroth, K., & Delp, S. L. (2010). Orderly recruitment of motor units under optical control in vivo. *Nature Medicine*, *16*(10), 1161–1165. https://doi.org/10.1038/nm.2228

Lokugamage, M. P., Vanover, D., Beyersdorf, J., Hatit, M. Z. C., Rotolo, L., Echeverri, E. S., Peck, H. E., Ni, H., Yoon, J. K., Kim, Y. T., Santangelo, P. J., & Dahlman, J. E. (2021). Optimization of lipid nanoparticles for the delivery of nebulized therapeutic mRNA to the lungs. *Nature Biomedical Engineering*, *5*(9), 1059–1068. https://doi.org/10.1038/s41551-021-00786-x

Lopes, B., Sousa, P., Alvites, R., Branquinho, M., Sousa, A. C., Mendonça, C., Atayde, L. M., Luís, A. L., Varejão, A. S. P., & Maurício, A. C. (2022). Peripheral Nerve Injury Treatments and Advances: One Health Perspective. *International Journal of Molecular Sciences*, *23*(2). https://doi.org/10.3390/ijms23020918

Lovering, R. M., Iyer, S. R., Edwards, B., & Davies, K. E. (2020). Alterations of neuromuscular junctions in Duchenne muscular dystrophy. *Neuroscience Letters*, *737*, 135304. https://doi.org/10.1016/j.neulet.2020.135304

Lovering, R. M., Porter, N. C., & Block, R. J. (2005). The muscular dystrophies: From genes to therapies. *Physical Therapy*, *85*(12), 1372–1388. https://doi.org/10.1093/ptj/85.12.1372

Lower, R. (1665). The method observed in transfusing the bloud out of one live animal into another: and how this experiment is like to be improved. Some considerations concerning the same. *Philosophical Transactions of the Royal Society of London*, *1*(20), 353–358. https://doi.org/10.1098/rstl.1665.0128

Lu, Q. L., Bou-Gharios, G., & Partridge, T. A. (2003). Non-viral gene delivery in skeletal muscle: A protein factory. *Gene Therapy*, *10*(2), 131–142. https://doi.org/10.1038/sj.gt.3301874

Lupa, M. T., & Caldwell, J. H. (1994). Sodium channels aggregate at former synaptic sites in innervated and denervated regenerating muscles. *Journal of Cell Biology*, *124*(1–2), 139–147. https://doi.org/10.1083/jcb.124.1.139

Magown, P., Shettar, B., Zhang, Y., & Rafuse, V. F. (2015). Direct optical activation of skeletal muscle fibres efficiently controls muscle contraction and attenuates denervation atrophy. *Nature Communications*, *6*. https://doi.org/10.1038/ncomms9506

Mahley, R. W., & Rall, S. C. (2000). Apolipoprotein E: Far more than a lipid transport protein. *Annual Review of Genomics and Human Genetics*, *1*(2000), 507–537. https://doi.org/10.1146/annurev.genom.1.1.507

Marshall, L. M., Sanes, J. R., & McMahan, U. J. (1977). Reinnervation of original synaptic sites on muscle fiber basement membrane after disruption of the muscle cells. *Proceedings of the National Academy of Sciences of the United States of America*, *74*(7), 3073–3077. https://doi.org/10.1073/pnas.74.7.3073

Martyn, J. A. J., Jonsson Fagerlund, M., & Eriksson, L. I. (2009). Basic principles of neuromuscular transmission. *Anaesthesia*, *64*(SUPPL. 1), 1–9. https://doi.org/10.1111/j.1365-2044.2008.05865.x

Matsuno-Yagi, A., & Mukohata, Y. (1977). Two possible roles of bacteriorhodopsin; a comparative study of strains of Halobacterium halobium differing in pigmentation. *Biochemical and Biophysical Research Communications*, *78*(1), 237–243. https://doi.org/10.1016/0006-291X(77)91245-1

Maugeri, G., D'Agata, V., Trovato, B., Roggio, F., Castorina, A., Vecchio, M., di Rosa, M., & Musumeci, G. (2021). The role of exercise on peripheral nerve regeneration: from animal model to clinical application. *Heliyon*, *7*(11), e08281. https://doi.org/10.1016/j.heliyon.2021.e08281

Maughan, R. J., Watson, J. S., & Weir, J. (1983). Strength and cross-sectional area of human skeletal muscle. *The Journal of Physiology*, *338*(1), 37–49. https://doi.org/10.1113/jphysiol.1983.sp014658

Maurer, N., Wong, K. F., Stark, H., Louie, L., McIntosh, D., Wong, T., Scherrer, P., Semple, S. C., & Cullis, P. R. (2001). Spontaneous entrapment of polynucleotides upon electrostatic interaction with ethanol-destabilized cationic liposomes. *Biophysical Journal*, *80*(5), 2310–2326. https://doi.org/10.1016/S0006-3495(01)76202-9

Mauro, A. (1961). Satellite cell of skeletal muscle fibers. *The Journal of Biophysical and Biochemical Cytology*, *9*, 493–495. https://doi.org/10.1083/jcb.9.2.493

Maynard, F. M., Bracken, M. B., Creasey, G., Ditunno, J. F., Donovan, W. H., Ducker, T. B., Garber, S. L., Marino, R. J., Stover, S. L., Tator, C. H., Waters, R. L., Wilberger, J. E., & Young, W. (1997). International standards for neurological and functional classification of spinal cord injury. *Spinal Cord*, *35*(5), 266–274. https://doi.org/10.1038/sj.sc.3100432

Mcdonald, J. W., & Sadowsky, C. (2002). *Spinal-cord injury*. *359*, 417–425.

McIntosh, J., Mekrouda, I., Dashti, M., Giuraniuc, C. V., Banks, R. W., Miles, G. B., & Bewick, G. S. (2023). Development of abnormalities at the neuromuscular junction in the SOD1-G93A mouse model of ALS: dysfunction then disruption of postsynaptic structure precede overt motor symptoms. *Frontiers in Molecular Neuroscience*, *16*. https://doi.org/10.3389/fnmol.2023.1169075

McKinnell, I. W., Ishibashi, J., Le Grand, F., Punch, V. G. J., Addicks, G. C., Greenblatt, J. F., Dilworth, F. J., & Rudnicki, M. A. (2008). Pax7 activates myogenic genes by recruitment of a histone methyltransferase complex. *Nature Cell Biology*, *10*(1), 77–84. https://doi.org/10.1038/ncb1671

Melamed, J. R., Yerneni, S. S., Arral, M. L., LoPresti, S. T., Chaudhary, N., Sehrawat, A., Muramatsu, H., Alameh, M. G., Pardi, N., Weissman, D., Gittes, G. K., & Whitehead, K. A. (2023). Ionizable lipid nanoparticles deliver mRNA to pancreatic β cells via macrophage-mediated gene transfer. *Science Advances*, *9*(4). https://doi.org/10.1126/sciadv.ade1444

Mendell, J. R., Kissel, J. T., Amato, A. A., King, W., Signore, L., Prior, T. W., Sahenk,

Z., Benson, S., McAndrew, P. E., Rice, R., Nagaraja, H., Stephens, R., Lantry, L., Morris, G. E., & Burghes, A. H. M. (1995). Myoblast Transfer in the Treatment of Duchenne's Muscular Dystrophy. *New England Journal of Medicine*, *333*(13), 832–838. https://doi.org/10.1056/NEJM199509283331303

Metzler, E., Escobar, H., Sunaga-Franze, D. Y., Sauer, S., Diecke, S., & Spuler, S. (2022). Generation of hiPSC-Derived Skeletal Muscle Cells: Exploiting the Potential of Skeletal Muscle-Derived hiPSCs. *Biomedicines*, *10*(5). https://doi.org/10.3390/BIOMEDICINES10051204

Meyer, G. A. (2018). Evidence of induced muscle regeneration persists for years in the mouse. *Muscle and Nerve*, *58*(6), 858–862. https://doi.org/10.1002/mus.26329

Mickle, A. D., Won, S. M., Noh, K. N., Yoon, J., Meacham, K. W., Xue, Y., McIlvried, L. A., Copits, B. A., Samineni, V. K., Crawford, K. E., Kim, D. H., Srivastava, P., Kim, B. H., Min, S., Shiuan, Y., Yun, Y., Payne, M. A., Zhang, J., Jang, H., … Rogers, J. A. (2019). A wireless closed-loop system for optogenetic peripheral neuromodulation. *Nature*, *565*(7739), 361–365. https://doi.org/10.1038/s41586-018-0823-6

Mierzejewski, B., Ciemerych, M. A., Streminska, W., Janczyk-Ilach, K., & Brzoska, E. (2023). miRNA-126a plays important role in myoblast and endothelial cell interaction. *Scientific Reports*, *13*(1), 1–15. https://doi.org/10.1038/s41598-023-41626-z

Miller, R. G., Sharma, K. R., Pavlath, G. K., Gussoni, E., Mynhier, M., Yu, P., Lanctot, A. M., Greco, C. M., Steinman, L., & Blau, H. M. (1997). Myoblast implantation in Duchenne muscular dystrophy: The San Francisco study. *Muscle & Nerve*, *20*(4), 469–478. https://doi.org/10.1002/(SICI)1097-4598(199704)20:4<469::AID-MUS10>3.0.CO;2-U

Miner, J. H., & Wold, B. J. (1991). c-myc Inhibition of MyoD and Myogenin-Initiated Myogenic Differentiation . *Molecular and Cellular Biology*, *11*(5), 2842–2851. https://doi.org/10.1128/mcb.11.5.2842-2851.1991

Mingozzi, F., & High, K. A. (2013). Immune responses to AAV vectors: Overcoming barriers to successful gene therapy. *Blood*, *122*(1), 23–36. https://doi.org/10.1182/blood-2013-01-306647

Morgan, J. E., Pagel, C. N., Sherrratt, T., & Partridge, T. A. (1993). Long-term persistence and migration of myogenic cells injected into pre-irradiated muscles of mdx mice. *Journal of the Neurological Sciences*, *115*(2), 191–200. https://doi.org/10.1016/0022-510X(93)90224-M

Morgan, J. E., & Partridge, T. A. (2003). Muscle satellite cells. *International Journal of Biochemistry and Cell Biology*, *35*(8), 1151–1156. https://doi.org/10.1016/S1357-2725(03)00042-6

Moss, F. P., & Leblond, C. P. (1971). Satellite cells as the source of nuclei in muscles of growing rats. *The Anatomical Record*, *170*(4), 421–435. https://doi.org/10.1002/ar.1091700405

Mukai, H., Ogawa, K., Kato, N., & Kawakami, S. (2022). Recent advances in lipid nanoparticles for delivery of nucleic acid, mRNA, and gene editing-based therapeutics. *Drug Metabolism and Pharmacokinetics*, *44*, 100450. https://doi.org/10.1016/j.dmpk.2022.100450

Mukund, K., & Subramaniam, S. (2020). Skeletal muscle: A review of molecular structure and function, in health and disease. *Wiley Interdisciplinary Reviews: Systems Biology and Medicine*, *12*(1), 1–46. https://doi.org/10.1002/wsbm.1462

Müller, M., Bamann, C., Bamberg, E., & Kühlbrandt, W. (2011). Projection structure of channelrhodopsin-2 at 6 Å resolution by electron crystallography. *Journal of Molecular Biology*, *414*(1), 86–95. https://doi.org/10.1016/j.jmb.2011.09.049

Murphy, M. M., Lawson, J. A., Mathew, S. J., Hutcheson, D. A., & Kardon, G. (2011). Satellite cells, connective tissue fibroblasts and their interactions are crucial for muscle regeneration. *Development*, *138*(17), 3625–3637. https://doi.org/10.1242/dev.064162

Nabeshlma, Y., Hanaokat, K., Hayasakat, M., Esuml, E., & Li, S. (1993). Myogenin gene disruption muscle defect. *Nature*, *364*(August), 8–11.

Nagata, Y., Kobayashi, H., Umeda, M., Ohta, N., Kawashima, S., Zammit, P. S., & Matsuda, R. (2006). Sphingomyelin levels in the plasma membrane correlate with the activation state of muscle satellite cells. *Journal of Histochemistry and Cytochemistry*, *54*(4), 375–384. https://doi.org/10.1369/jhc.5A6675.2006

Nagel, G., Brauner, M., Liewald, J. F., Adeishvili, N., Bamberg, E., & Gottschalk, A. (2005). Light activation of Channelrhodopsin-2 in excitable cells of caenorhabditis elegans triggers rapid behavioral responses. *Current Biology*, *15*(24), 2279–2284. https://doi.org/10.1016/j.cub.2005.11.032

Nagel, G., Ollig, D., Fuhrmann, M., Kateriya, S., Musti, A. M., Bamberg, E., & Hegemann, P. (2002). Channelrhodopsin-1: A light-gated proton channel in green algae. *Science*, *296*(5577), 2395–2398. https://doi.org/10.1126/science.1072068

Nagel, G., Szellas, T., Huhn, W., Kateriya, S., Adeishvili, N., Berthold, P., Ollig, D., Hegemann, P., & Bamberg, E. (2003). Channelrhodopsin-2, a directly light-gated cation-selective membrane channel. *Proceedings of the National Academy of Sciences of the United States of America*, *100*(SUPPL. 2), 13940–13945. https://doi.org/10.1073/pnas.1936192100

Nance, M. E., Shi, R., Hakim, C. H., Wasala, N. B., Yue, Y., Pan, X., Zhang, T., Robinson, C. A., Duan, S. X., Yao, G., Yang, N. N., Chen, S. jie, Wagner, K. R., Gersbach, C. A., & Duan, D. (2019). AAV9 Edits Muscle Stem Cells in Normal and Dystrophic Adult Mice. *Molecular Therapy*, *27*(9), 1568–1585. https://doi.org/10.1016/j.ymthe.2019.06.012

Naso, M. F., Tomkowicz, B., Perry, W. L., & Strohl, W. R. (2017). Adeno-Associated Virus (AAV) as a Vector for Gene Therapy. *BioDrugs*, *31*(4), 317–334. https://doi.org/10.1007/s40259-017-0234-5

Natasha, G., Tan, A., Farhatnia, Y., Rajadas, J., Hamblin, M. R., Khaw, P. T., & Seifalian, A. M. (2013). Channelrhodopsins: visual regeneration and neural activation by a light switch. *New Biotechnology*, *30*(5), 461–474. https://doi.org/10.1016/j.nbt.2013.04.007

Negroni, E., Bigot, A., Butler-Browne, G. S., Trollet, C., & Mouly, V. (2016). Cellular Therapies for Muscular Dystrophies: Frustrations and Clinical Successes. *Human Gene Therapy*, *27*(2), 117–126. https://doi.org/10.1089/hum.2015.139

Neumeyer, A. M., Cross, D., McKenna-Yasek, D., Zawadzka, A., Hoffman, E. P., Pegoraro, E., Hunter, R. G., Munsat, T. L., & Brown, R. H. (1998). Pilot study of myoblast transfer in the treatment of Becker muscular dystrophy. *Neurology*, *51*(2), 589–592. https://doi.org/10.1212/WNL.51.2.589

Nguyen, Q. T., Son, Y. J., Sanes, J. R., & Lichtman, J. W. (2000). Nerve terminals form but fail to mature when postsynaptic differentiation is blocked: In vivo analysis using mammalian nerve-muscle chimeras. *Journal of Neuroscience*, *20*(16), 6077–6086. https://doi.org/10.1523/jneurosci.20-16-06077.2000

Nuriel, T., Peng, K. Y., Ashok, A., Dillman, A. A., Figueroa, H. Y., Apuzzo, J., Ambat, J., Levy, E., Cookson, M. R., Mathews, P. M., & Duff, K. E. (2017). The endosomal-lysosomal pathway is dysregulated by APOE4 expression in vivo. *Frontiers in Neuroscience*, *11*(DEC), 1–12. https://doi.org/10.3389/fnins.2017.00702

Nyns, E. C. A., Poelma, R. H., Volkers, L., Bart, C. I., Van Brakel, T. J., Zeppenfeld, K., Schalij, M. J., Zhang, G. Q., De Vries, A. A. F., & Pijnappels, D. A. (2019). Continuous shock-free termination of atrial fibrillation by local optogenetic therapy and arrhythmia-triggered activation of an implanted light source. *European Heart Journal*, *40*(Supplement_1), 2160. https://doi.org/10.1093/eurheartj/ehz748.0090

Nyns, E. C. A., Poelma, R. H., Volkers, L., Plomp, J. J., Bart, C. I., Kip, A. M., van Brakel, T. J., Zeppenfeld, K., Schalij, M. J., Zhang, G. Q., de Vries, A. A. F., & Pijnappels, D. A. (2019). An automated hybrid bioelectronic system for autogenous restoration of sinus rhythm in atrial fibrillation. *Science Translational Medicine*, *11*(481). https://doi.org/10.1126/scitranslmed.aau6447

Oesterhelt, D., & Stoeckenius, W. (1971). Rhodopsin-like Protein from the Purple Membrane of Halobacterium halobium. *Nature New Biology*, *233*(39), 149–152. https://doi.org/10.1038/newbio233149a0

Ohtsuki, I., & Morimoto, S. (2008). Troponin: Regulatory function and disorders. *Biochemical and Biophysical Research Communications*, *369*(1), 62–73. https://doi.org/10.1016/j.bbrc.2007.11.187

Olguin, H. C., & Olwin, B. B. (2004). Pax-7 up-regulation inhibits myogenesis and cell cycle progression in satellite cells: a potential mechanism for self-renewal. *Developmental Biology*, *275*(2), 375–388. https://doi.org/10.1016/j.ydbio.2004.08.015

Olguín, H. C., & Pisconti, A. (2012). Marking the tempo for myogenesis: Pax7 and the regulation of muscle stem cell fate decisions. *Journal of Cellular and Molecular Medicine*, *16*(5), 1013–1025. https://doi.org/10.1111/j.1582-4934.2011.01348.x

Oud, T., Beelen, A., Eijffinger, E., & Nollet, F. (2007). Sensory re-education after nerve injury of the upper limb: A systematic review. *Clinical Rehabilitation*, *21*(6), 483–494. https://doi.org/10.1177/0269215507074395

Palanki, R., Bose, S. K., Dave, A., White, B. M., Berkowitz, C., Luks, V., Yaqoob, F., Han, E., Swingle, K. L., Menon, P., Hodgson, E., Biswas, A., Billingsley, M. M., Li, L., Yiping, F., Carpenter, M., Trokhan, A., Yeo, J., Johana, N., … Peranteau, W. H. (2023). Ionizable Lipid Nanoparticles for Therapeutic Base Editing of Congenital Brain Disease. *ACS Nano*, *17*(14), 13594–13610. https://doi.org/10.1021/acsnano.3c02268

Pallarès-Masmitjà, M., Ivančić, D., Mir-Pedrol, J., Jaraba-Wallace, J., Tagliani, T., Oliva, B., Rahmeh, A., Sánchez-Mejías, A., & Güell, M. (2021). Find and cut-and-transfer (FiCAT) mammalian genome engineering. *Nature Communications*, *12*(1), 1–9. https://doi.org/10.1038/s41467-021-27183-x

Paolini, C., Quarta, M., Nori, A., Boncompagni, S., Canato, M., Volpe, P., Allen, P. D., Reggiani, C., & Protasi, F. (2007). Reorganized stores and impaired calcium handling in skeletal muscle of mice lacking calsequestrin-1. *Journal of Physiology*, *583*(2), 767–784. https://doi.org/10.1113/jphysiol.2007.138024

Parhiz, H., Shuvaev, V. V., Pardi, N., Khoshnejad, M., Kiseleva, R. Y., Brenner, J. S., Uhler, T., Tuyishime, S., Mui, B. L., Tam, Y. K., Madden, T. D., Hope, M. J., Weissman, D., & Muzykantov, V. R. (2018). PECAM-1 directed re-targeting of exogenous mRNA providing two orders of magnitude enhancement of vascular delivery and expression in lungs independent of apolipoprotein E-mediated uptake. *Journal of Controlled Release*, *291*(October), 106–115. https://doi.org/10.1016/j.jconrel.2018.10.015

Partridge, T. A., Morgan, J. E., Coulton, G. R., Hoffman, E. P., & Kunkel, L. M. (1989). Conversion of mdx myofibres from dystrophin-negative to -positive by injection of normal myoblasts. *Nature*, *337*(6203), 176–179. https://doi.org/10.1038/337176a0

Patel, N., Davis, Z., Hofmann, C., Vlasak, J., Loughney, J. W., DePhillips, P., & Mukherjee, M. (2023). Development and Characterization of an In Vitro Cell-Based Assay to Predict Potency of mRNA–LNP-Based Vaccines. *Vaccines*, *11*(7). https://doi.org/10.3390/vaccines11071224

Patton, B. L. (2003). Basal lamina and the organization of neuromuscular synapses. *Journal of Neurocytology*, *32*(5–8), 883–903. https://doi.org/10.1023/B:NEUR.0000020630.74955.19

Paulin, D., & Li, Z. (2004). Desmin: A major intermediate filament protein essential for the structural integrity and function of muscle. *Experimental Cell Research*, *301*(1), 1–7. https://doi.org/10.1016/j.yexcr.2004.08.004

Paz, J. T., & Huguenard, J. R. (2014). Optogenetics and epilepsy: Past, present and future. *Epilepsy Currents*, *15*(1), 34–38. https://doi.org/10.5698/1535-7597-15.1.34

Penaud-Budloo, M., Le Guiner, C., Nowrouzi, A., Toromanoff, A., Chérel, Y., Chenuaud, P., Schmidt, M., von Kalle, C., Rolling, F., Moullier, P., & Snyder, R. O. (2008). Adeno-Associated Virus Vector Genomes Persist as Episomal Chromatin in Primate Muscle. *Journal of Virology*, *82*(16), 7875–7885. https://doi.org/10.1128/jvi.00649-08

Petersen, Z. Q., & Huard, J. (2000). The influence of muscle fiber type in myoblast-mediated gene transfer to skeletal muscles. *Cell Transplantation*, *9*(4), 503–517. https://doi.org/10.1177/096368970000900407

Pette, D. (1985). Metabolic heterogeneity of muscle fibres. *Journal of Experimental Biology*, *VOL. 115*, 179–189. https://doi.org/10.1242/jeb.115.1.179

Pette, D., & Staron, R. S. (1990). Cellular and molecular diversities of mammalian skeletal muscle fibers. *Reviews of Physiology, Biochemistry and Pharmacology*, *116*, 1–76. https://doi.org/10.1007/3540528806_3

Pette, D., & Staron, R. S. (2000). Myosin isoforms, muscle fiber types, and transitions. *Microscopy Research and Technique*, *50*(6), 500–509. https://doi.org/10.1002/1097-0029(20000915)50:6<500::AID-JEMT7>3.0.CO;2-7

Pham, S., & Puckett, Y. (2023). *Physiology, Skeletal Muscle Contraction*. Statpearls. https://www.ncbi.nlm.nih.gov/books/NBK559006/

Plant, D. R., Colarossi, F. E., & Lynch, G. S. (2006). Notexin causes greater myotoxic damage and slower functional repair in mouse skeletal muscles than bupivacaine. *Muscle and Nerve*, *34*(5), 577–585. https://doi.org/10.1002/mus.20616

Plenk, H. (2011). The Role of Materials Biocompatibility for Functional Electrical Stimulation Applications. *Artificial Organs*, *35*(3), 237–241. https://doi.org/10.1111/j.1525-1594.2011.01221.x

Polack, F. P., Thomas, S. J., Kitchin, N., Absalon, J., Gurtman, A., Lockhart, S., Perez, J. L., Pérez Marc, G., Moreira, E. D., Zerbini, C., Bailey, R., Swanson, K. A., Roychoudhury, S., Koury, K., Li, P., Kalina, W. V., Cooper, D., Frenck, R. W., Hammitt, L. L., … Gruber, W. C. (2020). Safety and Efficacy of the BNT162b2 mRNA Covid-19 Vaccine. *New England Journal of Medicine*, *383*(27), 2603–2615. https://doi.org/10.1056/nejmoa2034577

Prochazka, A., Mushahwar, V. K., & McCreery, D. B. (2001). Neural prostheses. *Journal of Physiology*, *533*(1), 99–109. https://doi.org/10.1111/j.1469-7793.2001.0099b.x

Purves D, Augustine GJ, Fitzpatrick D, et al., E. (2001). Neuroscience. 2nd edition. In *Neuroscience. 2nd edition*. Sinauer Associates.

Quarta, M., Cromie, M., Chacon, R., Blonigan, J., Garcia, V., Akimenko, I., Hamer, M., Paine, P., Stok, M., Shrager, J. B., & Rando, T. A. (2017). Bioengineered constructs combined with exercise enhance stem cell-mediated treatment of volumetric muscle loss. *Nature Communications*, *8*, 1–17. https://doi.org/10.1038/ncomms15613

Rafuse, V. F., Milner, L. D., & Landmesser, L. T. (1996). Selective innervation of fast and slow muscle regions during early chick neuromuscular development. *Journal of Neuroscience*, *16*(21), 6864–6877. https://doi.org/10.1523/jneurosci.16-21-06864.1996

Rafuse, V. F., Pattullo, M. C., & Gordon, T. (1997). Innervation ratio and motor unit force in large muscles: A study of chronically stimulated cat medial gastrocnemius. *Journal of Physiology*, *499*(3), 809–823. https://doi.org/10.1113/jphysiol.1997.sp021970

Raney, S., Wilson, K., Sekirov, L., Chikh, G., de Jong, S., Cullis, P., & Tam, Y. (2008). The effect of circulation lifetime and drug-to-lipid ratio of intravenously administered lipid nanoparticles on the biodistribution and immunostimulatory activity of encapsulated CpG-ODN. *Journal of Drug Targeting*, *16*(7–8), 564–577. https://doi.org/10.1080/10611860802228756

Rayagiri, S. S., Ranaldi, D., Raven, A., Mohamad Azhar, N. I. F., Lefebvre, O., Zammit, P. S., & Borycki, A. G. (2018). Basal lamina remodeling at the skeletal muscle stem cell niche mediates stem cell self-renewal. *Nature Communications*, *9*(1), 1–12. https://doi.org/10.1038/s41467-018-03425-3

Redondo-Castro, E., & Navarro, X. (2013). Peripheral nerve alterations after spinal cord injury in the adult rat. *Spinal Cord*, *51*(8), 630–633. https://doi.org/10.1038/sc.2013.57

Relaix, F., Bencze, M., Borok, M. J., Der Vartanian, A., Gattazzo, F., Mademtzoglou, D., Perez-Diaz, S., Prola, A., Reyes-Fernandez, P. C., Rotini, A., & Taglietti. (2021). Perspectives on skeletal muscle stem cells. *Nature Communications*, *12*(1), 1–11. https://doi.org/10.1038/s41467-020-20760-6

Relaix, F., & Zammit, P. S. (2012). Satellite cells are essential for skeletal muscle regeneration: The cell on the edge returns centre stage. *Development (Cambridge)*, *139*(16), 2845–2856. https://doi.org/10.1242/dev.069088

Ribeiro, A. F., Souza, L. S., Almeida, C. F., Ishiba, R., Fernandes, S. A., Guerrieri, D. A., Santos, A. L. F., Onofre-Oliveira, P. C. G., & Vainzof, M. (2019). Muscle satellite cells and impaired late stage regeneration in different murine models for muscular dystrophies. *Scientific Reports*, *9*(1), 1–11. https://doi.org/10.1038/s41598-019-48156-7

Richardson, P. M., McGuinness, U. M., & Aguayo, A. J. (1980). Axons from CNS neurones regenerate into PNS grafts. *Nature*, *284*(5753), 264–265. https://doi.org/10.1038/284264a0

Rietwyk, S., & Peer, D. (2017). Next-Generation Lipids in RNA Interference Therapeutics. *ACS Nano*, *11*(8), 7572–7586. https://doi.org/10.1021/acsnano.7b04734

Robin, G., & Allard, B. (2013). Major contribution of sarcoplasmic reticulum Ca2+ depletion during long-lasting activation of skeletal muscle. *Journal of General Physiology*, *141*(5), 557–565. https://doi.org/10.1085/jgp.201310957

Rodríguez Cruz, P. M., Cossins, J., Beeson, D., & Vincent, A. (2020). The Neuromuscular Junction in Health and Disease: Molecular Mechanisms Governing Synaptic Formation and Homeostasis. *Frontiers in Molecular Neuroscience*, *13*(December), 1–22. https://doi.org/10.3389/fnmol.2020.610964

Rogers, R. S., & Nishimune, H. (2017). The role of laminins in the organization and function of neuromuscular junctions. *Matrix Biology*, *57–58*, 86–105. https://doi.org/10.1016/j.matbio.2016.08.008

Romanul, F. C. A., & Van Der Meulen, J. (1967). Slow and Fast Muscles After Cross Innervation. *Archives of Neurology*, *17*(4), 387. https://doi.org/10.1001/archneur.1967.00470280053006

Rousseau, E., Raman, R., Tamir, T., Bu, A., Srinivasan, S., Lynch, N., Langer, R., White, F. M., & Cima, M. J. (2023). Actuated tissue engineered muscle grafts restore functional mobility after volumetric muscle loss. *Biomaterials*, *302*(September), 122317. https://doi.org/10.1016/j.biomaterials.2023.122317

Rudolf, R., & Straka, T. (2019). Nicotinic acetylcholine receptor at vertebrate motor endplates: Endocytosis, recycling, and degradation. *Neuroscience Letters*, *711*(July), 134434. https://doi.org/10.1016/j.neulet.2019.134434

Rungta, R. L., Choi, H. B., Lin, P. J. C., Ko, R. W. Y., Ashby, D., Nair, J., Manoharan, M., Cullis, P. R., & MacVicar, B. A. (2013). Lipid nanoparticle delivery of sirna to silence neuronal gene expression in the brain. *Molecular Therapy Nucleic Acids*, *2*(April 2014). https://doi.org/10.1038/mtna.2013.65

Rungta, R. L., Choi, H. B., Tyson, J. R., Malik, A., Dissing-Olesen, L., Lin, P. J. C., Cain, S. M., Cullis, P. R., Snutch, T. P., & Macvicar, B. A. (2015). The cellular mechanisms of neuronal swelling underlying cytotoxic edema. *Cell*, *161*(3), 610–621. https://doi.org/10.1016/j.cell.2015.03.029

Rupp, R. (2020). Spinal cord lesions. In *Handbook of Clinical Neurology* (pp. 51–65). https://doi.org/10.1016/B978-0-444-63934-9.00006-8

Rurik, J. G., Tombácz, I., Yadegari, A., Méndez Fernández, P. O., Shewale, S. V., Li, L., Kimura, T., Soliman, O. Y., Papp, T. E., Tam, Y. K., Mui, B. L., Albelda, S. M., Puré, E., June, C. H., Aghajanian, H., Weissman, D., Parhiz, H., & Epstein, J. A. (2022). CAR T cells produced in vivo to treat cardiac injury. *Science*, *375*(6576), 91–96. https://doi.org/10.1126/science.abm0594

Russell, S. (2015). *Examination of Peripheral Nerve Injuries: An Anatomical Approach* (2nd ed.). Thieme.

Sago, C. D., Lokugamage, M. P., Paunovska, K., Vanover, D. A., Monaco, C. M., Shah, N. N., Castro, M. G., Anderson, S. E., Rudoltz, T. G., Lando, G. N., Tiwari, P. M., Kirschman, J. L., Willett, N., Jang, Y. C., Santangelo, P. J., Bryksin, A. V., & Dahlman, J. E. (2018). High-throughput in vivo screen of functional mRNA delivery identifies nanoparticles for endothelial cell gene editing. *Proceedings of the National Academy of Sciences of the United States of America*, *115*(42), E9944–E9952. https://doi.org/10.1073/pnas.1811276115

Samaridou, E., Heyes, J., & Lutwyche, P. (2020). Lipid nanoparticles for nucleic acid delivery: Current perspectives. *Advanced Drug Delivery Reviews*, *154–155*, 37–63. https://doi.org/10.1016/j.addr.2020.06.002

Sanes, J. R. (2003). The basement membrane/basal lamina of skeletal muscle. *Journal of Biological Chemistry*, *278*(15), 12601–12604. https://doi.org/10.1074/jbc.R200027200

Scardigli, M., Müllenbroich, C., Margoni, E., Cannazzaro, S., Crocini, C., Ferrantini, C., Coppini, R., Yan, P., Loew, L. M., Campione, M., Bocchi, L., Giulietti, D., Cerbai, E., Poggesi, C., Bub, G., Pavone, F. S., & Sacconi, L. (2018). Real-time optical manipulation of cardiac conduction in intact hearts. *The Journal of Physiology*, *596*(17), 3841–3858. https://doi.org/10.1113/JP276283

Scheib, J., & Höke, A. (2013). Advances in peripheral nerve regeneration. *Nature Reviews Neurology*, *9*(12), 668–676. https://doi.org/10.1038/nrneurol.2013.227

Schiaffino, S., & Reggiani, C. (2011). Fiber types in Mammalian skeletal muscles. *Physiological Reviews*, *91*(4), 1447–1531. https://doi.org/10.1152/physrev.00031.2010

Schmalbruch, H., & Lewis, D. M. (2000). Dynamics of nuclei of muscle fibers and connective tissue cells in normal and denervated rat muscles. *Muscle and Nerve*, *23*(4), 617–626. https://doi.org/10.1002/(SICI)1097-4598(200004)23:4<617::AID-MUS22>3.0.CO;2-Y

Schmidt, M., Schüler, S. C., Hüttner, S. S., von Eyss, B., & von Maltzahn, J. (2019). Adult stem cells at work: regenerating skeletal muscle. *Cellular and Molecular Life Sciences*, *76*(13), 2559–2570. https://doi.org/10.1007/s00018-019-03093-6

Schüler, S. C., Liu, Y., Dumontier, S., Grandbois, M., Le Moal, E., Cornelison, D. D. W., & Bentzinger, C. F. (2022). Extracellular matrix: Brick and mortar in the skeletal muscle stem cell niche. *Frontiers in Cell and Developmental Biology*, *10*(November), 1–21. https://doi.org/10.3389/fcell.2022.1056523

Schultz, E., Gibson, M. C., & Champion, T. (1978). Satellite cells are mitotically quiescent in mature mouse muscle: An EM and radioautographic study. *Journal of Experimental Zoology*, *206*(3), 451–456. https://doi.org/10.1002/jez.1402060314

Scott, W., Stevens, J., & Binder-Macleod, S. A. (2001). Human skeletal muscle fiber type classifications. *Physical Therapy*, *81*(11), 1810–1816. https://doi.org/10.1093/ptj/81.11.1810

Seale, P., Sabourin, L. A., Girgis-Gabardo, A., Mansouri, A., Gruss, P., & Rudnicki, M. A. (2000). Pax7 is required for the specification of myogenic satellite cells. *Cell*, *102*(6), 777–786. https://doi.org/10.1016/S0092-8674(00)00066-0

Seddon, H. J., Medawar, P. B., & Smith, H. (1943). Rate of regeneration of peripheral nerves in man. *The Journal of Physiology*, *102*(2), 191–215. https://doi.org/10.1113/jphysiol.1943.sp004027

Semple, S. C., Klimuk, S. K., Harasym, T. O., Dos Santos, N., Ansell, S. M., Wong, K. F., Maurer, N., Stark, H., Cullis, P. R., Hope, M. J., & Scherrer, P. (2001). Efficient encapsulation of antisense oligonucleotides in lipid vesicles using ionizable aminolipids: Formation of novel small multilamellar vesicle structures. *Biochimica et Biophysica Acta - Biomembranes*, *1510*(1–2), 152–166. https://doi.org/10.1016/S0005-2736(00)00343-6

Sercombe, L., Veerati, T., Moheimani, F., Wu, S. Y., Sood, A. K., & Hua, S. (2015). Advances and challenges of liposome assisted drug delivery. *Frontiers in Pharmacology*, *6*(DEC), 1–13. https://doi.org/10.3389/fphar.2015.00286

Singer, M. L., Benevides, E. S., Rana, S., Sunshine, M. D., Martinez, R. C., Barral, B. E., Byrne, B. J., & Fuller, D. D. (2023). Optogenetic activation of the tongue in spontaneously breathing mice. *Respiratory Physiology and Neurobiology*, *309*, 1–13. https://doi.org/10.1016/j.resp.2022.103998

Singh, K., & Dilworth, F. J. (2013). Differential modulation of cell cycle progression distinguishes members of the myogenic regulatory factor family of transcription factors. *FEBS Journal*, *280*(17), 3991–4003. https://doi.org/10.1111/febs.12188

Slavin, B. R., Sarhane, K. A., von Guionneau, N., Hanwright, P. J., Qiu, C., Mao, H. Q., Höke, A., & Tuffaha, S. H. (2021). Insulin-Like Growth Factor-1: A Promising Therapeutic Target for Peripheral Nerve Injury. *Frontiers in Bioengineering and Biotechnology*, *9*(June), 1–12. https://doi.org/10.3389/fbioe.2021.695850

Smania, N., Berto, G., La Marchina, E., Melotti, C., Midiri, A., Roncari, L., Zenorini, A., Ianes, P., Picelli, A., Waldner, A., Faccioli, S., & Gandolfi, M. (2012). Rehabilitation of brachial plexus injuries in adults and children. *European Journal of Physical and Rehabilitation Medicine*, *48*(3), 483–506.

Smith, T. H., Block, N. E., Rhodes, S. J., Konieczny, S. F., & Miller, J. B. (1993). *(Smith) A unique pattern of expression of the four muscle regulatory factor proteins distinguishes somitic from embryonic... [[]] [[]]*. *1133*, 1125–1133.

Snow, M. (1978). An autoradiographic study of satellite cell differentiation into regenerating myotubes following transplantation of muscles in young rats. *Cell and Tissue Research*, *186*(3). https://doi.org/10.1007/BF00224941

Snow, M. H. (1977). Myogenic cell formation in regenerating rat skeletal muscle injured by mincing II. An autoradiographic study. *The Anatomical Record*, *188*(2), 201–217. https://doi.org/10.1002/ar.1091880206

Sousa-Victor, P., García-Prat, L., & Muñoz-Cánoves, P. (2022). Control of satellite cell function in muscle regeneration and its disruption in ageing. *Nature Reviews Molecular Cell Biology*, *23*(3), 204–226. https://doi.org/10.1038/s41580-021-00421-2

Srikuea, R., Pholpramool, C., Kitiyanant, Y., & Yimlamai, T. (2010). Satellite cell activity in muscle regeneration after contusion in rats. *Clinical and Experimental Pharmacology and Physiology*, *37*(11), 1078–1086. https://doi.org/10.1111/j.1440-1681.2010.05439.x

Srinivasan, S. S., Maimon, B. E., Diaz, M., Song, H., & Herr, H. M. (2018). Closed-loop functional optogenetic stimulation. *Nature Communications*, *9*(1), 5303. https://doi.org/10.1038/s41467-018-07721-w

Steinbach, J. H. (1981). *Ul.S.A.* 513–528.

Stewart, R., Flechner, L., Montminy, M., & Berdeaux, R. (2011). Creb is activated by muscle injury and promotes muscle regeneration. *PLoS ONE*, *6*(9). https://doi.org/10.1371/journal.pone.0024714

Swetha, K., Kotla, N. G., Tunki, L., Jayaraj, A., Bhargava, S. K., Hu, H., Bonam, S. R., & Kurapati, R. (2023). Recent Advances in the Lipid Nanoparticle-Mediated Delivery of mRNA Vaccines. *Vaccines*, *11*(3). https://doi.org/10.3390/vaccines11030658

Swingle, K. L., Hamilton, A. G., & Mitchell, M. J. (2021). Lipid Nanoparticle-Mediated Delivery of mRNA Therapeutics and Vaccines. *Trends in Molecular Medicine*, *27*(6), 616–617. https://doi.org/10.1016/j.molmed.2021.03.003

Syama, K., Jakubek, Z. J., Chen, S., Zaifman, J., Tam, Y. Y. C., & Zou, S. (2022). Development of lipid nanoparticles and liposomes reference materials (II): cytotoxic profiles. *Scientific Reports*, *12*(1), 1–11. https://doi.org/10.1038/s41598-022-23013-2

Talbot, J., & Mavez, L. (2016). Resistance To Muscle Disease. *Wiley Interdisciplinary Reviews: Developmental Biology*, *5*(4), 518–534. https://doi.org/10.1002/wdev.230.Skeletal

Tanaka, S., & Okusa, M. D. (2018). Optogenetics in understanding mechanisms of acute kidney injury. *Nephron*, *140*(2), 152–155. https://doi.org/10.1159/000491498

Tang, X., Zhang, Y., & Han, X. (2023). Ionizable Lipid Nanoparticles for mRNA Delivery. *Advanced NanoBiomed Research*, *3*(8). https://doi.org/10.1002/anbr.202300006

Tedesco, F. S., Dellavalle, A., Diaz-manera, J., Messina, G., & Cossu, G. (2010). Repairing skeletal muscle: regenerative potential ... [J Clin Invest. 2010] - PubMed result. *J. Clin. Invest.*, *120*(1), 11–19. https://doi.org/10.1172/JCI40373.and

Tenchov, R., Bird, R., Curtze, A. E., & Zhou, Q. (2021). Lipid Nanoparticles from Liposomes to mRNA Vaccine Delivery, a Landscape of Research Diversity and Advancement. *ACS Nano*, *15*(11), 16982–17015. https://doi.org/10.1021/acsnano.1c04996

Thatte, M., Babhulkar, S., & Hiremath, A. (2013). Brachial plexus injury in adults: Diagnosis and surgical treatment strategies. *Annals of Indian Academy of Neurology*, *16*(1), 26. https://doi.org/10.4103/0972-2327.107686

Thomas, C. K., & Noga, B. R. (2003). Physiological methods to measure motor function in humans and animals with spinal cord injury. *Journal of Rehabilitation Research and Development*, *40*(4 SUPPL. 1), 25–33. https://doi.org/10.1682/JRRD.2003.08.0025

Thomas, C. K., Zaidner, E. Y., Calancie, B., Broton, J. G., & Bigland-Ritchie, B. R. (1997). Muscle Weakness, Paralysis, and Atrophy after Human Cervical Spinal Cord Injury. *Experimental Neurology*, *148*(2), 414–423. https://doi.org/10.1006/exnr.1997.6690

Thomas, C. K., & Zijdewind, I. (2006). Fatigue of muscles weakened by death of motoneurons. *Muscle and Nerve*, *33*(1), 21–41. https://doi.org/10.1002/mus.20400

Thomas, K., Engler, A. J., & Meyer, G. A. (2015). Extracellular Matrix Regulation in the Muscle. *Connect Tissue Res*, *56*(1), 1–8. https://doi.org/10.3109/03008207.2014.947369.EXTRACELLULAR

Thompson, L. D. V. (2002). Skeletal muscle adaptations with age, inactivity, and therapeutic exercise. *Journal of Orthopaedic and Sports Physical Therapy*, *32*(2), 44–57. https://doi.org/10.2519/jospt.2002.32.2.44

Thorogood, N. P., Noonan, V. K., Chen, X., Fallah, N., Humphreys, S., Dea, N., Kwon, B. K., & Dvorak, M. F. (2023). Incidence and prevalence of traumatic spinal cord injury in Canada using health administrative data. *Frontiers in Neurology*, *14*(July), 1–10. https://doi.org/10.3389/fneur.2023.1201025

Towne, C., Montgomery, K. L., Iyer, S. M., Deisseroth, K., & Delp, S. L. (2013). Optogenetic Control of Targeted Peripheral Axons in Freely Moving Animals. *PLoS ONE*, *8*(8). https://doi.org/10.1371/journal.pone.0072691

Tremblay, J. P., Bouchard, J. P., Malouin, F., Théau, D., Cottrell, F., Collin, H., Rouche, A., Gilgenkrantz, S., Abbadi, N., Tremblay, M., Tomé, F. M. S., & Fardeau, M. (1993). Myoblast transplantation between monozygotic twin girl carriers of Duchenne muscular dystrophy. *Neuromuscular Disorders*, *3*(5–6), 583–592. https://doi.org/10.1016/0960-8966(93)90121-Y

Tremblay, J. P., Malouin, F., Roy, R., Huard, J., Bouchard, J. P., Satoh, A., & Richards, C. L. (1993). Results of a Triple Blind Clinical Study of Myoblast Transplantations without Immunosuppressive Treatment in Young Boys with Duchenne Muscular Dystrophy. *Cell Transplantation*, *2*(2), 99–112. https://doi.org/10.1177/096368979300200203

Turner, N. J., & Badylak, S. F. (2012). Regeneration of skeletal muscle. *Cell and Tissue Research*, *347*(3), 759–774. https://doi.org/10.1007/s00441-011-1185-7

van Bremen, T., Send, T., Sasse, P., & Bruegmann, T. (2017). Spot light on skeletal muscles: optogenetic stimulation to understand and restore skeletal muscle function. *Journal of Muscle Research and Cell Motility*, *38*(3–4), 331–337. https://doi.org/10.1007/s10974-017-9481-9

Venuti, J. M., Morris, J. H., Vivian, J. L., Olson, E. N., & Klein, W. H. (1995). Myogenin is required for late but not early aspects of myogenesis during mouse development. *Journal of Cell Biology*, *128*(4), 563–576. https://doi.org/10.1083/jcb.128.4.563

Vijayavenkataraman, S. (2020). Nerve guide conduits for peripheral nerve injury repair: A review on design, materials and fabrication methods. *Acta Biomaterialia*, *106*, 54–69. https://doi.org/10.1016/j.actbio.2020.02.003

Vilquin, J. T., Wagner, E., Kinoshita, I., Roy, R., & Tremblay, J. P. (1995). Successful histocompatible myoblast transplantation in dystrophin-deficient mdx mouse despite the production of antibodies against dystrophin. *Journal of Cell Biology*, *131*(4), 975–988. https://doi.org/10.1083/jcb.131.4.975

Vogel, A. B., Kanevsky, I., Che, Y., Swanson, K. A., Muik, A., Vormehr, M., Kranz, L. M., Walzer, K. C., Hein, S., Güler, A., Loschko, J., Maddur, M. S., Ota-Setlik, A., Tompkins, K., Cole, J., Lui, B. G., Ziegenhals, T., Plaschke, A., Eisel, D., … Sahin, U. (2021). BNT162b vaccines protect rhesus macaques from SARS-CoV-2. *Nature*, *592*(7853), 283–289. https://doi.org/10.1038/s41586-021-03275-y

Vogel, M., & Landmesser, L. (1987). Distribution of fiber types in embryonic chick limb muscles innervated by foreign motoneurons. *Developmental Biology*, *119*(2), 481–495. https://doi.org/10.1016/0012-1606(87)90051-0

Von Maltzahn, J., Bentzinger, C. F., & Rudnicki, M. A. (2014). *Characteristics of Satellite Cells and Multipotent Adult Stem Cells in the Skeletal Muscle* (pp. 63–73). https://doi.org/10.1007/978-94-017-8032-2_6

Von Maltzahn, J., Jones, A. E., Parks, R. J., & Rudnicki, M. A. (2013). Pax7 is critical for the normal function of satellite cells in adult skeletal muscle. *Proceedings of the National Academy of Sciences of the United States of America*, *110*(41), 16474–16479. https://doi.org/10.1073/pnas.1307680110

Wang, D., Tai, P. W. L., Gao, G., Systems, P., & Tai, P. W. L. (2019). *Adeno-associated virus vector as a platform for gene therapy delivery* (Vol. 18, Issue 5). https://doi.org/10.1038/s41573-019-0012-9.Adeno-associated

Wang, H., Sugiyama, Y., Hikima, T., Sugano, E., Tomita, H., Takahashi, T., Ishizuka, T., & Yawo, H. (2009). Molecular determinants differentiating photocurrent properties of two channelrhodopsins from Chlamydomonas. *Journal of Biological Chemistry*, *284*(9), 5685–5696. https://doi.org/10.1074/jbc.M807632200

Wang, M. L., Rivlin, M., Graham, J. G., & Beredjiklian, P. K. (2019). Peripheral nerve injury, scarring, and recovery. *Connective Tissue Research*, *60*(1), 3–9. https://doi.org/10.1080/03008207.2018.1489381

Wang, Y., Lobb-Rabe, M., Ashley, J., Anand, V., & Carrillo, R. A. (2021). Structural and Functional Synaptic Plasticity Induced by Convergent Synapse Loss in the Drosophila Neuromuscular Circuit. *The Journal of Neuroscience*, *41*(7), 1401–1417. https://doi.org/10.1523/JNEUROSCI.1492-20.2020

Weng, J., Zhang, P., Yin, X., & Jiang, B. (2018). The whole transcriptome involved in denervated muscle atrophy following peripheral nerve injury. *Frontiers in Molecular Neuroscience*, *11*(March), 1–15. https://doi.org/10.3389/fnmol.2018.00069

Wernig, A., Irintchev, A., & Lange, G. (1995). Functional effects of myoblast implantation into histoincompatible mice with or without immunosuppression. *The Journal of Physiology*, *484*(2), 493–504. https://doi.org/10.1113/jphysiol.1995.sp020681

Wernig, A., Zweyer, M., & Irintchev, A. (2000). Function of skeletal muscle tissue formed after myoblast transplantation info irradiated mouse muscles. *Journal of Physiology*, *522*(2), 333–345. https://doi.org/10.1111/j.1469-7793.2000.t01-2-00333.x

Wheeler, J. J., Palmer, L., Ossanlou, M., Maclachlan, I., Graham, R. W., Zhang, Y. P., Hope, M. J., Scherrer, P., & Cullis, P. R. (1999). *Stabilized plasmid-lipid particles : construction and characterization*. 271–281.

Whitehead, K. A., Langer, R., & Anderson, D. G. (2009). Knocking down barriers: Advances in siRNA delivery. *Nature Reviews Drug Discovery*, *8*(2), 129–138. https://doi.org/10.1038/nrd2742

Wilson, K. D., de Jong, S. D., Kazem, M., Lall, R., Hope, M. J., Cullis, P. R., & Tam, Y. K. (2009). The combination of stabilized plasmid lipid particles and lipid nanoparticle encapsulated CpG containing oligodeoxynucleotides as a systemic genetic vaccine. *The Journal of Gene Medicine*, *11*(1), 14–25. https://doi.org/10.1002/jgm.1267

Wilson, M. H., & Deschenes, M. R. (2005). The neuromuscular junction: Anatomical features and adaptations to various forms of increased, or decreased neuromuscular activity. *International Journal of Neuroscience*, *115*(6), 803–828. https://doi.org/10.1080/00207450590882172

Wolfe, R. R. (2006). The underappreciated role of muscle in health and disease. *American Journal of Clinical Nutrition*, *84*(3), 475–482. https://doi.org/10.1093/ajcn/84.3.475

Wong, A., Garcia, S. M., Tamaki, S., Striedinger, K., Barruet, E., Hansen, S. L., Young, D. M., & Pomerantz, J. H. (2021). Satellite cell activation and retention of muscle regenerative potential after long-term denervation. *Stem Cells*, *39*(3), 331–344. https://doi.org/10.1002/stem.3316

Wu, X., Corona, B. T., Chen, X., & Walters, T. J. (2012). A standardized rat model of volumetric muscle loss injury for the development of tissue engineering therapies. *BioResearch Open Access*, *1*(6), 280–290. https://doi.org/10.1089/biores.2012.0271

Xiao, X., Li, J., & Samulski, R. J. (1996). Efficient long-term gene transfer into muscle tissue of immunocompetent mice by adeno-associated virus vector. *Journal of Virology*, *70*(11), 8098–8108. https://doi.org/10.1128/jvi.70.11.8098-8108.1996

Xu, C., Tabebordbar, M., Iovino, S., Ciarlo, C., Liu, J., Castiglioni, A., Price, E., Liu, M., Barton, E. R., Kahn, C. R., Wagers, A. J., & Zon, L. I. (2013). XA zebrafish embryo culture system defines factors that promote vertebrate myogenesis across species. *Cell*, *155*(4), 909. https://doi.org/10.1016/j.cell.2013.10.023

Xu, X., Talifu, Z., Zhang, C. J., Gao, F., Ke, H., Pan, Y. Z., Gong, H., Du, H. Y., Yu, Y., Jing, Y. L., Du, L. J., Li, J. J., & Yang, D. G. (2023). Mechanism of skeletal muscle atrophy after spinal cord injury: A narrative review. *Frontiers in Nutrition*, *10*. https://doi.org/10.3389/fnut.2023.1099143

Yablonka-Reuveni, Z. (2011). The Skeletal Muscle Satellite Cell: Still Young and Fascinating at 50. *Journal of Histochemistry and Cytochemistry*, *59*(12), 1041–1059. https://doi.org/10.1369/0022155411426780

Yablonka-Reuveni, Z., & Rivera, A. J. (1994). Temporal expression of regulatory and structural muscle proteins during myogenesis of satellite cells on isolated adult rat fibers. *Developmental Biology*, *164*(2), 588–603. https://doi.org/10.1006/dbio.1994.1226

Yan, X., Kuipers, F., Havekes, L. M., Havinga, R., Dontje, B., Poelstra, K., Scherphof, G. L., & Kamps, J. A. A. M. (2005). The role of apolipoprotein E in the elimination of liposomes from blood by hepatocytes in the mouse. *Biochemical and Biophysical Research Communications*, *328*(1), 57–62. https://doi.org/10.1016/j.bbrc.2004.12.137

Yang, T., Zhang, W., Cheng, J., Nie, Y., Xin, Q., Yuan, S., & Dou, Y. (2019). Formation mechanism of ion channel in channelrhodopsin-2: Molecular dynamics simulation and steering molecular dynamics simulations. *International Journal of Molecular Sciences*, *20*(15), 1–15. https://doi.org/10.3390/ijms20153780

Yannascoli, S. M., Stwalley, D., Saeed, M. J., Olsen, M. A., & Dy, C. J. (2018). A Population-Based Assessment of Depression and Anxiety in Patients With Brachial Plexus Injuries. *Journal of Hand Surgery*, *43*(12), 1136.e1-1136.e9. https://doi.org/10.1016/j.jhsa.2018.03.056

Yin, H., Price, F., & Rudnicki, M. A. (2013). Satellite cells and the muscle stem cell niche. *Physiological Reviews*, *93*(1), 23–67. https://doi.org/10.1152/physrev.00043.2011

Yin, X., Yu, T., Chen, B., Xu, J., Chen, W., Qi, Y., Zhang, P., Li, Y., Kou, Y., Ma, Y., Han, N., Wan, P., Luo, Q., Zhu, D., & Jiang, B. (2019). Spatial distribution of motor endplates and its adaptive change in skeletal muscle. *Theranostics*, *9*(3), 734–746. https://doi.org/10.7150/thno.28729

Yizhar, O., Fenno, L. E., Davidson, T. J., Mogri, M., & Deisseroth, K. (2011). Optogenetics in Neural Systems. *Neuron*, *71*(1), 9–34. https://doi.org/10.1016/j.neuron.2011.06.004

Yohn, D. C., Miles, G. B., Rafuse, V. F., & Brownstone, R. M. (2008). Transplanted mouse embryonic stem-cell-derived motoneurons form functional motor units and reduce muscle atrophy. *Journal of Neuroscience*, *28*(47), 12409–12418. https://doi.org/10.1523/JNEUROSCI.1761-08.2008

Zaglia, T., Pianca, N., Borile, G., Da Broi, F., Richter, C., Campione, M., Lehnart, S. E., Luther, S., Corrado, D., Miquerol, L., & Mongillo, M. (2015). Optogenetic determination of the myocardial requirements for extrasystoles by cell type-specific targeting of ChannelRhodopsin-2. *Proceedings of the National Academy of Sciences*, *112*(32). https://doi.org/10.1073/pnas.1509380112

Zammit, P. S. (2017). Function of the myogenic regulatory factors Myf5, MyoD, Myogenin and MRF4 in skeletal muscle, satellite cells and regenerative myogenesis. *Seminars in Cell and Developmental Biology*, *72*, 19–32. https://doi.org/10.1016/j.semcdb.2017.11.011

Zammit, P. S., Golding, J. P., Nagata, Y., Hudon, V., Partridge, T. A., & Beauchamp, J. R. (2004). Muscle satellite cells adopt divergent fates: A mechanism for self-renewal? *Journal of Cell Biology*, *166*(3), 347–357. https://doi.org/10.1083/jcb.200312007

Zammit, P. S., Partridge, T. A., & Yablonka-Reuveni, Z. (2006). The skeletal muscle satellite cell: The stem cell that came in from the cold. *Journal of Histochemistry and Cytochemistry*, *54*(11), 1177–1191. https://doi.org/10.1369/jhc.6R6995.2006

Zammit, P. S., Relaix, F., Nagata, Y., Ruiz, A. P., Collins, C. A., Partridge, T. A., & Beauchamp, J. R. (2006). Pax7 and myogenic progression in skeletal muscle satellite cells. *Journal of Cell Science*, *119*(9), 1824–1832. https://doi.org/10.1242/jcs.02908

Zimmermann, T. S., Lee, A. C. H., Akinc, A., Bramlage, B., Bumcrot, D., Fedoruk, M. N., Harborth, J., Heyes, J. A., Jeffs, L. B., John, M., Judge, A. D., Lam, K., McClintock, K., Nechev, L. V., Palmer, L. R., Racie, T., Röhl, I., Seiffert, S., Shanmugam, S., … MacLachlan, I. (2006). RNAi-mediated gene silencing in non-human primates. *Nature*, *441*(1), 111–114. https://doi.org/10.1038/nature04688

Appendix One- Chapter Two Movies

Video 2.1. Optical activation of ES cell-derived myotubes/myofibres expressing ChR2. This video demonstrates the optical activation of 15-day-old ES cell-derived myotube/myofibre cultures expressing ChR2. The cultures were stimulated using 470 nm blue light, visibly inducing muscle contraction upon light exposure.

Video 2.2. Optical activation of ES cell-derived myotubes/myofibres transduced with AAV-PHP.eB-CAG-ChR2-EYFP. This video demonstrates the optical activation of 15-day-old ES cell-derived myotube/myofibre cultures expressing ChR2 via AAV-PHP.eB-CAG-ChR2-EYFP transduction 2 days earlier (day 13). The cultures were stimulated using 470 nm blue light, visibly inducing muscle contraction upon light exposure.

Appendix Two - Chapter Three Movies

Video 3.1. *Ex Vivo* Optical Activation of Regenerated Soleus Muscle Following ChR2-Expressing Myoblast Transplantation. This video shows the ex vivo optical activation of regenerated soleus muscle 30 days post-transplantation of ChR2-expressing myoblasts into irradiated and notexin-injected muscle tissue. Muscle contractions are obvious in response to 470 nm blue light stimulation, occurring independently of nerve stimulation.

Video 3.2. *Ex Vivo* Optical Activation of Regenerated Soleus Muscle Following AAV-PHP.eB-CAG-ChR2-EYFP transduced Myoblast Transplantation. This video shows the ex vivo optical activation of regenerated soleus muscle 60 days post-transplantation of AAV-PHP.eB-CAG-ChR2-EYFP transduced myoblasts into irradiated and notexin-injected muscle tissue. Muscle contraction is obvious in response to 470 nm blue light stimulation, occurring independently of nerve stimulation.